Bulletin 99

A Model for Predicting Flood Hazards Due to Specific Land-Use Practices

B. B. Ross
D. N. Contractor
E. A. Li
V. O. Shanholtz
J. C. Carr

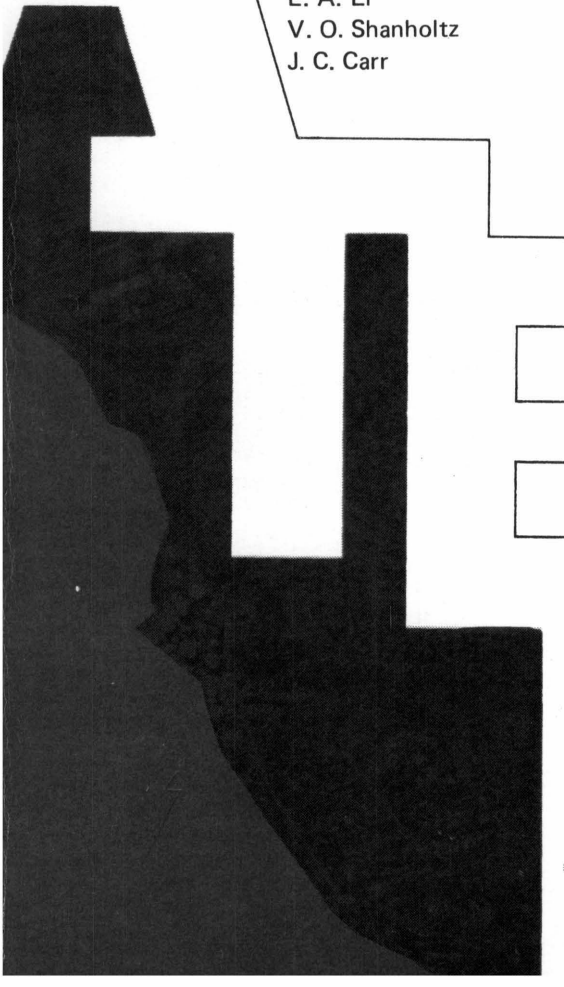

Bulletin 99
September 1976

A Model for Predicting Flood Hazards Due to Specific Land-Use Practices

B. B. Ross
D. N. Contractor

Department of Civil Engineering

E. A. Li
V. O. Shanholtz
J. C. Carr

Department of Agricultural Engineering

The work upon which this report is based was supported in part by funds provided by the United States Department of the Interior Office of Water Resources Research, as authorized by the Water Resources Research Act of 1964 (P.L. 88-379), and in part by the Virginia Polytechnic Institute and State University Research Division

OWRT Project A-062-VA
VPI-VWRRC-BULL 99

A publication of
Virginia Water Resources Research Center
Virginia Polytechnic Institute and State University
Blacksburg, Virginia 24061

TABLE OF CONTENTS

(continued)

LIST OF TABLES

LIST OF FIGURES

ABSTRACT

This investigation developed a finite element model for mathematically routing overland and channel flow when rainfall excess is known. To determine rainfall excess, a procedure was developed to subdivide a drainage area into similarly responding units, defined as hydrologic response units. These units were functions of soil texture, soil depth, land use, and hydrology group classification. A computer model, based on the Mein and Larson and Holtan infiltration equations, was developed to generate excess precipitation for each hydrologic response unit. A finite element grid, devised for both the watershed and the main streams, allowed use of the hydrologic response units within an element to obtain weighted rainfall excess values for each element.

A one-dimensional finite element scheme, in conjunction with Galerkin's residual method, simulated overland and open channel flow. Hurricane Camille (August, 1969) provided an event by which the model was tested and calibrated on the South River watershed in Augusta County, Virginia. Having the ability to report changes in land use, the finite element procedure allowed several arbitrary land-use changes to be incorporated into the model in order to observe the river's response under flood conditions. The effects of changes in the number and size of the elements in the watershed and in the streams also were observed, along with changes in the size of the time increment.

ACKNOWLEDGMENTS

Data for the development and evaluation of the precipitation excess model relating hydrologic response units to readily obtainable soils and vegetative parameters were collected jointly by the USDA Agricultural Research Service (ARS) and the Research Division, Virginia Polytechnic Institute and State University. This phase of the study utilized data from one of the watersheds monitored by this group, the Rocky Run Branch Watershed, Brunswick County, Virginia. Computer funds were made available by the Departments of Agricultural Engineering and Civil Engineering.

Special acknowledgment is accorded the following who generously gave their time to a critical review of the manuscript: Dr. C. T. Haan, Professor, Department of Agricultural Engineering, University of Kentucky, and Dr. J. T. Ligon, Professor, Department of Agricultural Engineering, Clemson University. South Carolina. Acknowledgment is also made to Victoria C. Esarey, who did the typesetting.

INTRODUCTION

With the recent occurrences of major flood events in the past few decades, particularly in the Eastern part of the United States, the importance of careful planning and accurate flood prediction models has become more evident. Many cities have developed near streams because water for drinking, irrigation, power, industry and water disposal is readily available. The expansion of cities has caused stress on the water supply as the demand for water has increased. At the same time, too much water in the form of runoff from urban areas has seriously increased the frequency and magnitude of floods. During the last 20 years, man has begun to realize the extent to which his use of land affects the earth's water resources, and how this use affects the response of a river. Quality and quantity of river discharges are now important issues in many parts of the world.

Physical models of watersheds and river systems were used in earlier years to simulate the response of a watershed system, but more recently the advent of high-speed digital computers and the availablility of data have made detailed mathematical modeling feasible. Mathematical flood routing by a computer, for example, has proven to be superior to the physical model because of the ease with which changes may be made in the geometry of the watershed system.

During the past decade, research efforts have focused on the development of hydrologic models which have the capability to simulate flow response when a drainage area is subjected to some rainfall distribution. These models have been lumped-parameter models, where parameters are based on a weighted average of such factors as soils, land use, and topography. The models are relatively easy to use when necessary data requirements are available, but they are not readily adaptable to situations where spatial variations are extreme and must be considered.

This report covers a cooperative research effort sponsored by the Virginia Water Resources Research Center and conducted jointly by Virginia Military Institute and Virginia Polytechnic Institute and State University. The VMI effort will be reported in Virginia WRRC Bulletin 103. The work at VPI&SU was conducted jointly by the Departments of Civil Engineering and Agricultural Engineering. The Department of Civil Engineering had the responsibility for developing a routing routine utilizing the the finite element technique to provide temporal and spatial history of overland and channel flows. Input to this routine was precipitation excess, and this phase was conducted by the Department of Agricultural Engineering.

Since the precipitation excess generator and the routing routine were developed as separate entities, the development of each is discussed separately in this report. In a final section the application of each to the South River drainage system is presented.

LITERATURE REVIEW

Considerable research effort has been expended nationally towards equation fitting and mathematical modeling of problems related to hydrology [Dawdy, 1969]. Much emphasis has been placed on the development of comprehensive simulation models. These developments have followed three basic approaches: (a) parametric, (b) deterministic and (c) stochastic. In recent years, some attention has been focused on the development of combination models, e.g. deterministic-parametric.

Linsley and Crawford [1962, 1966] are generally recognized as the early leaders in the development of comprehensive watershed models to simulate flows through watershed systems. The Stanford model is basically a lumped-parameter model, although large watersheds can be divided into sub-watersheds if sufficient data are available to define model parameters. The model has gained widespread use and as a result has undergone numerous modifications [e.g. James, 1965; Claborn and Moore, 1970; Ligon et al., 1969; National Weather Service, 1972; Shanholtz et al., 1972; Ricca, 1974].

Holtan and Lopez [1971] describe a lumped model. Attempts were made to define spatial variability by dividing the area into land capability classes. Dawdy et al. [1970] recently reported on a model similar to the Stanford model, which describes surface flow from small watersheds. Freeze and Harlan [1969] proposed a three-dimensional approach. TVA [1972] recently described a daily streamflow model with five parameters that require optimization and 11 constants (parameters) readily determinable. Reasonable success was noted in predicting streamflows. Examples also were given which illustrate the utility of the model for water quality predictions.

Woolhiser [1973], in a recent paper, outlines the state-of-the-art in watershed models and specifically defines different model classes. Larson [1973] discusses the hydrologic effects of modifying small watersheds and the possibility of prediction by hydrologic modeling.

A series of publications in preparation under Southern Regional Reserarch Project S-53 [1975] also describe several watershed models and their applicability to small agricultural watersheds. Many other notable contributions have been made to watershed modeling in the past fifteen years. Most of these are included for the interested reader in a supporting bibliography.

Although considerable effort has been expended toward mathematical modeling in the past, much less effort has been devoted to the development of reliable prediction models for defining land use change. However, with the present state-of-the-art in hydrologic model development, more attention can be focused on the problem of watershed change and streamflow predictions on ungaged areas. This is particularly true since several hydrologic models have been structured which have demonstrated

reliability for those situations where an historical record is available to calibrate the model.

The following review specifically summarizes research relative to the development of a storm hydrograph model. Methods for predicting precipitation excess with particular emphasis on infiltration techniques are presented and this discussion is followed by a critique of flood-routing methods.

I. Precipitation Excess

Description of the runoff process accounts for the discharge of excess rainfall during any rainfall event. In recent years, many hydrologic models have been developed to simulate this process [e.g., Schulze, 1966]. Most techniques involve moisture accounting as a function of infiltration. Consequently, this review will be limited to pertinent infiltration models. The different models can be divided into two major groups: theoretical and empirical methods.

II. Theoretical Methods

Most theoretical methods for predicting precipitation excess are based on Darcy's Law as applied to the wetting front in the soil. All display a dependency on soil properties, but differ in dependency on time and rainfall intensity.

A. The Green and Ampt Equation

Green and Ampt [1911] developed a relationship to predict the flow of water through the soil based on Darcy's Law and the assumption that the soil acts as an aggregate of capillary tubes differing in area, direction, and shape. A homogeneous deep soil with a uniform initial moisture content and a ponded surface are also basic assumptions in their equation. Infiltration capacity is determined from the relationship:

$$f = Sn \, Log_e \frac{F + nS}{nS} + Ks\,(t) \qquad [1]$$

where:

f = infiltration capacity;
F = volume of infiltration;
Ks = conductivity at the wetted zone;
S = capillary potential at the wetting front;
n = the initial moisture deficit, and
t = the time.

The head of water on the surface and capillary potential at the wetting front are difficult to obtain under field conditions, seriously limiting the applicability of the method.

B. The Richards Flow Equation

Richards [1931] combined Darcy's Law with the equation of continuity to obtain the following nonlinear partial differential equation for vertical water movement in the soil during unsaturated conditions:

$$\frac{\partial \theta}{\partial t} = -\frac{\partial}{\partial x}\left[K(\theta)\frac{\partial h(\theta)}{\partial x}\right] - \frac{\partial K(\theta)}{\partial x} \qquad [2]$$

where:

θ = volumetric moisture content of the soil;
t = time;
x = distance of the wetted front below surface;
h = capillary potential at the wetted front, and
K = unsaturated hydraulic conductivity.

Like the Green and Ampt equation, the Richards equation requires knowledge of the capillary potential at the wetted front. In addition, the unsaturated hydraulic conductivity of the soil must be determined, which is difficult, particularly under field conditions. The equation stresses time-dependency, but involves no direct dependency on rainfall intensity. Despite obvious disadvantages, the method is considered to be a theoretically sound procedure for determining vertical movement of water in a soil column.

C. The Philip Equation

Philip [1957] solved the soil moisture flow equation assuming a homogeneous deep soil with a ponded surface. The solution is in the form of an infinite time series (t), with the diffusivity and moisture retention characteristics of the soil defining the coefficient for each term. Since the series converges quite rapidly, usually only the first two terms are retained to give:

$$F = st^{1/2} + At \qquad [3]$$

where:

F = volume of infiltration to time t, and
s,A = constants dependent on soil type and initial soil moisture content.

This equation is simple when limited to the first few terms in the series. Like the Green and Ampt equation, however, the constants s and A must be obtained by fitting the equation to actual data. This equation, like the theoretical methods previously discussed, is not a direct function of rainfall intensity, but is clearly time-variant.

D. The Mein and Larson Equation

Mein and Larson [1971] developed a set of two equations to predict infiltration based on Darcy's Law. They considered three conditions in the development of their model. Case A was defined to include all periods during which the rainfall intensity was less than the saturated hydraulic conductivity (Ks); that is , by definition no runoff will occur until the soil becomes saturated at which time runoff equals precipitation.

Case B was defined to include the condition in which the rainfall rate exceeded the saturated hydraulic conductivity but was less than the maximum infiltration rate. The model developed for this case was:

$$F_s = \frac{(S_{av})\ (IMD)}{(I/K_s) - 1} \qquad [4]$$

where:

F_s = infiltration volume prior to the start of runoff;
IMD = initial soil moisture deficit;
I = rainfall intensity
K_s = saturated hydraulic conductivity, and
S_{av} = capillary potential at the wetted front, represented by the area under the capillary suction (S) versus relative conductivity of the soil (K) curve, from K = 0.01 to 1.0.

Finally, Case C was defined to include the condition when rainfall rate exceeded the the infiltration capacity of the soil. In their method they stated that:

$$f_p = (K_s)\ (1 + \frac{(IMD)\ S_{av}}{F}) \qquad [5]$$

where:

f_p = infiltration capacity;
K_s = saturated hydraulic conductivity;
IMD = initial soil moisture deficit;
S_{av} = capillary potential at the wetted front, and
F = infiltration volume.

This method, like others, is cumbersome to use because of the difficulty associated with determining S_{av}. However, it is a definite improvement over previous methods because it attempts to define threshold conditions. The model is a function of rainfall intensity and is time-invariant.

III. Empirical Methods

In addition to the numerous theoretical methods for predicting precipitation excess,

there exist a number of methods based on the relationship of decreasing infiltration capacity to an increasing volume of water in the soil profile. These models attempt to fit observed infiltration to a decay-type function. Most empirical methods require fitting of the equation to actual data to obtain one or more necessary parameters.

A. The Kostyakov Equation

The Kostyakov equation [1932] takes the general form:

$$F = at^b \qquad [6]$$

where:

F = total infiltration volume;
t = time from onset of infiltration;
a = constant dependent on soil type and initial soil moisture content, and
b = constant dependent on soil type that ranges between 0 and 1.0.

Mein and Larson [1971] noted that the simplicity of this model and its adaptations have promoted its widespread use. However, the constants a and b must be fitted by use of field data, and threshold conditions must be estimated. The equation is time-variant but does not consider rainfall rate.

B. The Horton Equation

Horton [1939]proposed the following model for predicting precipitation excess:

$$f_p = f_c + (f_o - f_c)\, e^{-kt} \qquad [7]$$

where:

f_p = infiltration capacity at time, t;
f_o = initial infiltration capacity;
f_c = final or equilibrium infiltration, and
k = constant dependent on soil type and initial moisture conditions.

The equation is easy to use once the constants are defined. The constants f_o, f_c, and k must be fitted to field data. The model does not provide a means for direct computation of infiltration recovery—a distinct disadvantage in continuous modeling of watershed systems. The initial infiltration rate is also very difficult to estimate with reasonable reliability.

C. The Non-Linear Loss Relation

The U.S. Army Corps of Engineers [1973] developed the following non-linear relationship between rainfall and runoff:

$$L = KP^E \quad [8]$$

where:

L = loss rate (infiltration) in in/hr;
K = coefficient which decreases with increasing ground wetness;
P = average rainfall rate in in/hr for given basin, and
E = exponent which varies between 0.0 and 1.0.

The exponent E is a function of land use and soil characteristics and usually ranges from 0.3 to 0.9. The loss rate becomes independent of rainfall intensity when E is set to 0.

The coefficient K is estimated from:

$$K = K_0 C^{-(L/10)} \quad [9]$$

where:

K_0 = initial loss coefficient, in inches;
C = coefficient controlling rate of decrease of K, and
L = accumulated loss during storm, in inches.

To account for initial soil moisture deficit, Equation 9 was redefined by the Corps [1973] as:

$$L = (K + K')\, P^E \quad [10]$$

where:

$K' = 0.2D\ (L/D)^2$ where $L/D \leqslant 1.0$.
D = initial soil moisture deficit in inches.

This method is indirectly dependent on both rainfall intensity and time, but constants K, E, K_O, C, and D must be fitted from field or laboratory data.

D. The Soil Conservation Service Method

The Soil Conservation Service [1972] developed a method for predicting precipitation excess based on the soil-vegetative complex. Initial soil moisture content is reflected in Ia, referred to as the initial abstraction. The Soil Conservation Service (SCS) recommends Ia be set to 20 percent of the potential maximum storage (S). Actual retention is represented by (P-Ia-Q), where Q is the precipitation excess and P is the rainfall in

in/hr. The ratio of actual retention to the potential maximum retention (S) is equal to the ratio of actual runoff to potential maximum runoff (P-Ia).

$$Q = \frac{(P - Ia)^2}{(P - Ia) + S} \qquad [11]$$

S can be estimated by runoff curve numbers, CN, for any particular soil-cover complex using the following:

$$Cn = \frac{1000}{S + 10} \qquad [12]$$

As retention (S) approaches infinity, CN approaches zero and when S becomes 0, CN is equal to precipitation. This method has attained wide usage, particularly within the SCS, but the determination of CN requires the use of a weighted average based on the existing soil-vegetative complex. Depending upon the size and detail of the watershed, this can entail many calculations.

E. The Holtan Equation

Holtan [1961] developed the following empirical equation which defines infiltration as a function of soil water volume:

$$f = a\,(S - F)^n + f_c \qquad [13]$$

where:

- f = rate of infiltration in in/hr;
- S = unfilled storage potential in a soil above the impeding strata, in inches. Initially equal to available storage minus antecedent soil moisture.
- F = accumulated infiltration in inches;
- f_c = constant rate of infiltration after prolonged wetting, in in/hr, and
- a,n = constants for a particular soil-vegetative complex.

The constant f_c, in general, ranges from 0.45 to 0.30 for hydrologic group A; 0.30 to 0.15 for hydrologic group B; 0.15 to 0.05 for hydrologic group C; and 0.05 to 0.0 for hydrologic group D.

The value for n is generally set to 1.4, but constant a must be fitted from actual data for a specific area. Estimates are available for various cover crops [Holtan and Lopez, 1971].

Infiltration recovery is achieved through evapotranspiration and deep seepage. Time and rainfall intensity indirectly influence the precipitation excess value generated by this method.

IV. Flood Routing

The basic hydrodynamic equations used in most analyses of overland flow and streamflow were originally published by Saint-Venant in 1871. Because there is no known analytical method available for the solution of these complete equations, special cases have been solved by arranging them in simpler forms [Yevjevich, 1964]. Convergence and high computation time are among the many difficulties that have been encountered with the various numerical and graphical methods that have been devised.

A. Numerical Methods

In the past, the two most common numerical methods used for the solution of the Saint-Venant equations have been the method of characteristics and various finite difference techniques. Stoker [1953], with the aid of a digital computer, performed the first important numerical studies in flood routing while working with floods on the Ohio River. He used an explicit finite difference method and found that the size of the time step had to be restricted to achieve stability in his solution. The explicit method has also been used by Garrison et al. [1969] and Balloffet [1969].

The implicit method in finite differencing has been used with success by Strelkoff [1970], Contractor and Wiggert [1972], Morgali and Linsley [1965], and Greco and Panattoni [1975]. Greco and Panattoni [1975] observed that the implicit method exhibited rapid convergence and had limited storage requirements. Complex geometry, complex boundary conditions and instability have been general problems experienced with finite difference techniques.

Amein and Fang [1970] used the method of characteristics and the explicit finite difference method to compute hydrographs from a natural river and found that when compared with the hydrographs generated by the implicit finite difference method [Amein 1968], the implicit method gave better results and stability was not a problem. The method of characteristics has also been used by Wylie [1970], and Baltzer and Lai [1968] in investigating flows in open channels. Most investigators agree that when the various numerical methods are compared, implicit schemes give the most accurate results. However, Liggett and Woolhiser [1967], in a study involving these methods, found that stability and convergence problems were exhibited by both the explicit and implicit schemes and observed that the method of characteristics was the more reliable of the three, although it contains certain disadvantages and limitations [Vreugdenhill, 1968].

Price [1974] compared four numerical methods for flood routing, and concluded that the implicit method of Amein [1968] was the most efficient. He also stated that Galerkin and finite element techniques may be an improvement over finite difference methods and the method of characteristics although no details were presented in his paper.

B. The Finite Element Method

The recent introduction of the finite element method to solve flow problems has been encouraging since it has been demonstrated that many of the problems encountered by other numerical methods can be eliminated. Computation time can usually be reduced because the method requires less elements and can accommodate larger time steps than other numerical methods. The method can also handle large spatial variations.

In addition to the above advantages, additional attributes given by Desai and Abel [1972] are as follows:

1. Boundary conditions need not be introduced into the algebraic equations for the individual elements, but only into the algebraic equations for the assemblage.
2. The method easily accommodates complex geometry and complex boundary conditions.
3. It can handle complicated formulations involving material properties such as anistropy, nonlinearity, and time dependency.
4. The property of nonhomogeneity is very easily accounted for since different properties may be designated to different elements.
5. The finite element method can be applied readily to a wide range of problems.

Oden [1969] also gives some of the generalized properties and advantages of the finite element method.

Desai [1972] lists the major steps in the finite element method, for general applications, as follows:

1. Discretization of the continuum.
2. Selection of the field variable models.
3. Derivation of the finite element equations.
4. Assembly of the algebraic equations for the overall discretized continuum.
5. Solution of the nodal field variables vector.
6. Computation of the element resultants from the nodal field variable amplitudes.

Although finite element methods have been employed in solid mechanics since the 1950's, their use in flow problems did not become prominent until the late 1960's. One of the earliest applications of the finite element method to the problem of flow computations was made by Zienkiewicz and Cheung [1965] who reported on a seepage flow analysis. More recently, investigators such as Oden and Somogyi [1969] and Tong [1971] have applied the method to incompressible and compressible transient flow problems.

Al-Mashidani and Taylor [1974] used the Galerkin form of the finite element method to solve for the non-dimensional form of the shallow water equations for surface runoff. When compared with other numerical methods, it was found to have more stability, more rapid convergence, and to be computationally fast.

Judah [1972] used the finite element method and Galerkin's residual method in developing a flood routing model. He found, when the model was applied to a natural watershed, that this method gave accurate results and he reported that a finite element model can easily handle complex geometry, diverse land use, and variable rainfall distribution. These results are especially significant because Judah [1972] had considered a constant Manning coefficient for the entire overland flow part of the model and a separate Manning coefficient for the entire channel part of the model. He also considered rainfall to be distributed evenly over the entire watershed and, consequently, the rainfall excess value to be distributed evenly over the entire watershed. Assignment of specific Manning coefficient and rainfall excess values to specific elements presumably could improve the accuracy of results.

Either weighted residual methods or variational principles such as the Ritz method, Gurtin's variational principle, and Hamilton's principle, may be used for the formulation of the finite element equations. Several weighted residual methods include the orthogonal collocation, least squares, and Galerkin's residual methods.

C. Galerkin's Residual Method

The residual methods have proven to be more general and do not encounter some of the mathematical limitations that some of the variational methods may encounter. A problem also arises in some cases where no variational principle exists and a residual method must be chosen.

Galerkins's residual method was chosen for this finite element formulation because it has been demonstrated in recent years to be the best formulation procedure for flow problems. Recent investigators, such as Judah [1972] and Al-Mashidani and Taylor [1974] have employed it with great success.

In Galerkin's method the shape function is generally used as the weighting function and a trial function is chosen to represent the field function. Because the trial function is not the exact function, an error must be introduced. It is this error which must be normalized by the weighting function.

The trial function which represents the dependent variables can be written in terms of the nodal point unknown. From Zienkiewicz and Parekh [1970], the general form is as follows:

$$\phi = \sum_{i=1}^{n} N_i (x, y, z)\, \phi_i (t) \qquad [14]$$

where:

ϕ = the unknown field variable;
N_i = the shape function, and
$\phi_i(t)$ = the field variable as a function of time only.

Galerkin's method specifies that:

$$\int_D [N_i]^T R_D \, dD \qquad [15]$$

be a minimum where D represents the domain containing the elements and R_D represents the residuals to be weighted by the transpose of the shape function, $[N_i]^T$. The integral is taken over each element of the domain.

D. Kinematic Wave Approximation

Regardless of the numerical method used, either the dynamic wave or the kinematic wave approximation can be used. The kinematic wave approximation is the best choice when applicable because initial and boundary conditions need only be applied to the continuity equation.

This approximation requires that there be a balance between the gravitational and frictional forces involved in the momentum equation, and that flow is a function of depth alone. This assumption is true in most cases of overland flow with the exception of "flash flood" conditions. Generally, gradually varied flow will satisfy the conditions for the kinematic wave approximation.

Lighthill and Whitham [1955], in a discussion of the development of the kinematic wave approximation, state that for flow to be classified as kinematic, the Froude number should be less than two. Liggett and Woolhiser [1967] state that the kinematic wave approximation gives very accurate results providing that a single dimensionless parameter K is less than 10 when defined as:

$$K = c^2 s^2 L / v^2 F^2 \qquad [16]$$

where:

L = length of the flow plane;
s = bed slope of the flow plane;
v = uniform velocity of the flow;
F = Froude number, and
c = Chezy coefficient.

Eagleson [1970] suggested that both these conditions be upheld for the use of the kinematic wave approximation to be accurate in estimation of surface runoff, but

Al-Mashidani and Taylor [1974] have shown where the Froude number may be greater than two provided that K is large.

Ishihara [1963] reported on one of the first successful applications of the kinematic wave approximation and it has also been demonstrated to work well by other investigators [e.g. Brakensiek, 1967; Morgali, 1970; and Rastogi, 1971]. All of the latter found that comparison of hydrographs generated by the kinematic wave approximation were in good agreement with those found by using dynamic wave theories. Langford and Turner [1973] used results from physical model experiments to compare with results from analysis using the kinematic wave approximation and observed close agreement between the two. Errors were found to be minimal. Wooding [1967a, 1965b, 1966] presented a convincing argument in favor of the kinematic wave approximation in a set of papers in which he applied the kinematic wave approximation to a hypothetical V-shaped watershed and obtained good agreement between hydrographs generated by the model and those generated by a natural catchment.

Al-Mashidani and Taylor [1974], in their finite element solutions for surface runoff, found the kinematic wave approximation to be an adequate representation of the problem in a comparison between it and the complete equations solution. Judah [1972] also utilized the finite element method and found the kinematic wave approximation to be very applicable to the problem of routing overland and channel flow.

OBJECTIVES

Most hydrologic models have been structured to predict streamflows based on the lumped parameter concept. This technique has been successful, particularly for water yield predictions. However, recent emphasis on land use planning has created a need for models with sufficient flexibility and reliability to predict the impact of watershed change and/or modification on the stream system draining the area.

In response to this need, this project began with a general goal to develop a hydrologic model to predict the effects of land use change. This report focuses on the following specific objectives:

1. Develop a technique for defining areas which are hydrologically homogeneous from readily determinable watershed conditions.
2. Develop a computer algorithm to predict excess precipitation on each hydrologic response unit.
3. Develop a computer model to route excess precipitation from its origin to some downstream point.
4. Construct the routing algorithm with sufficient flexibility to handle the introduction of flow retardance structures such as reservoirs.
5. Verify the two models on the South River Watershed, Augusta County, Virginia.
6. Predict the effect of population growth on flood flows.
7. Evaluate the effect of element size on streamflow predictions.

PRECIPITATION EXCESS MODEL

I. Defining Hydrologic Response Units

Since the objective of this study was to develop criteria for describing the effects of land-use change on the discharge from a drainage area, parameters changing the effect of these factors on runoff must be incorporated into any model. It is important that spatial uniqueness be maintained so that runoff contribution from a specific point in the watershed can be traced. To meet these requirements, the area was subdivided into units defined as hydrologic response units. The following section describes the vegetative-soil characteristics that were used to identify a given unit. Data from the Rocky Run Watershed (located in Brunswick County, Virginia) are used to describe the procedures.

Data contained in detailed soils and land-use maps contained the type and extent of cover, while soil maps identified soil type, erosion class, and land surface slope class. Typical land-use classifications were fallow, row crop, small grain, pasture, woods, ponds and paved area. As many classifications can be included as may be needed to describe the existing cover.

Soil maps, as mentioned above, are based on soil type, erosion class and surface slope. Often, however, soil types differ in such characteristics as color or parent material, yet have the same texture, hydrology grouping, and horizon depth. For the purposes of this model, such soil types were grouped together. Overlays of the two maps were used as guides to determine the hydrologic response unit. In using overlays it is very important that maps have the same scale. It was found beneficial to grid the maps and enter the grid points into a data file accessible by a computer. Each soil type and land use was assigned a different symbol, for example, W for woods. Grid points falling within these response areas were entered with the corresponding symbol. After these grid points have been entered into a data file, they can be manipulated easily on a computer terminal in an interactive edit mode. For example, soil type A and soil type B have similar hydrologic characteristics and should be grouped as one unit. This can be accomplished by simply redefining the symbols for A and B to a common symbol.

In addition to simplifying the process of regrouping, gridding provides a technique whereby maps with different scales can be easily compared. A transparent grid network drawn to the desired scale can be placed over the map to be rescaled. The grid data resulting from this network redefines the area coverage to the scale represented by the transparency.

After appropriate groupings are completed, computer printouts similar to Figures 1 and 2 can be obtained. Transparencies were made of computer printouts (e.g. Figures 1 and 2) for corresponding soil and land use maps, i.e., maps of the same area. These

FIGURE 1

Digitized Soils Map for Rocky Run Watershed

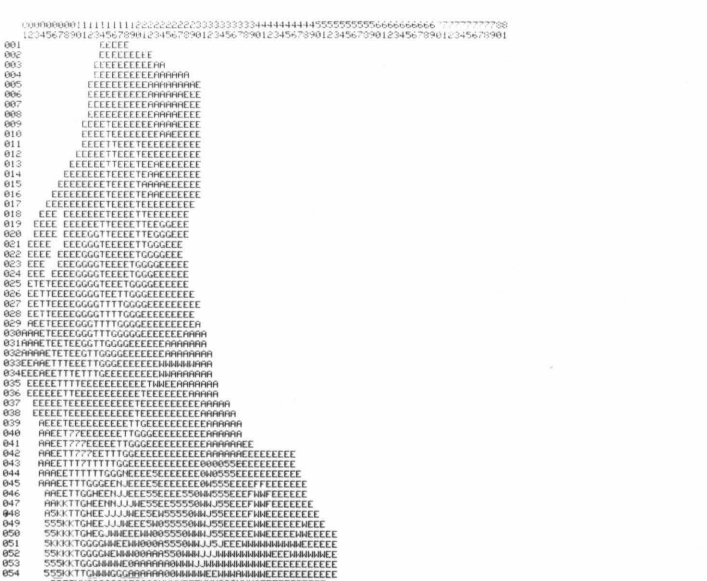

FIGURE 2

Digitized Land-Use Map for Rocky Run Watershed

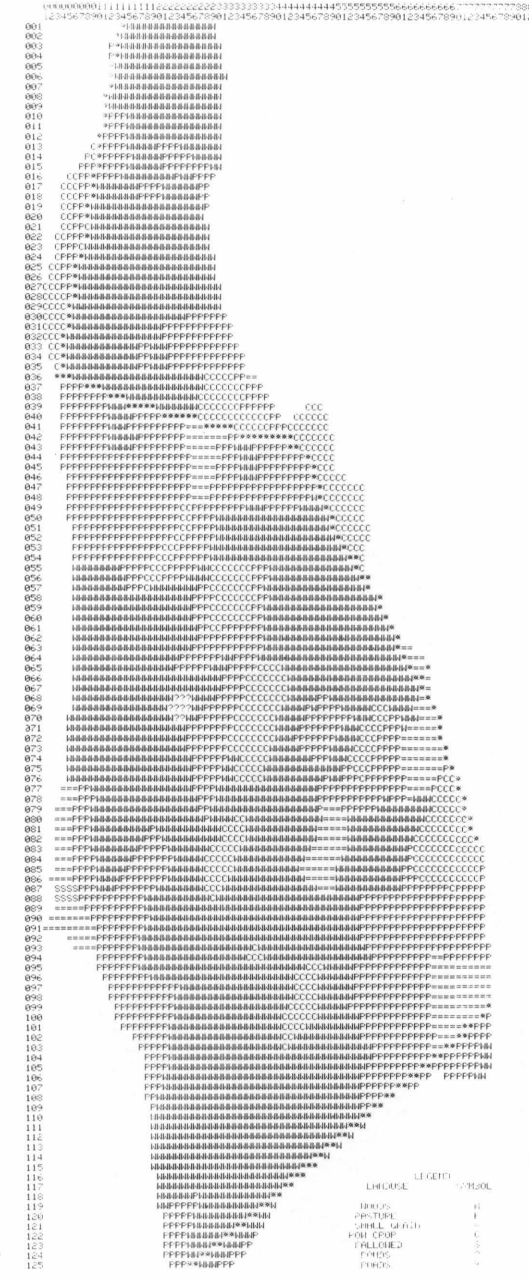

transparencies were then overlaid. Each set of soil and land-use characteristics was assigned a new symbol. The procedure is illustrated in the schematic given in Figure 3. Figure 3a represents part of a soils map with two soils, coded A and B. Figure 3b represents the corresponding land-use map of that area with three fields, woods coded as W, pasture coded as P, and small grain coded as S. Figure 3c represents an overlay of these two maps, showing new delineations based on both the soil and the land-use characteristics. For example, small grain on soil B is redefined as 5, woods on soil B is redefined as 4; the area defined as 2 is pasture on soil A. This procedure is continued until the entire area of interest is redefined. Figure 4 is the map that resulted when the soils and land use maps were combined using the above procedure. It represents the initial categorization of Rocky Run Watershed into hydrologic response units. In a later section, procedures to refine these groupings based on the results of a precipitation excess generator will be discussed.

FIGURE 3

Schematic Illustration of the Process for Determining Hydrologic Response Units

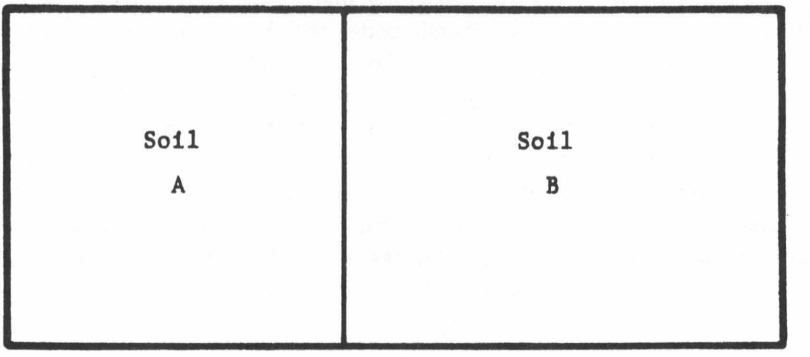

Soils map

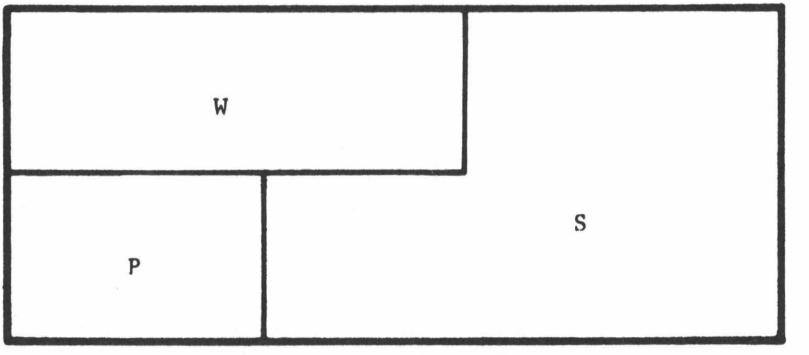

Land use map

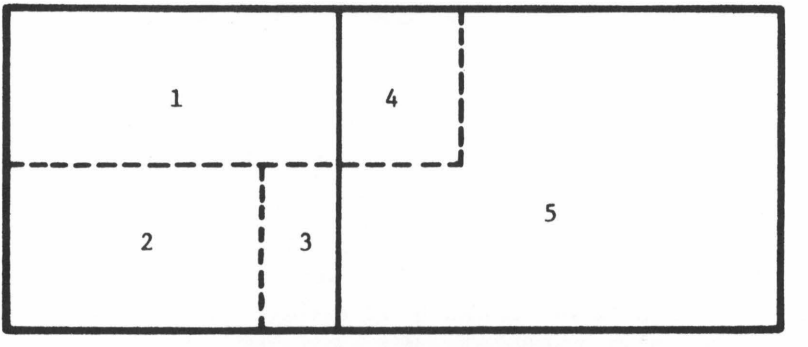

Overlay of soils and land use maps

FIGURE 4

Digitized Hydrologic Response Unit Map for Rocky Run Watershed

MODEL TO COMPUTE PRECIPITATION EXCESS

Infiltration equations developed by Mein and Larson [1971] and Holtan [1961] were selected to be used in this study. The recent work of Mein and Larson [1971] was appealing because their method attempted to define threshold conditions necessary for runoff to occur. The Holtan equation, although empirical, has obvious advantages for continuous modeling and takes into account storage recovery, vegetative cover, soil characteristics, soil moisture content, and if necessary, ponding effects. The equation has been shown to fit a wide variety of data and is easy to apply [Holtan et al, 1967]. In addition, the required parameters parallel the criteria for determining a hydrologic response unit.

The Mein and Larson equation is more difficult to apply, because the unsaturated hydraulic conductivity of the soil must be available. This presents an immediate difficulty since unsaturated hydraulic conductivities are available for a very limited number of soils and locations. In addition, unlike Holtans's equation, this method does not account for storage recovery or provide a direct way of introducing variations in vegetative cover. It does, however, define the conditions prior to and after flooding. Thus it has an advantage over methods such as the Green and Ampt equation and the Philip equation, which presuppose the presence of a ponded surface.

A study by Skaggs et al. [1978] determined a correlation coefficient for the Green and Ampt, Horton, Philip and Holtan equations. All coefficients were above 0.90 with the Holtan equation being 0.988, the Horto equation 0.987, the Philip equation 0.936, and the Green and Ampt equation 0.935. Since Mein and Larsons's equation has Darcy's Law as its basis, one would expect a correlation coefficient for that method of over 0.90, consistent with the results displayed by the Green and Ampt and Philip equations. Thus it appears that the correlation coefficients for both methods chosen would lie within an acceptable range, provided parameters for these models can be determined.

I. Model Parameters

A. Storage Capacity

Storage capacity within a soil profile is defined in this study as the percentage of pore space in a unit volume. A typical unit of soil is composed of solids and pore space. The pore space is occupied by both air and water. This breakdown is illustrated by the schematic given in Figure 5. The hygroscopic water is moisture that can be removed only by oven drying and therefore is unavailable to plants. Normally, this water is not considered in modeling because it does not enter into the evapotranspiration process. The point at which water becomes available for plant use is called the wilting point. There is a small and insignificant amount of soil water held below the wilting point and above the hygroscopic coefficient. Soil water readily available

FIGURE 5

Schematic Representation of the Volume Composition of Soil

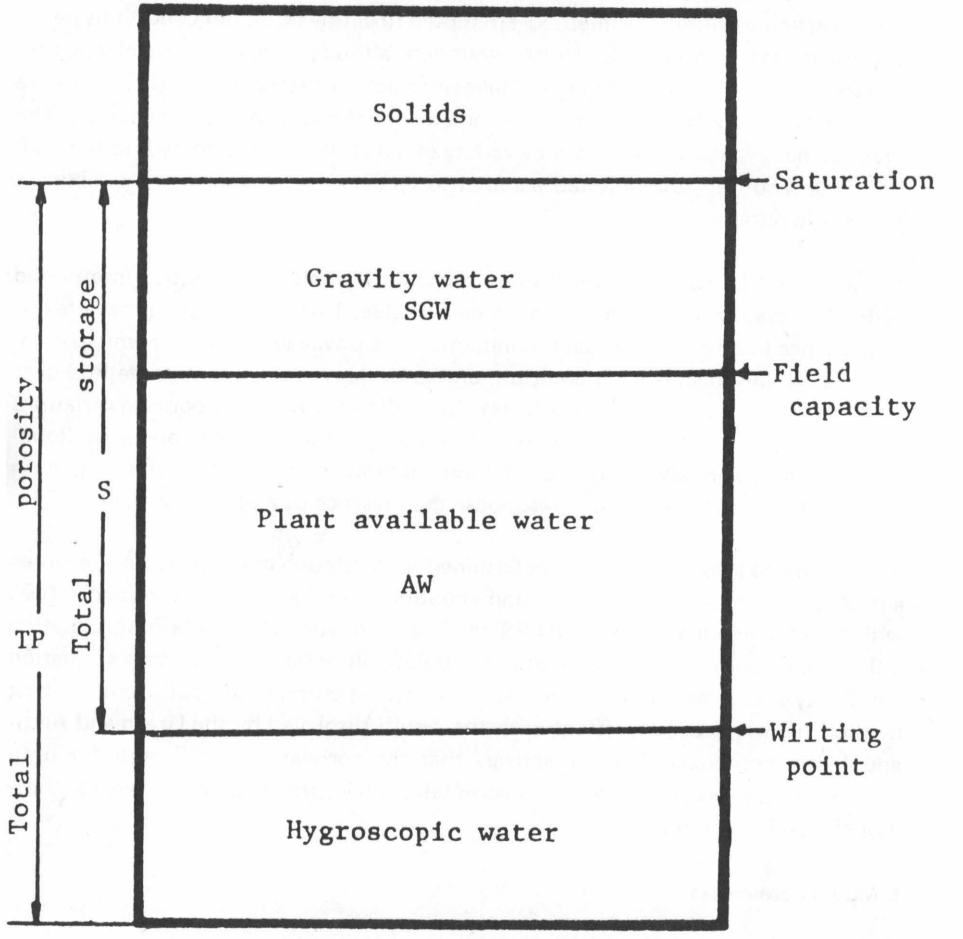

TABLE 1

Estimates by Texture of the Total Water Storage Capacity of a Soil

Soil texture	Gravity water storage (SGW) (in./in.)	Available water storage (AW) (in./in.)	Total storage (S) (in./in.)
cS	.177	.067	.244
cSL	.153	.087	.245
S	.190	.133	.323
LS	.269	.101	.370
LfS	.272	.054	.326
SL	.186	.123	.309
fSL	.235	.131	.366
vfSL	.210	.117	.327
L	.144	.156	.300
SiL	.114	.199	.313
SCL	.134	.119	.253
CL	.130	.127	.257
SiCL	.084	.149	.233
SC	.116	.078	.194
SiC	.091	.123	.214
C	.073	.115	.188

for plant use is designated as AW, and its upper limit is defined as field capacity. The remaining voids, designated SGW, when filled with water are defined as gravity water because water in these large pores is moved through the soil profile by gravitational forces. The upper limit of the volume is defined as the saturation point, or total porosity. The remaining volume consists of solids.

The potential water storage capacity for a specific soil is determined by its textural class. Both infiltration equations used in this study utilize the potential water storage capacity of the soil. Infiltration is related to the volume of unfilled pore space, i.e., pore space not containing water. If the volume of water is defined as V_w, then the volume of unfilled pore space becomes:

$$S = SGW + AW - V_w \qquad [17]$$

where:

S = total available storage per unit depth, in/in;
SWG = gravity water per unit depth, in/in, and
AW = plant available water per unit depth, in/in.

Typical volumes of S, SGW, and AW for sixteen textural classes are summarized in Table 1 [England, 1970].

TABLE 2

A Typical Soil Profile Description for an Appling Series, Gritty Sandy Loam Phase

Horizon	Depth	Description
AP	0"-5"	Yellowish-brown (10 RY 5/4) very friable gritty sandy loam; weak fine granualr structure; many small roots; strongly acid; 4 to 12 in. thick; clear smooth boundary.
B25	5"-26"	Yellowish-red (5 YR 5/6) with common medium faint mottles of yellowish-brown (10 YR 5/8) and pale brown (10 YR 6/3) friable clays; moderate medium subangular blocky structure; few small roots; distinct and continuous clay films on most peds; strongly acid; 15 to 25 in. thick; gradual wavy boundary.
B3	26"-38"	Yellowish-brown (10 YR 5/8) with common medium and distinct mottles of yellowish-red (5 YR 5/6) and pale brown (10 YR 6/3) friable clay loam; moderate medium subangular structure; thin discontinuous clay films on a few peds; strongly acid; 8 to 18 in. thick, gradual wavy boundary.
C	38"-42"	Mottles yellowish-red (5 YR 5/6), yellowish-brown (10 Yr 5/6) and red (2.5 YR 5/6 clay loam with numerous highly weathered rock fragments.

B. Soil Depth

The Holtan equation relates infiltration to the potential water storage in a finite depth. It has been shown that the depth to the first impeding horizon gives a reasonable approximation of the infiltration rate. This depth was defined by Holtan and Lopez [1971] as the depth of the A horizon. However, the Mein and Larson equation assumes a homogeneous soil with an unconfined depth. The equation was modified by the authors to provide for a finite soil depth, because most rainfall intensities were less than the saturated hydraulic conductivity and were assumed to infiltrate. The finite depth assumption proved more reasonable when using the model under the conditions of this study.

The depth of the A horizon was determined from typical profile descriptions which are normally included in a detailed soil survey. The typical profile is usually a class B slope with an erosion class 2. A typical profile description for an Appling series, gritty sand loam phase is shown in Table 2.

There will be other soils in the same series that have a different slope or erosion classification. When these are not described, the description of the typical profile can be extended, with modification, to determine the depth of the A horizon for these other

phases. For example, an Appling series—gritty sand loam phase with a D slope (10 to 15 percent)—would probably have a depth of the A horizon of four inches. If the soil is also severely eroded, the A horizon could be as shallow as three inches. The occurrance to a great extent of rock outcrops is also an indication of a shallow soil.

C. Initial Soil Moisture

The initial soil moisture content (IMC) is necessary for both models. It is required in defining the initial moisture deficit (IMD) in the Mein and Larson equation and must be known to calculate the total available storage (SWS) in the Holtan equation. The IMC is defined as the soil water content antecedent to the rainfall event minus the moisture content at wilting point. It is usually given as the percentage of total storage, SWS, and ranges between 0 and 1;

Correcting storage in the Mein and Larson equation for initial soil moisture content gives:

$$IMD = (SGW + AW) - (SGW + AW)\, IMC \qquad [18]$$

where the variables are as previously identified.

Correcting storage in the Holtan equation for IMC gives:

$$SWS = [S - (S)\,(IMC)]\, DEPTH \qquad [19]$$

D. Constants for the Mein and Larson Equation

Two constants that are needed specifically for the Mein and Larson equation include the saturated hydraulic conductivity (SKS) and the capillary potential at the wetted front (SSAV).

The saturated hydraulic conductivity is directly dependent upon soil texture, since it determines the number and size of soil capillaries [Mein and Larson, 1971]. Using the data of Holtan et al. [1968] and by arranging textural class averages of saturated hydraulic conductivities for several hundred soils on a textural triangle (Figure 6), it was noted that SKS was approximately logarithmic on the basis of percentage of clay. Combining this with a linear least squares analysis in order to fit the data to an equation resulted in the following relationship for determining saturated hydraulic conductivity based on soil texture:

$$SKS = \frac{4\,(1 - Si)}{C^2} \qquad [20]$$

where:

FIGURE 6

Illustration of the Logarithmic Characteristics of Saturated Hydraulic Conductivities as Related to Textural Class

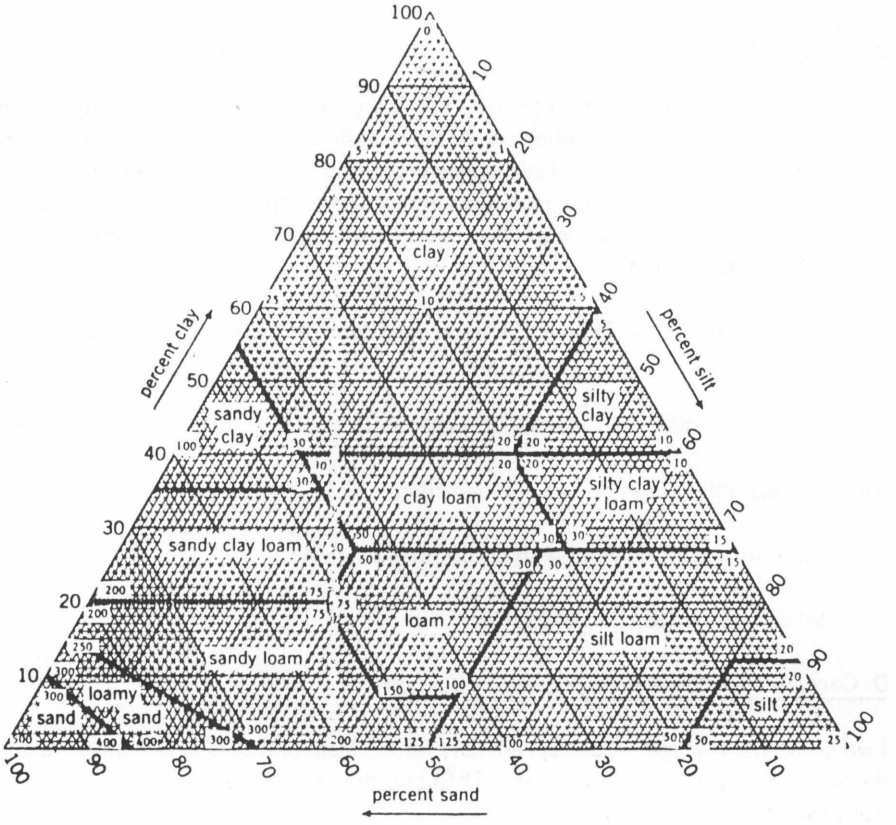

SKS = saturated hydraulic conductivity in cm/day;
Si = percent silt in the soil, expressed as a decimal, and
C = percent clay in the soil, expressed as a decimal.

The capillary potential at the wetted front (SSAV) can be represented by the area under the relative hydraulic conductivity versus soil moisture tension curve, where K_r is the ratio of unsaturated to saturated hydraulic conductivity. Data for the unsaturated hydraulic conductivity at differing moisture tensions for textural classes is usually not available and difficult to obtain under field conditions. However, as the moisture tension approaches zero, the soil approaches saturation and hence, the unsaturated hydraulic conductivity approaches the saturated hydraulic conductivity at this point for all soil textures. Therefore, one point on the curve is obtainable. (Equation 20).

FIGURE 7

Hydraulic Conductivity Versus Soil Moisture Content Relationship for Various Soil Textures

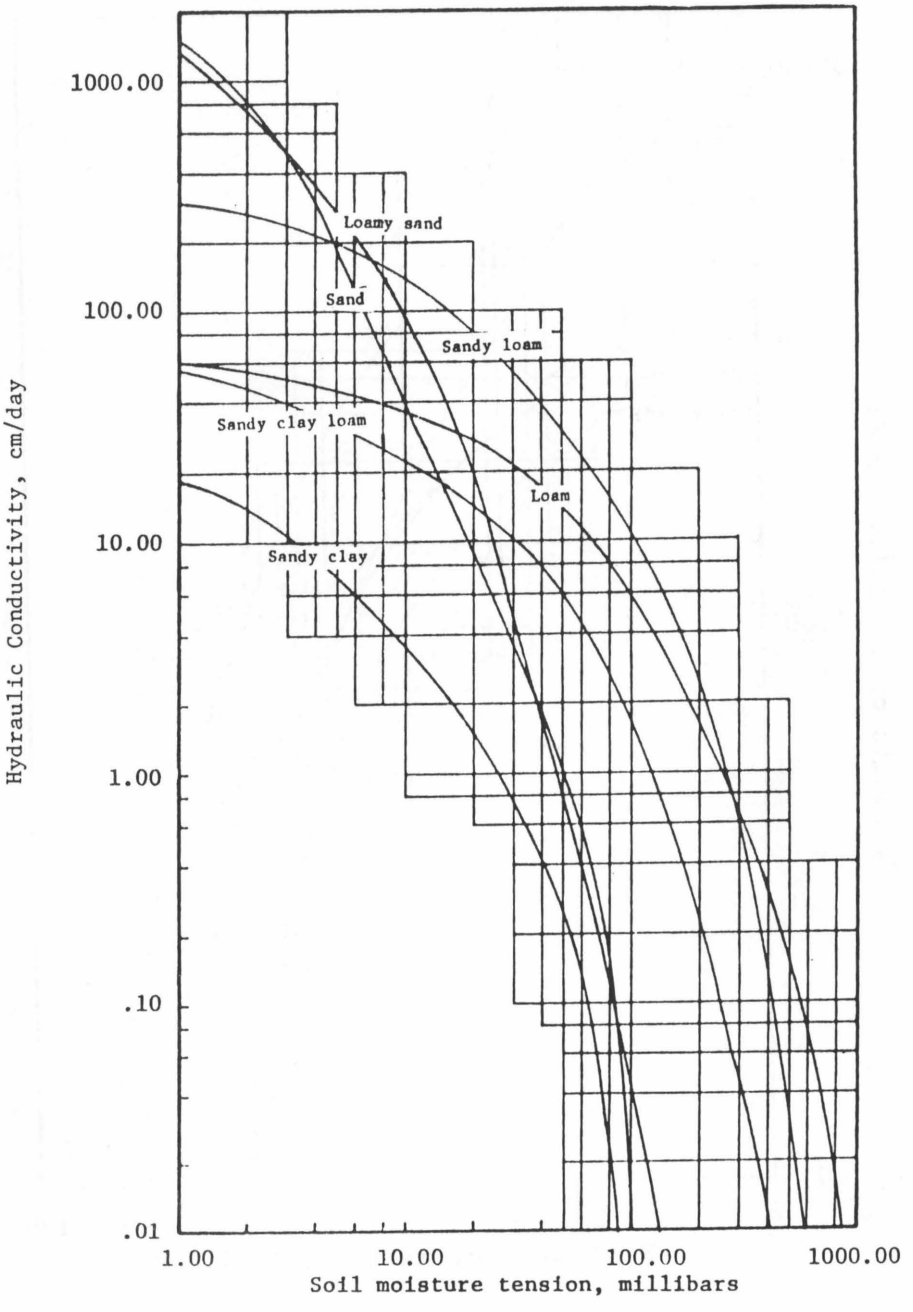

FIGURE 8

Hydraulic Conductivity Versus Soil Moisture tension Relationship for Various Soil Textures

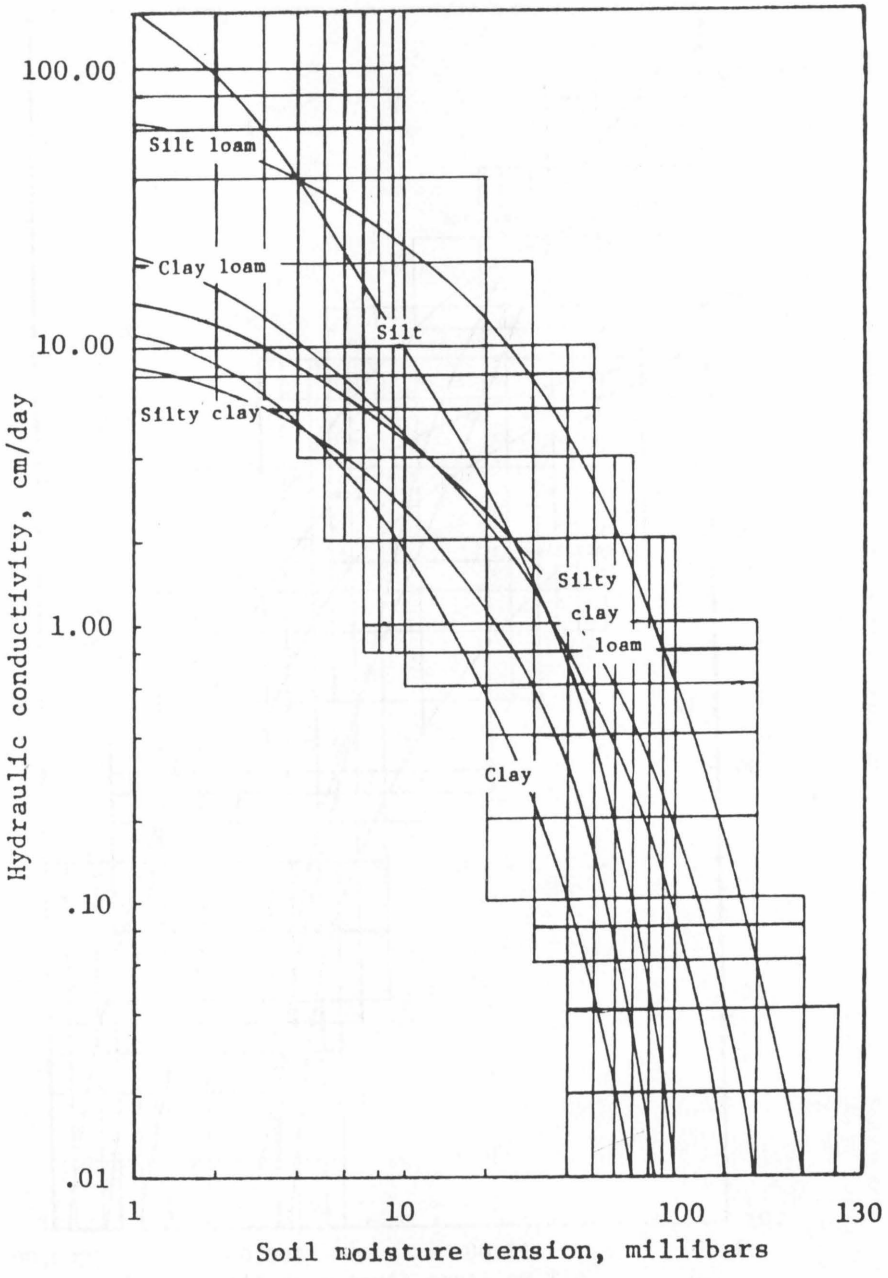

TABLE 3

Estimates Based on Soil Texture for the Saturated Hydraulic Conductivity (SKS) and Capillary Suction at the Wetting Front (SSAV) for the Mein and Larson Equation

Soil Texture	SKS (in./hr.)	SSAV (in.)
cSL	15.000	3.00
S	24.934	1.98
LS	22.310	1.00
SL	4.921	9.99
fSL	3.000	11.00
L	0.984	14.17
SiL	1.020	4.63
SCL	0.892	6.74
CL	0.348	2.96
SiCL	0.241	4.68
SC	0.308	2.37
SiC	0.144	3.32
Si	2.625	0.996
C	0.181	2.03

Further, in a study by Bouma et al. [1971], curves of soil moisture tension versus hydraulic conductivity were determined for several different textural classes. Curves were constructed for each textural class (Figures 7 and 8) using these as a guideline for their general shape and range. The curves were then transferred to coordinate paper, cut and weighed to determine the area under the curve for each textural class. As suggested by Mein and Larson [1971], only that area between K_r = 0.01-1.0 was used in determining SSAV. This is due to the difficulties in defining the curve as it approaches zero. Table 3 shows both the saturated hydraulic conductivity (Equation 20) and the capillary potential at the wetted front for fourteen classes. Values for textures involving the various sand sizes can be estimated by use of the curves from Figure 7. For example, the hydraulic conductivity of a very fine sandy loam would range somewhere between a fine sandy loam and a sandy clay loam.

E. Constants for the Holtan Equation

Three additional constants are necessary for the Holtan equation. These are the exponential constant, C, the final rate of infiltration, SFC, and the land-use factor, AH.

Although C was first thought to vary according to soil properties, it was later reported by Holtan et al. [1967] that C could be set to 1.4 with very little problem in accuracy.

TABLE 4

Estimates by Hydrology Group for the Final Rate of Infiltration, SFC, for the Holtan Equation

Hydrology Group	SFC (in./hr.)
A^+	0.450
A	0.400
A^-	0.350
B^+	0.300
B	0.250
B^-	0.200
C^+	0.150
C	0.100
C^-	0.075
D^+	0.050
D	0.025
D^-	0.001
Impervious	0.000

AH and SFC are based on properties concordant with the criteria for determining hydrologic response units. The final rate of infiltration was defined by Holtan and Lopez [1971] as a range of values for each of the hydrology groups A, B, C, and D. Analysis of available soil data by Holtan et al. [1968] enabled soils to be assigned intermediate hydrology groups. These were designated by plus and minus signs. Table 4 summarizes the SFC values for these hydrology groups.

The land use factor (AH) is given by Holtan [1961] as a range of values for a particular land use. Although his land use categorization was more detailed than that used in this study, it provided an excellent guideline for estimating the land-use factor for the hydrologic response units. For example, no distinction was made in the study between permanent pasture and temporary pasture. Table 5 shows the land-use and corresponding values for parameter AH (Holtan equation) used in the model development.

F. Evapotranspiration

Evapotranspiration is not normally considered as a parameter or constant in hydrologic models. In this study, however, emphasis is focused on modeling single storm periods capable of causing severe flooding. Evapotranspiration will not significantly affect streamflow generation during these types of events, simply because rates are very low.

TABLE 5

Estimates of the Vegetative Parameter, AH, for the Holtan Equation

Land Use	Vegetative Parameter (AH)
Impervious	0.00
Fallow	0.20
Row crops	0.20
Small grains	0.30
Pasture	0.60
Woods	1.00

For the purpose of this study evapotranspiration is entered as a constant with units of in/day. It is assumed to be zero during rain periods and between the hours of 6:00 p.m. to 6:00 a.m.

The Mein and Larson equation has no provision for infiltration recovery due to losses by evapotranspiration. The Holtan equation, however, provides an effective procedure for increasing infiltration potential because infiltration rate can be considered as a function of remaining soil water storage.

Evapotranspiration is assumed to prevail at the potential or maximum rate when the soil moisture is greater than or equal to field capacity. The unfilled pore space is adjusted according to the relationship:

$$SWS = SWS + \frac{ET}{12.0}(TINC) \qquad [21]$$

where:

ET = the evapotranspiration rate, in/day, and
TINC = duration of the period of no rainfall in hours.

However, when soil water content is less than field capacity, the actual evapotranspiration rate was assumed to be proportional to the ratio AWC/S.

The storage remaining was adjusted by the expression:

$$SWS = SWS + AWC/S\ (\frac{ET}{12.0})\ (TINC) \qquad [22]$$

The evapotranspiration rate varies with the location of the watershed and the time of year in which the storm occurs. The higher the evapotranspiration rate, the greater the storage recovery provided the storm conditions are conducive to evapotranspiration.

II. Computer Model

A computer program was developed to determine precipitation excess by hydrologic response units when rainfall, evapotranspiration, and program control cards are given as input. Computations were performed for each period during which the rainfall intensity was constant. These intervals were defined as a storm event. The basic procedure is essentially a moisture accounting technique whereby infiltration during any time interval is subtracted from the available storage. The procedure is repeated for each storm event. Infiltration can be determined by either the Mein and Larson or Holtan equation.

During the development of the model the following assumptions were made:

1. Homogeneity of the upper horizon: Although an actual soil profile is never homogeneous, for the purposes of modeling, the upper horizon is assumed to be homogeneous.
2. Evapotranspiration: It was assumed that water loss due to evapotranspiration was insignificant at night and during rain periods.
3. Depressional storage: Since the effect of water storage in surface depressions during a storm of large magnitude will be negligible compared to total amount of excess, it was not included in the model.
4. Plant interception: The effect of rainfall interception by the leaves of plants is also negligible during storms of large magnitude, and was not included in the model.
5. Sealing of the soil: Certain types of soils, particularly certain clays, expand when wetted, thus sealing the surface of the soil and making it somewhat impervious to infiltration. Although this is partially accounted for by the textural and hydrologic classifications, it is not directly accounted for by the model.
6. Model is worked in discrete time steps: Calculations for precipitation excess were performed assuming that the rainfall intensity during a time step was constant and that the infiltration taking place did not affect the available storage until the end of that time step.

A. Program Design

The computer program for this model was written in subroutines for ease in understanding and to allow future modifications to be accomplished without major changes in the entire program. The function of each subroutine is briefly discussed below.

B. Subroutines

1. Subroutine MAIN: Precipitation data and program control data are entered by this subroutine.

2. Subroutine PRECIP collects the constants necessary for the two infiltration models, passes them to the subroutines XMEIN and HOLTAN, summarizes and prints the results of the calculations.

3. Subroutine XMEIN calculates the precipitation excess for each storm event for all response units using the Mein and Larson equation.

4. Subroutine HOLTAN calculates the precipitation excess for each storm event for all response units using the Holtan equation.

5. Subroutine TOPLOT plots recorded data and accumulated simulated precipitation excess versus time. The plots are optional with the option coded by the user on the program control data card discussed in a later section on input.

6. Subroutine SOILS: The user must supply data for SKS, SSAV, DEPTH, AWC, GW, and SFC for each hydrologic response unit through this subroutine. The data are arranged in Fortran DATA statements. Each variable must be dimensioned in a Fortran DIMENSION statement, with the dimensional equal to the number of hydrologic response units.

A worksheet simplifies the process of determining this information. After the hydrologic response units are determined, the basic information, soil texture, land use, hydrology group, and depth of the A horizon, can be entered on the worksheet (Table 6) and the appropriate constants determined from Tables 1, 3, 4, and 5. After the worksheet is completed, DATA statements can be keypunched directly from the worksheet. The first value in each DATA will be the value of that constant for the first hydrologic response unit, the second value for the second hydrologic response unit, and so on.

III. Parameter Adjustment

The initial moisture content and land use parameters can be used to adjust the model to obtain a better match between simulated and actual flows. The values given for these parameters in initial computer runs can later be revised to try to fit the simulated to the recorded data. The plots generated must be studied, adjusted, and the program re-run until the match between recorded and simulated flow is acceptable.

A. Initial Soil Moisture Content (SMC)

Adjustment of the initial soil moisture content will affect the simulated excess values obtained by both infiltration models. The effect is greater with the Holtan equation since it bases storage on the entire depth of the first horizon. Therefore, by observing the plots of the simulated data from the Holtan equation in relation to the recorded data, the adjustment of the initial soil moisture content can be estimated. If the simulated curves for all response units show excess accumulation in advance of the recorded

TABLE 6

A Summary of the Soil and Vegetative Characteristics for Each Hydrologic Response Unit for Rocky Run Watershed

Map unit	Soil texture	HG	Land use	HRU No.	Depth	SFC	AH	AW	SGW	SKS	SSAV	Map Symbol
25B2	c/SL	B^+	woods	1	5.0	0.3	1.0	0.087	0.158	15.0	3.0	E
25B2	c/SL	B^+	pasture	2	5.0	0.3	0.6	0.087	0.158	15.0	3.0	e
25B2	c/SL	B^+	row crop	3	5.0	0.3	0.2	0.087	0.158	15.0	3.0	1
25B2	c/SL	B^+	small grain	4	5.0	0.3	0.3	0.087	0.158	15.0	3.0	°
49B2	c/SL	B^+	woods	5	7.5	0.3	1.0	0.087	0.158	15.0	3.0	A
49B2	c/SL	B^+	pasture	6	7.5	0.3	0.6	0.087	0.158	15.0	3.0	a
49B2	c/SL	B^+	row crop	7	7.5	0.3	0.2	0.087	0.158	15.0	3.0	2
49B2	c/SL	B^+	small grain	8	7.5	0.3	0.3	0.087	0.158	15.0	3.0	,
49B2	c/SL	B^+	fallow	9	7.5	0.3	0.2	0.087	0.158	15.0	3.0	<
49C2	c/SL	B^+	woods	10	6.0	0.3	1.0	0.087	0.158	15.0	3.0	B
49C2	c/SL	B^+	pasture	11	6.0	0.3	0.6	0.087	0.158	15.0	3.0	b
49C2	c/SL	B^+	small grain	12	6.0	0.3	0.3	0.087	0.158	15.0	3.0	;
49D2	c/SL	B^+	woods	13	5.0	0.3	1.0	0.087	0.158	15.0	3.0	C
49D2	c/SL	B^+	pasture	14	5.0	0.3	0.6	0.087	0.158	15.0	3.0	c
49D2	c/SL	B^+	row crop	15	5.0	0.3	0.2	0.087	0.158	15.0	3.0	3
49D2	c/SL	B^+	small grain	16	5.0	0.3	0.3	0.087	0.158	15.0	3.0	1
25B1	c/SL	B^+	woods	17	10.5	0.3	1.0	0.087	0.158	15.0	3.0	D
25B1	c/SL	B^+	pasture	18	10.5	0.3	0.6	0.087	0.158	15.0	3.0	d
25B1	c/SL	B^+	row crop	19	10.5	0.3	0.2	0.087	0.158	15.0	3.0	4
25B3	SCL	B	pasture	20	4.0	0.25	0.6	0.119	0.134	0.992	6.74	f
25C2	c/SL	B	woods	21	4.0	0.3	1.0	0.087	0.158	15.0	3.0	G
25C2	c/SL	B^+	pasture	22	4.0	0.3	0.6	0.087	0.158	15.0	3.0	g
25C2	c/SL	B^+	row crop	23	4.0	0.3	0.2	0.087	0.158	15.0	3.0	5
25C2	c/SL	B^+	small grain	24	4.0	0.3	0.3	0.087	0.158	15.0	3.0	?
25D2	c/SL	B^+	woods	25	3.0	0.3	1.0	0.087	0.158	15.0	3.0	H

25D2	c/SL	B^+	pasture	26	3.0	0.3	0.6	0.087	0.158	15.0	3.0	h
30C3	CL	B^-	woods	27	15.0	0.2	1.0	0.127	0.13	0.348	2.96	J
30C3	CL	B^-	pasture	28	15.0	0.2	0.6	0.127	0.13	0.348	2.96	j
30D3	CL	B^-	pasture	29	10.5	0.2	0.6	0.127	0.13	0.348	2.96	K
31B1	c/SL	B^+	woods	30	7.5	0.3	1.0	0.087	0.158	15.0	3.0	L
31B1	c/SL	B^+	pasture	31	7.5	0.3	0.6	0.087	0.158	15.0	3.0	I
31E1	c/SL	B^+	woods	32	7.5	0.3	1.0	0.087	0.158	15.0	3.0	M
26B3	CL	B^-	pasture	33	7.5	0.2	0.6	0.127	0.13	0.348	2.96	n
26D3	CL	B^-	woods	34	4.0	0.2	1.0	0.127	0.13	0.348	2.96	P
1A1	f/SL	D	woods	35	15.0	0.025	1.0	0.131	0.235	3.0	11.0	S
1A1	f/SL	D	row crop	36	15.0	0.025	0.2	0.131	0.235	3.0	11.0	6
10B1	f/SL	D	woods	37	15.0	0.025	1.0	0.131	0.235	3.0	11.0	T
10B1	f/SL	D	pasture	38	15.0	0.025	0.6	0.131	0.235	3.0	11.9	t
10B1	f/SL	D	row crop	39	15.0	0.025	0.2	0.131	0.235	3.0	11.9	7
8B1	c/SL	C^+	woods	40	15.0	0.15	1.0	0.087	0.158	15.0	3.0	W
3B1	c/SL	C^+	pasture	41	15.0	0.15	0.6	0.087	0.158	15.0	3.0	w
8B1	c/SL	C^+	row crop	42	15.0	0.15	0.2	0.087	0.158	15.0	3.0	8
8B1	c/SL	C^+	small grain	43	15.0	0.15	0.3	0.087	0.158	15.0	3.0	(
8B1	c/SL	C^+	fallow	44	15.0	0.15	0.2	0.087	0.158	15.0	3.0	=
26C3	CL	B^-	woods	45	5.0	0.20	1.0	0.127	0.13	0.348	2.96	X
26C3	CL	B^-	pasture	46	5.0	0.20	0.6	0.127	0.13	0.348	2.96	x
26C3	CL	B^-	row crop	47	5.0	0.20	0.2	0.127	0.13	0.348	2.96	9
30B3	CL	B^-	woods	48	15.0	0.20	1.0	0.127	0.13	0.348	2.96	Y
30B3	CL	B^-	pasture	49	15.0	0.20	0.6	0.124	0.13	0.348	2.96	y
30B3	CL	B	row crop	50	15.0	0.20	0.2	0.127	0.13	0.348	2.96	θ
30B3	CL	B^-	small grain	51	15.0	0.20	0.3	0.127	0.13	0.348	2.96	''
25C3	SCL	B	woods	52	3.0	0.25	1.0	0.119	0.134	0.892	6.74	Z
25C3	SCL	B	pasture	53	3.0	0.25	0.6	0.119	0.134	0.892	6.74	z
—	—	—	road	54	0.0	0.0	0.0	0.0	0.0	0.0	0.0	*
—	—	—	pond	55	0.0	0.0	0.0	0.0	0.0	0.0	0.0	+

curves, the initial moisture content is too high. This is because the initial soil moisture content determines the amount of storage remaining. If the initial soil moisture content is too high, too much of the storage will be modeled as occupied by water at the beginning of the storm, and too little storage will be modeled as available for infiltration. Generated precipitation excess will then begin sooner than the recorded data show.

It should be noted that since recorded data consists of flow from the entire watershed, a time lag between simulated and recorded curves approximately equal to the watershed time of concentration would be expected. The excess generated for a point is immediately apparent, however, the response is not noted at downstream locations until a later time. A technique for obtaining time lag is discussed in succeeding sections.

B. Land Use (AH)

Adjusting the land use factor will not affect the excess generated by the Mein and Larson equation, since this parameter is not considered in determining precipitation excess. It does, however, greatly affect the excess generated by the Holtan equation.

Increasing AH for any given land use classification will decrease the amount of excess produced. The final value for the land use parameter, however, must lie between 0 for a completely impervious area, and 1 for a completely pervious region.

IV. Regrouping Hydrologic Response Data

Once the model has been calibrated and precipitation excess generated for each hydrologic unit, units producing similar excess values should be grouped together. Parameters for the new response units can be taken as the parameters of any of the units included in the new grouping.

The excess precipitation for all hydrologic response units approaches the total rainfall as the magnitude and duration of the storm increases and because the storage approaches zero. Therefore, if the regrouping is based on a storm of relatively small magnitude and intensity, it should be the same as that for a storm of larger intensity and duration.

V. Ranking Response Units

Similar units can be grouped together, since a hydrologic response unit was previously defined as an area which responds similarly to a given rainfall input. If this grouping could be predicted, much of the initial effort needed to define these units could be eliminated. Therefore, an attempt was made to find an equation which would predict the relative amounts of excess for each response unit.

The data used to produce this equation was generated using storm data from the Rocky Run Watershed. The initial moisture content was taken to be 99 percent and the evapotranspiration rate as 0.20 inches per day. The hydrologic response units are shown ranked in ascending order according to simulated precipitation excess (Table 7). After many trials the following equation was developed:

$$C = \left(\frac{ALU}{6} + \frac{D}{5ALU}\right)\left(2.0 - \frac{AW}{SWS}\right)^{2.8} + HG + \left(\frac{AW^{2.5}}{11SWS}\right) \qquad [23]$$

where:

ALU = a land use factor;
HG = a hydrology group factor;
AW = available water based on soil texture;
SWS = total storage based on soil texture;
C = rank of hydrologic response unit (increasing C indicates higher excess),
D = depth of the A horizon.

This equation gave an acceptable ranking for the hydrologic response units given in Table 7. However, the storm-to-storm variation of total rainfall, evapotranspiration rate, and initial soil moisture content is not considered. Therefore, the equation needs further testing, which is being undertaken in a separate study, to validate its practical usefulness. The equation does show, however, that the four characteristics used to develop the hydrologic response units do not interact in a linear fashion, but rather in a highly complex manner which illustrates the difficulty of problems encountered in developing reliable mathematical models.

VI. Comparison of Two Infiltration Models

Five storm periods were chosen from the Rocky Run record, including the dates of 7/10/70, 7/21/70, 10/22/71, 6/20/72, and 10/5/72. These storms were major events and were selected for an evaluation of the model because it was structured to predict excess precipitation during potential flood producting storms.

Excess of precipitation was computed for 54 response units described in previous sections. A summary of the results are given in Table 8. A survey of these data show that excess estimates range from zero on some response units to several inches on other units during most storms. These results obviously illustrate the variability of response over a drainage area.

These data also illustrate that significantly different results were obtained from the two infiltration equations. For most response units, the amount of excess generated by the Mein and Larson equation was equal to or greater than that of the Holtan equation. However, there were several units where the reverse was true, for example, see the results from storms 1 and 2, response unit 19, in Table 8.

TABLE 7

Hydrologic Response Units Ranked in Ascending Order Based on Total Precipitation Excess Predicted by the Holton Equation

HRU	Texture	Hydrology group	Depth of "A" horizon	Land use	% area	Total excess	Weighted excess
37	fSL	D	15.0	Woods	0.0304	0.00010	0.0000
35	fSL	D	15.0	Woods	0.0235	0.00010	0.0000
38	fSL	D	15.0	Row crop	0.0085	0.20210	0.0017
40	cSL	C^+	15.0	Woods	0.0356	0.33157	0.0118
27	CL	B^-	15.0	Woods	0.0015	0.53363	0.0008
48	CL	B^-	15.0	Woods	0.0048	0.53363	0.0026
41	cSL	C^+	15.0	Pasture	0.0289	0.61281	0.0177
17	cSL	B^+	10.5	Woods	0.0033	0.65800	0.0022
28	CL	B^-	15.0	Pasture	0.0032	0.76577	0.0024
49	CL	B^-	15.0	Pasture	0.0074	0.76577	0.0057
18	cSL	B^+	10.5	Pasture	0.0007	0.85114	0.0006
36	fSL	D	15.0	Row crop	0.0022	0.89783	0.0020
39	fSL	D	15.0	Row crop	0.0004	0.89783	0.0003
5	cSL	B^+	7.5	Woods	0.1016	0.92012	0.0935
30	cSL	B^+	7.5	Woods	0.0007	0.92012	0.0006
32	cSL	B^+	7.5	Woods	0.0043	0.92012	0.0039
43	cSL	C^+	15.0	Small grain	0.0035	0.94891	0.0033
29	CL	B^-	10.5	Pasture	0.0039	1.02979	0.0040
10	cSL	B^+	6.0	Woods	0.0120	1.04908	0.0126
51	CL	B^-	15.0	Small grain	0.0017	1.05518	0.0018
31	cSL	B^+	7.5	Pasture	0.0009	1.05528	0.0010
6	cSL	B^+	7.5	Pasture	0.0943	1.05528	0.0995
1	cSL	B^+	5.0	Woods	0.1903	1.13295	0.2156
13	cSL	B^+	5.0	Woods	0.0296	1.13295	0.0336
44	cSL	C^+	15.0	Fallow	0.0004	1.13436	0.0004

TABLE 7 (continued)

HRU	Texture	Hydrology group	Depth of "A" horizon	Land use	% area	Total excess	Weighted excess
42	cSL	C^+	15.0	Row crop	0.0026	1.13436	0.0029
11	cSL	B^+	6.0	Pasture	0.0104	1.16885	0.0121
50	CL	B^-	15.0	Row crop	0.0006	1.20815	0.0007
19	cSL	B^+	10.5	Row crop	0.0015	1.20975	0.0018
33	CL	B^-	7.5	Pasture	0.0022	1.21804	0.0027
21	cSL	B^+	4.0	Woods	0.1110	1.22483	0.1359
2	cSL	B^+	5.0	Pasture	0.0730	1.24053	0.0906
14	cSL	B^+	5.0	Pasture	0.0007	1.24053	0.0009
8	cSL	B^+	7.5	Small grain	0.0328	1.24114	0.0407
45	CL	B^-	5.0	Woods	0.0015	1.28392	0.0019
22	cSL	B^+	4.0	Pasture	0.0264	1.30891	0.0347
12	cSL	B^+	6.0	Small grain	0.0002	1.31022	0.0002
25	cSL	B^+	3.0	Woods	0.0145	1.31081	0.0189
9	cSL	B^+	7.5	Fallow	0.0015	1.31912	0.0020
7	cSL	B^+	7.5	Row crop	0.0334	1.31912	0.0441
4	cSL	B^+	5.0	Small grain	0.0073	1.35371	0.0099
16	cSL	B^+	5.0	Small grain	0.0004	1.35371	0.0005
34	CL	B^-	4.0	Woods	0.0063	1.36600	0.0086
26	cSL	B^+	3.0	Pasture	0.0006	1.37420	0.0008
46	CL	B^-	5.0	Pasture	0.0041	1.37720	0.0056
20	SCL	B	4.0	Pasture	0.0013	1.39079	0.0018
52	SCL	B	3.0	Woods	0.0002	1.39499	0.0003
24	cSL	B^+	4.0	Small grain	0.0030	1.39909	0.0041
3	cSL	B^+	5.0	Row crop	0.0402	1.40499	0.0000
15	cSL	B^+	5.0	Row crop	0.0019	1.40499	0.0026
23	cSL	B^+	4.0	Row crop	0.0007	1.43828	0.0011
53	SCL	B	3.0	Pasture	0.0015	1.45198	0.0022
47	CL	B^-	5.0	Row crop	0.0004	1.53736	0.0006
74	–	–	–	Paved	0.0252	2.07000	0.0522

TABLE 8

Comparison of Precipitation Excess Generated by Two Infiltration Models by Hydrologic Response Unit for Five Storm Periods

	Storm 1 7/10/70 P_e		Storm 2 7/21/70 P_e		Storm 3 10/22/71 P_e		Storm 4 6/20/72 P_e		Storm 5 10/5/72 P_e	
HRU	Mein	Holtan	Mein	Holtan	Mein	Holtan	Mein	Holtan	Mein	Holtan
1	0.9535	1.0684	3.4939	2.8354	3.1855	0.7315	5.0550	4.2553	7.9643	6.4342
2	0.9535	1.1857	3.4939	2.8354	3.1355	0.8921	5.0450	4.2734	7.9643	6.4430
3	0.9535	1.3784	3.4939	2.8826	3.1855	1.1336	5.0450	4.2931	7.9643	6.4523
4	0.9535	1.3207	3.4939	2.8354	3.1355	1.1321	5.0450	4.2878	7.9643	6.4498
5	0.3954	0.7545	2.9358	2.2773	2.6383	0.5079	4.5630	3.9690	7.4714	5.9413
6	0.3954	0.9366	2.9358	2.3174	2.6383	0.6865	4.5630	3.9690	7.4714	5.9501
7	0.3954	1.2556	2.9358	2.6379	2.6383	0.9082	4.5630	3.9690	7.4714	6.1779
8	0.3954	1.1530	2.9358	2.5119	2.6383	0.8999	4.5630	3.9690	7.4714	6.0755
9	0.3954	1.2556	2.9358	2.6379	2.6383	0.9082	4.5630	3.9690	7.4714	6.1779
10	0.7302	0.9489	3.2707	2.6122	2.9666	0.5478	4.8522	4.2011	7.7671	6.2371
11	0.7302	1.0805	3.2707	2.6122	2.9666	0.7388	4.8522	4.2357	7.7671	6.2459
12	0.7302	1.2565	3.2707	2.6967	2.9666	1.0282	4.8522	4.2382	7.7671	6.2932
13	0.9535	1.0684	3.4939	2.8354	3.1855	0.7315	0.0450	4.2553	7.9643	6.4342
14	0.9535	1.1857	3.4939	2.8354	3.1855	0.8921	5.0450	4.2734	7.9643	6.4430
15	0.9535	1.3784	3.4939	2.8826	3.1855	1.1336	5.0450	4.2931	7.9643	6.4523
16	0.9535	1.3207	3.4939	2.8354	3.1855	1.1321	5.0450	4.2878	7.9643	6.4498
17	0.0000	0.4002	2.2661	1.6329	1.9816	0.4645	3.9846	3.3907	6.8799	5.3499
18	0.0000	0.6503	2.2661	1.8236	1.9816	0.4784	3.9846	3.3907	6.8799	5.4737
19	0.0000	1.0987	2.2661	2.3318	1.9816	0.5219	3.9846	3.3907	6.8799	5.7330
20	1.1767	1.3216	3.7162	3.0587	3.4108	1.7725	5.2826	4.4439	8.1998	6.8294
21	1.1767	1.1925	3.7172	3.0587	3.4044	0.9989	5.2378	4.2773	8.1614	6.6314
22	1.1767	1.2844	3.7172	3.0587	3.4044	1.1566	5.2378	4.2877	8.1614	6.6402
23	1.1767	1.4263	3.7172	3.0587	3.4044	1.3525	5.2378	4.3024	8.1614	6.6495

24	1.1767	1.3829	3.7172	3.0587	3.4044	1.3525	5.2378	4.2970	8.1614	6.6470
25	1.4000	1.3141	3.9404	3.2101	3.6233	1.1165	5.4306	4.2773	8.3586	6.8385
26	1.4000	1.3768	3.9404	3.2459	3.6233	1.2742	5.4306	4.2877	8.3586	6.8373
27	0.3053	0.0303	1.2314	0.8929	0.9965	0.6000	3.2970	2.8544	6.1428	4.9742
28	0.3053	0.2727	1.2314	1.1989	0.9965	0.6002	3.2970	2.8544	6.1428	5.1500
29	0.3393	0.6830	2.2451	1.9108	1.9816	0.7916	4.1106	3.6680	6.9849	5.8870
30	0.3954	0.7645	2.9358	2.2773	2.6383	0.5079	4.5630	3.9690	7.4714	5.9413
31	0.3954	0.9366	2.9358	2.3174	2.6383	0.6865	4.5630	3.9690	7.4714	5.9501
32	0.3954	0.7645	2.9358	2.2773	2.6383	0.5079	4.5630	3.9690	7.4714	5.9513
33	0.3979	0.9816	2.9208	2.4268	2.6383	1.3841	1.3841	4.2104	7.5464	6.4369
34	1.1687	1.2556	3.7092	3.0773	3.4044	2.0031	5.2858	4.5493	8.2014	6.9995
35	0.0000	0.0000	0.0000	0.1040	0.0000	0.0000	1.6981	1.5872	4.5408	4.3520
36	0.0000	0.5970	0.0000	1.4741	0.0000	0.1608	1.6981	2.363	4.5408	4.6613
37	0.0000	0.0000	0.0000	0.1040	0.0000	0.0000	1.6981	1.5872	4.5408	4.3520
38	0.0000	0.0000	0.0000	0.3935	0.0000	0.0025	1.6981	1.6713	4.5408	4.3532
39	0.0000	0.5970	0.0000	1.4741	0.0000	0.1608	1.6981	2.3363	4.5408	4.6613
40	0.0000	0.0436	1.2614	0.9398	0.9965	0.6420	3.1170	2.7886	5.9928	4.9767
41	0.0000	0.2950	1.2614	1.2548	0.9965	0.6465	3.1170	2.7886	5.9928	5.0923
42	0.0000	0.9237	1.2614	2.0895	0.9965	0.6456	3.1170	3.0403	5.9928	5.3076
43	0.0000	0.7122	1.2614	1.7865	0.9965	0.6465	3.1039	2.9061	5.9928	5.1081
44	0.0000	0.9237	1.2614	2.0895	0.9956	0.6465	3.1170	3.0403	5.9928	5.3076
45	0.9435	1.1134	3.4839	2.8521	3.1855	1.7842	5.1050	4.5216	8.0143	6.8124
46	0.9435	1.2456	3.4839	2.821	3.1855	1.8122	5.1050	4.5402	8.0143	6.8714
47	0.9435	1.4679	3.4839	3.0734	3.1855	1.8255	5.1050	4.5683	8.0148	6.9197
48	0.3053	0.0303	1.2314	0.8929	0.9965	0.6000	3.2970	2.8544	6.1428	4.9742
49	0.3053	0.2727	1.2314	1.1989	0.9965	0.6002	3.2970	2.8544	6.1428	5.1500
50	0.3053	0.8871	1.2314	2.0218	0.9965	0.6465	3.2970	3.0444	6.1428	5.1750
51	0.3053	0.6811	1.2314	1.7201	0.9965	0.6266	3.2670	2.9483	6.1428	5.1713
52	1.4000	1.3606	3.9404	3.2423	3.6281	1.9073	5.4542	4.4337	8.3874	7.0104
53	1.4000	1.4233	3.9404	3.2819	3.6281	1.9119	5.4542	4.4525	8.3874	7.0170
54	2.0700	2.0700	4.6101	4.6101	4.2800	4.2800	6.0090	6.0090	8.9500	8.9500

In addition, it would appear that the results from the Mein and Larson equation are more uniform. This is because this equation does not explicitly acccount for either depth of the A horizon or land use. Therefore, the hydrologic response units for the Mein and Larson model are solely a function of soil texture. Hence, when soil depth and land use become unimportant in relation to the soil texture, the results from both models will, in general, be similar; see, for example, response unit 28, Table 8. However, when the textural properties of the soil are the limiting factor, the excess from the Holtan model will be higher if the soil depth is shallow and the land use factor AH is high. This is shown very clearly in Table 8, storm 2, response units 47 and 27, respectively.

Rainfall intensity is a very critical factor. If the storm is of high intensity, the soil depth and land use play a much lesser role than does the soil texture. This can be illustrated by referring again to response unit 19, storm 5, in Table 8 where the excess obtained by using the Mein and Larson equation exceeded that of the Holtan equation because storm intensities were much higher than storms 1 and 2. The Mein and Larson equation is a direct function of the soil's hydraulic conductivity and consequently is highly sensitive to the rainfall rates. Again, the complexity of the interactions among the four characteristics used to define the hydrologic response units and storm intensity clearly illustrates the problems encountered in hydrologic modeling.

VII. Comparison of Recorded and Simulated Runoff

The excess precipitation data for each element must be routed to an outlet point of interest (e.g., gaging stations) before a valid evaluation between recorded and simulated discharge can be made. However, a rough approximation can be obtained from the relationship:

$$Q_W = \sum_{i=1}^{n} \frac{A_i}{A_T} P_i \qquad [24]$$

where:

- n = number of hydrologic response units;
- A_i = area of the ith hydrologic response unit;
- A_T = area of the watershed;
- P = precipitation excess for the ith hydrologic response unit, and
- Q_W = accumulated weighted discharge.

Base flow and interflow must be separated from the recorded discharge hydrograph and the resultant surface flow must be separated into precipitation excess for each hydrologic response unit before the recorded data can be compared to the simulated precipitation excess.

Surface flow was separated from the total hydrograph following procedures outlined by Barnes [1940], as illustrated in Figure 9. Partitioning the surface flow to represent contributions by individual response units cannot be accomplished from the recorded flow sequence. Therefore, comparisons must be made based on a sum of the simulated excess precipitation from each response unit and the recorded hydrograph. An approximation is given by Equation 24; however, valid interpretation of the influence of each response unit can only be made by routing the flows from their point of origin to the gaging station. Examples will be given in a later applications section.

Accumulated simulated and corresponding recorded discharge are compared in Appendix E for two response units and five major storms. Results are presented for both the Mein and Larson and Holtan infiltration model. Note that the accumulated excess precedes recorded data, because the excess precipitation has not been adjusted for lag time.

The total accumulation provides some guideline as to how well the model is predicting flow volume. If the entire watershed consisted of the indicated response unit, then the recorded and simulated curves should match within some predefined error range. Otherwise, the weighted contribution from all elements must be combined by routing technique before goodness of fit can be properly judged.

To provide some continuity of thought, a brief description follows of the procedures that will be used to define the finite-sized elements for subsequent routing. The watershed is subdivided into elements based on topography. The element map, Figure 10, is overlaid with the hydrologic response unit map, Figure 4, and sub-elements defined as a function of the hydrologic response units and watershed topography. A precipitation excess value for each sub-element is then determined. These excess values are then routed, assuming one-dimensional flow, to the gaging station. This gives an estimate of runoff with respect to time and space, producing a hydrograph of the simulated excess values.

It should be noted that, in drawing the sub-element divisions, it is not always possible to divide an element into homogeneous sub-elements. Therefore, each sub-element must be assumed to be dominated by a particular response unit or a weighted average of the precipitation excesses must be calculated for all response units located within the sub-element. This point will be discussed more thoroughly in a later section.

VIII. Sensitivity Analysis

Several model runs were made with the Holtan equation to demonstrate the effects that varying initial soil moisture conditions, depth of the A horizon, soil texture, hydrology group, and land-use have on precipitation excess. All characteristics remained constant, except the one being studied, in an attempt to eliminate some of

FIGURE 9
Illustration of Hydrograph Separation Based on Barnes' Procedure

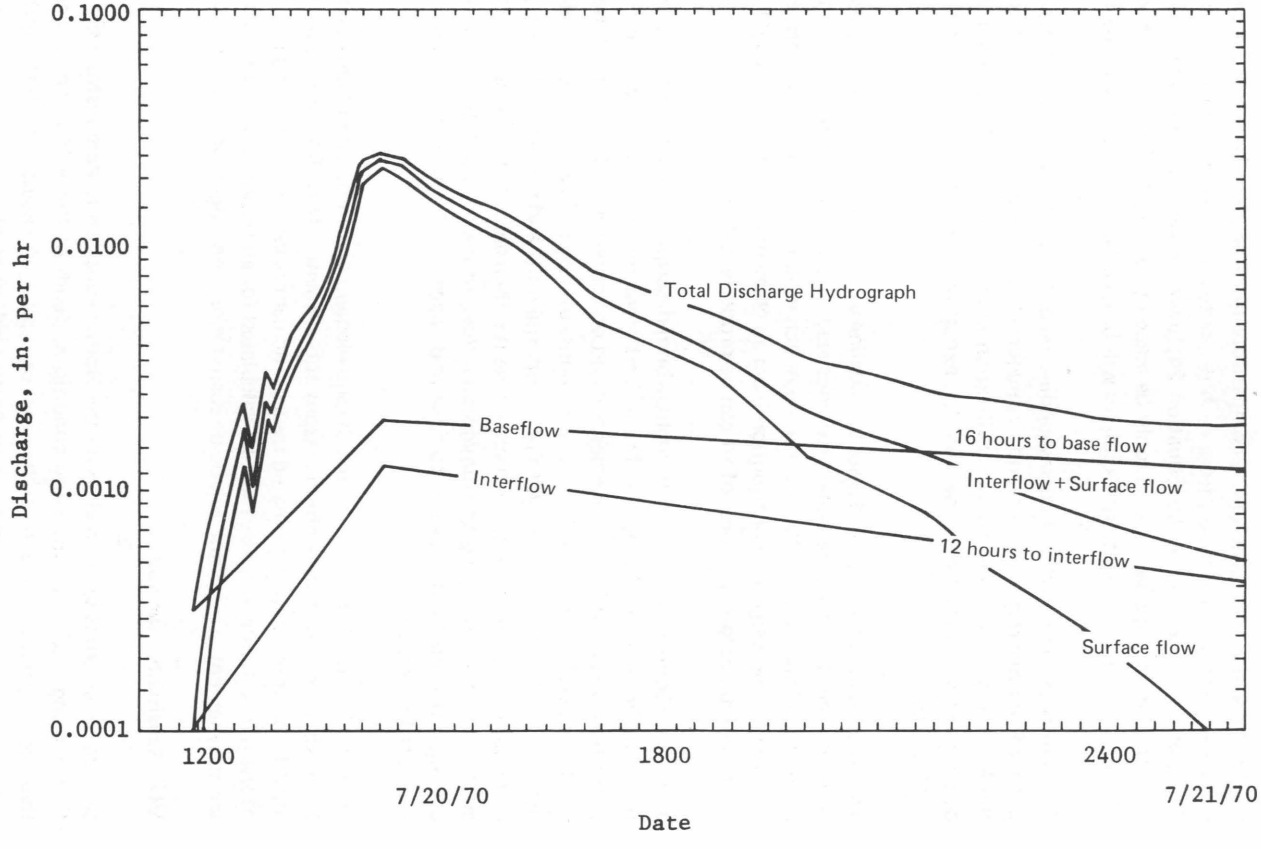

Figure 10
Digitized Map of the Element Breakdown
for the Routing Routine for Rocky Run Watershed

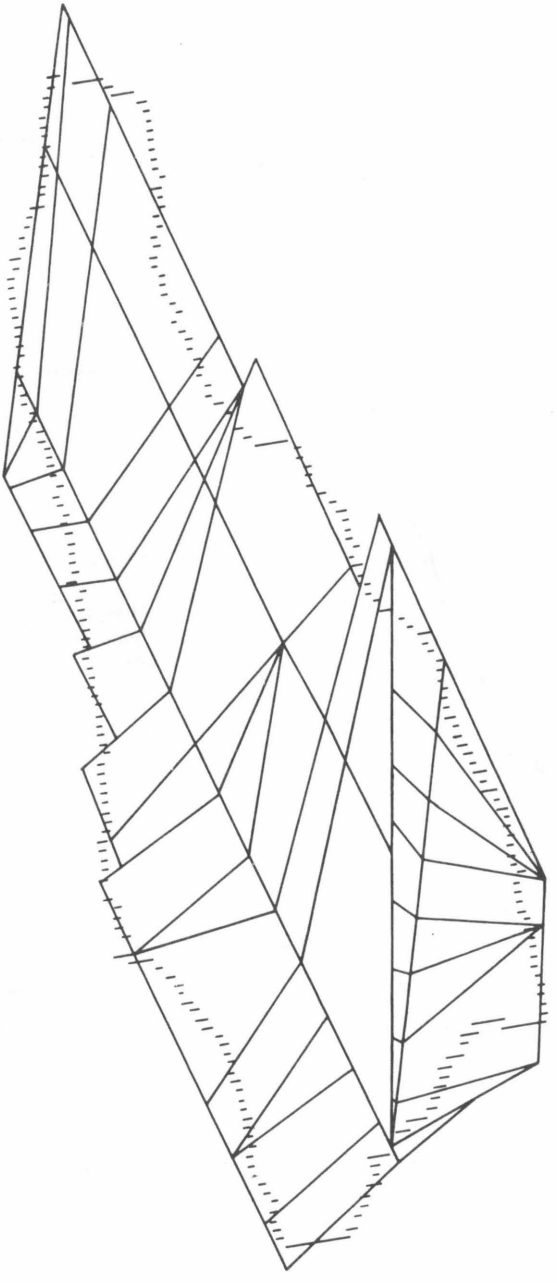

FIGURE 11

Illustration of the Effect of Initial Soil Moisture Condition on Precipitation Excess Obtained by the Holtan Model

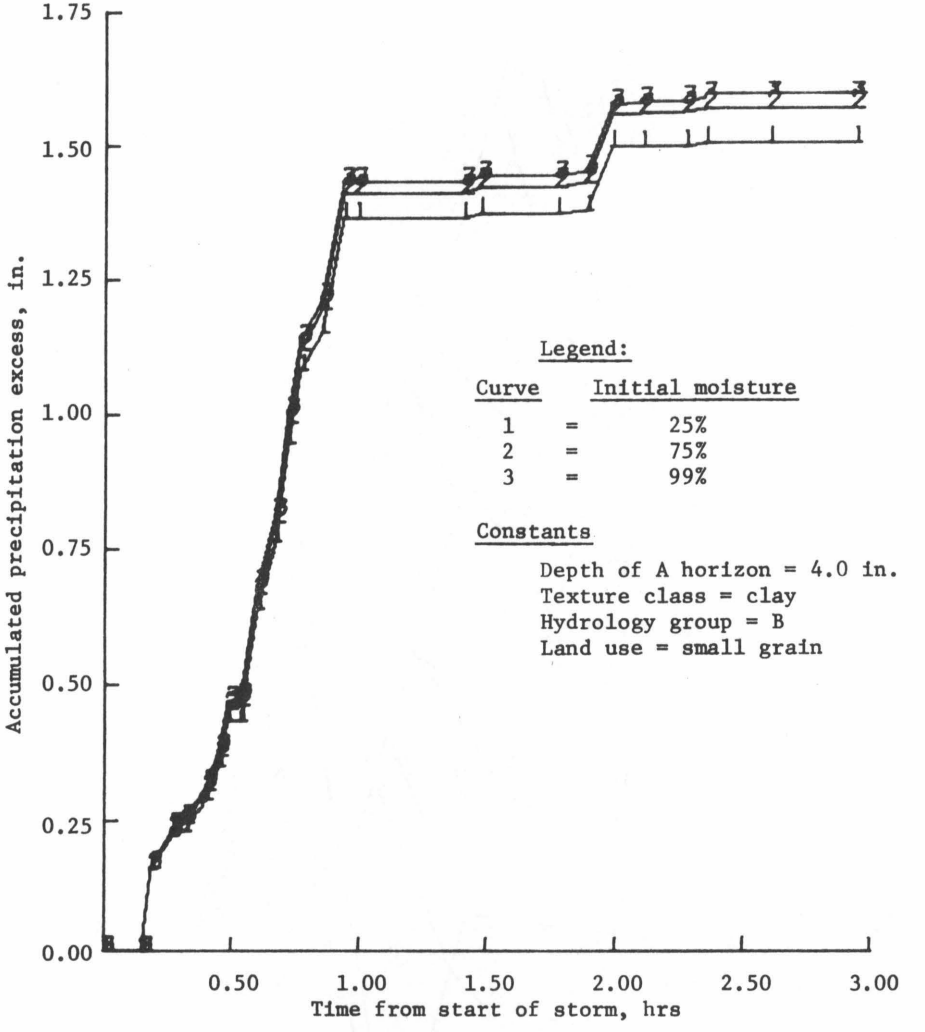

the confusing interactions among totally different hydrologic response units. For example, soil texture is usually related to the hydrology group, and two hydrologic response units with the same texture are usually classified in the same hydrology group. For the sensitivity analyses, however, it was assumed that soils within a specific textural class could have different hydrology groups.

A. Initial Soil Moisture Content

Figure 11 shows the effect of varying the initial soil moisture content from 25 percent to 99 percent. As the initial soil moisture increases, the amount of precipitation excess increases. This is due to a reduction in available storage, since the initial soil moisture represents that part of the storage occupied by water before infiltration begins. The parameters which were held constant soil texture (clay), hydrology group (B), and land use (row crop).

B. Depth of the A Horizon

The results of varying the depth of the A horizon from 1 to 15 inches is shown in Figure 12. As the depth increases, the storage increases and the precipitation excess decreases. The differences are evident early in the storm. The parameters held constant were initial soil moisture content (25 percent); soil texture (loam); hydrology group (B), and land use (row crop).

C. Soil Texture

The precipitation excess generated for four soil textures is shown in Figure 13 with hydrology group (B), soil depth (6.0 inches), and land-use (small grain) held constant. The loamy fine sand showed the least amount of precipitation excess, while the clay showed the most. These soils were all assumed to have an initial soil moisture content of 25 percent. The effect of texture is highly dependent on the ratio of AW to S and SGW to S.

D. Hydrology Group

Results of varying the hydrology group on precipitation excess generated for a silt loam with a 4.0 inch horizon in pasture can be seen in Figure 14. The initial soil moisture content was held constant at 25 percent. The precipitation excess increased as the hydrology group index was ranged from B^+ to D. The hydrology group classification is directly related to the infiltration properties of the soil. Infiltration potential decreases as the classification is increased from B to D; therefore, runoff should increase.

E. Land Use

The results of changing land use within a particular response unit is perhaps the most

FIGURE 12

Illustration of the Effect of Depth of the A Horizon on Precipitation Excess Obtained by the Holtan Model

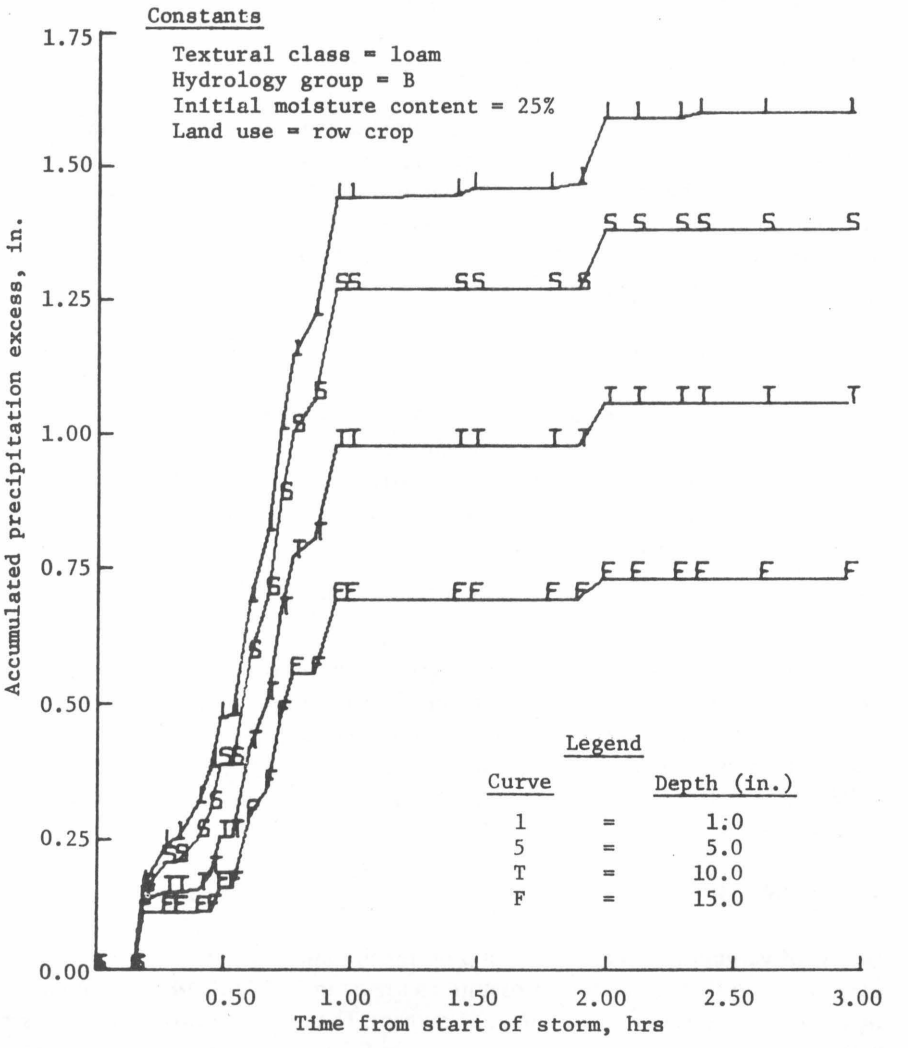

FIGURE 13

Illustration of the Effect of Soil Textural Classification On Precipitation Excess Obtained by the Holtan Method

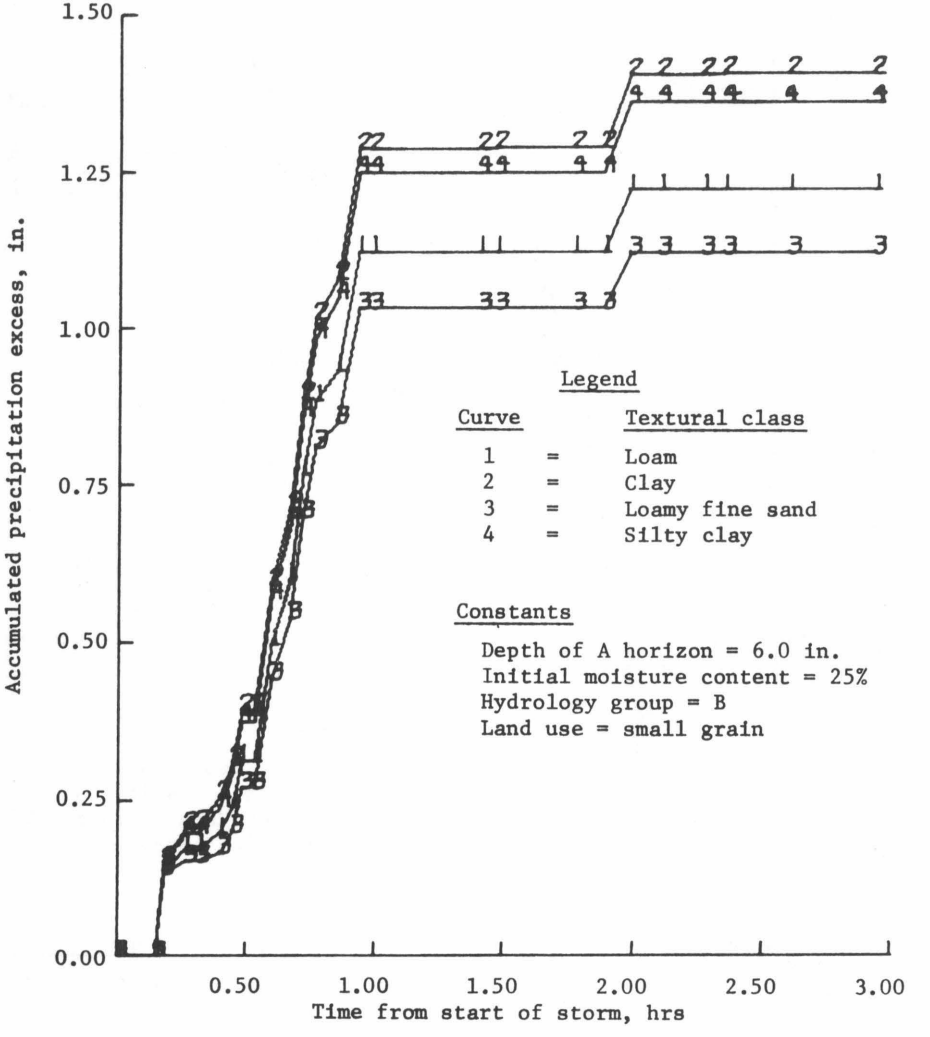

FIGURE 14

Illustration of the Effect of Hydrology Group Classification On Precipitation Excess Obtained by the Holtan Model

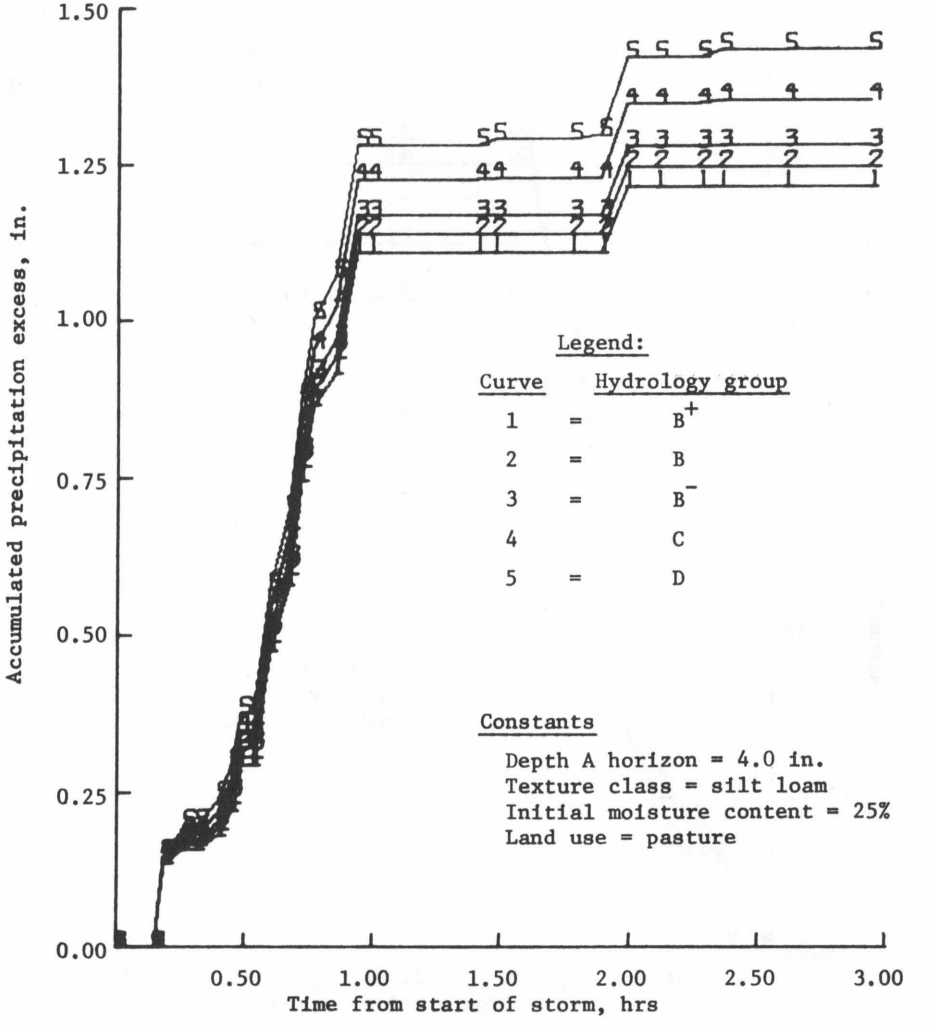

interesting and important application of this model. Figure 15 shows the effect of land use for an area with fine, sandy loam soil, hydrology group B, and a 6.0 inch A horizon. Wooded areas of this soil would produce the least amount of precipitation excess. If the area were paved, all precipitation would be modeled as excess, producing the line designated by "I."

Applications of these results are obvious. Suppose, for example, a watershed like Figure 16 exists. A city, marked X, has decided to build an airport in the field marked Y, which is presently in woods and pasture. Hydrologic response units are identified as 2, 3, 4, and 5. It is important to the downstream city, Z, to know the potential effect of this decision, because it is located within the 100-year flood zone.

The model could be used as follows: given an approximate rainfall distribution, the expected discharge would be simulated with the area in its present state. Then the proposed airport would be assumed to replace response units 2, 3, 4, and 5 and a new discharge created. A comparison of these results would give the effect of the airport.

The model can also be used to find an area where the change to impervious area will produce a less drastic change in the generated precipitation excess. For example, a shallow clay soil planted in row crops would produce a less drastic change than a deep loam covered by woods.

FIGURE 15

Illustration of the Effect of Land-Use Classification On Precipitation Excess Obtained by the Holtan Model

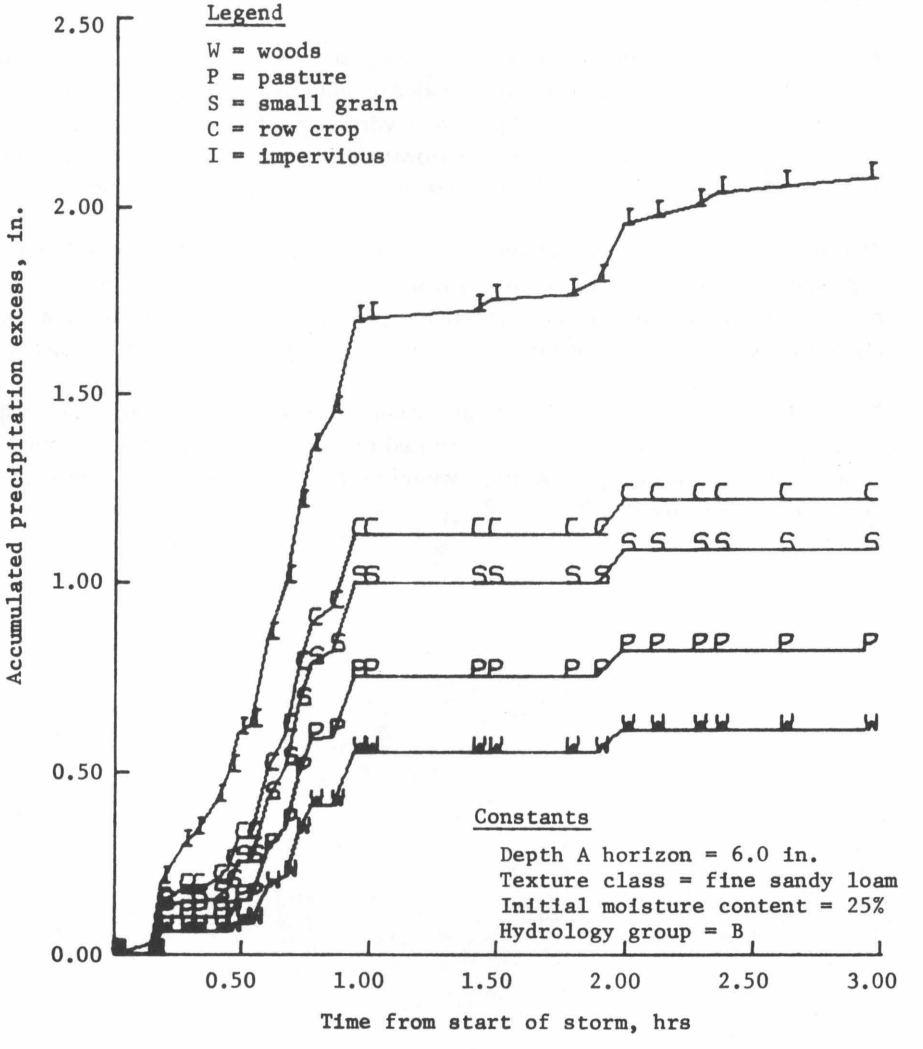

FIGURE 16

A Typical Watershed Sub-Divided by Hydrologic Response Units For Planning Analysis

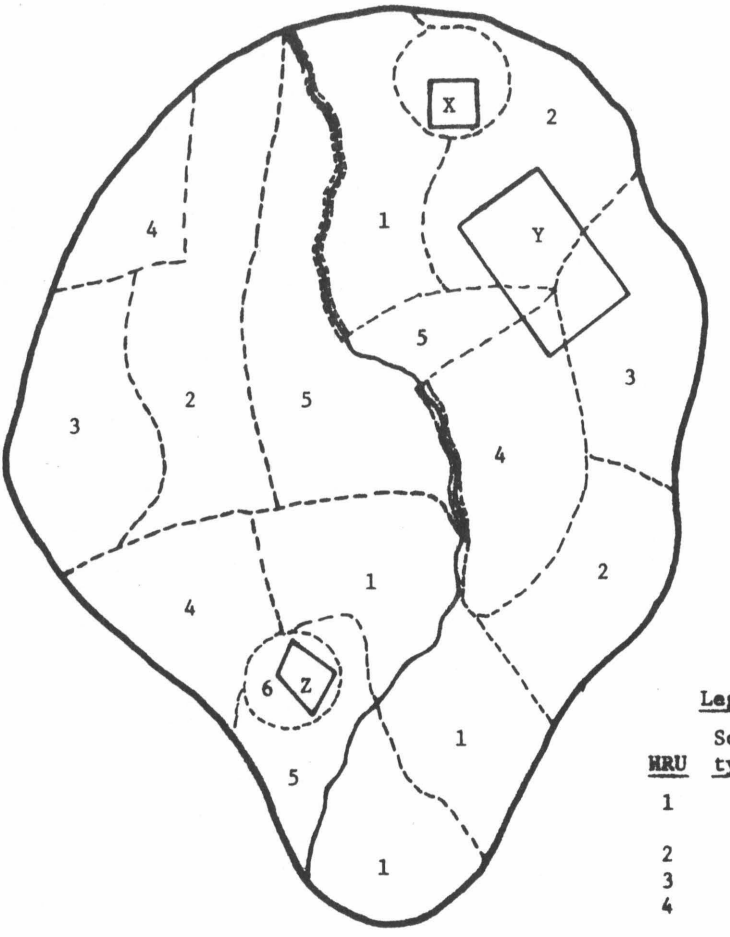

Legend

HRU	Soil type	Land use
1	A	small grain
2	B	woods
3	B	pasture
4	C	row crop
5	C	woods
6	B	impervious

GENERAL CONCLUSIONS FROM PRECIPITATION EXCESS MODEL

Data generated by the two infiltration models illustrate that, regardless of the method, vegetative-soil characteristics should not be ignored. Both equations produced widely varied results for different response units. When using only the Mein and Larson equation, hydrologic response units could be delineated solely on the basis of soil texture. An alternative to modifying the response units is to modify the Mein and Larson equation to include the characteristics of a hydrologic response unit. However, not only is the Holtan equation highly compatible with this concept, but also the nature of the equation itself suggests such a method.

A model based on the hydrologic response unit concept is not difficult to use because soil and land-use data are generally readily available. Gridding large areas can prove tedious, but since the digital computer is being applied to so many new fields, it is simply a matter of time before soils maps will be available in digitized (gridded) form. Land-use data are already being collected in this form by remote sensing, using aerial photographs. The technique still is not perfected, but the time of wide use of remote sensing is not far off.

The ability of the hydrologic response unit concept to maintain the spatial uniqueness of the area is an important aspect which provides many variations not possible with a lumped-parameter system. If rainfall data are available from gages scattered throughout a watershed, the hydrologic response unit concept provides the capability to account for non-uniform rainfall throughout the watershed. This is especially important in large watersheds, since storms over a large area are rarely uniform.

In addition, if delayed infiltration can be adequately described, many studies will be possible which require spatial uniqueness. This relationship would enhance our ability to model potential effect of urban expansion. For example, perhaps a golf course or forested park should be placed between a new subdivision and a stream. By application of zoning codes, building codes, and decisions concerning the location of pertinent city facilities such as schools, bus lines, roads, and sewage treatment plants, development can be restricted to areas less conducive to being flooded or to producing downstream flooding. Urban development can be orderly.

Applications of this model to agricultural problems are also possible. Erosion can be greatly slowed by planting row crops in soils with high infiltration rates or by bordering fields of row crops with pasture or wooded area. The effects of precipitation excess caused by changing the cover on a response unit can be determined readily by the model. Soil conservation would be one goal, water conservation another. By manipulatiing existing hydrologic response units, maximum efficiency in relation to these two goals can be achieved.

FIGURE 17
Flow Planes with Lateral Inflow

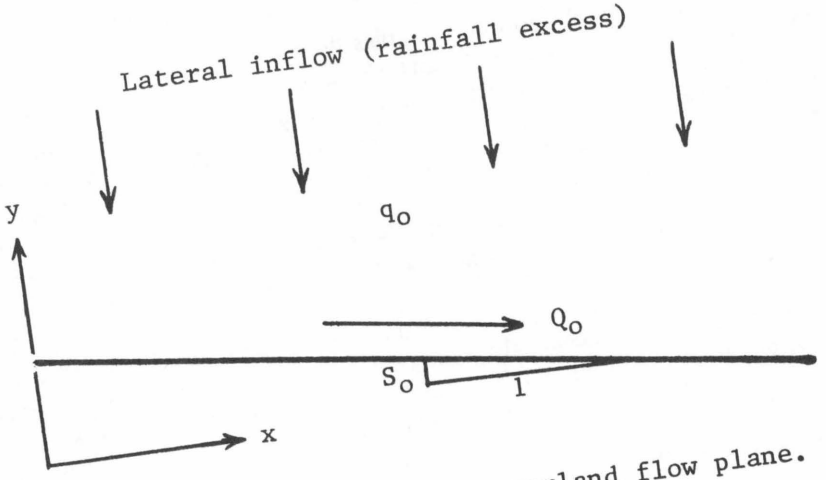

(a) Representation of the overland flow plane.

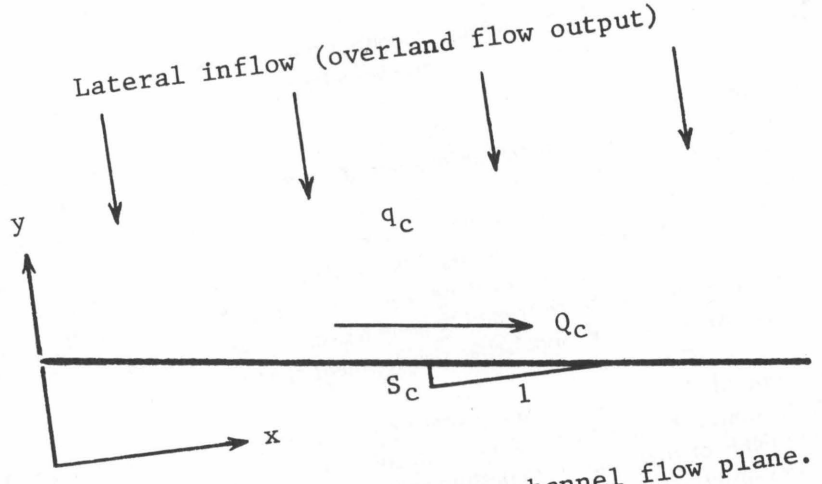

(b) Representation of the channel flow plane.

FORMULATION OF THE FLOW ROUTING MODEL

I. Governing Differential Equations

The hydrodynamic equations attributed to Saint-Venant are the equation of continuity and the equation of momentum for both overland flow and channel flow. These equations are the partial differential equations used in this finite element analysis. Figure 17 shows the plan views of the overland and channel flow that are represented by these equations. The equation of continuity can be expressed as:

$$\frac{\partial Q}{\partial x} + \frac{\partial A}{\partial t} - q = 0 \qquad [25]$$

and the equation of momentum as:

$$\frac{\partial Q}{\partial t} + \frac{\partial}{\partial x}\left(\frac{Q^2}{A}\right) = gA\,(S - S_f) - gA\frac{\partial y}{\partial x} \qquad [26]$$

where:

- Q = the discharge in the overland flow plane or channel;
- q = the lateral inflow per unit length of flow plane (rainfall excess for the overland flow plane and overland flow output for the channel);
- A = the area of flow in the overland flow plane or the channel;
- x = the distance in the direction of flow;
- t = time;
- S = the bed slope of the flow plane;
- S_f = the friction slope; and,
- y = the depth of flow.

After applying the kinematic wave approximation to the momentum equation, it can be reduced to the following form:

$$S = S_f \qquad [27]$$

To mathematically describe open channel flow, the above equation must be represented by an equation such as the Chezy or Manning equation. The Manning equation was chosen for this study because its applicability has been demonstrated by many investigators [e.g. Morgali and Linsley, 1965]. The Manning equation can be written as:

$$V = \frac{1.49}{\eta} R^{2/3} S^{1/2} \qquad [28]$$

or

$$Q = \frac{1.49}{\eta} R^{2/3} S^{1/2} A \qquad [29]$$

FIGURE 18
Actual and Discretized Domains of a Typical Watershed

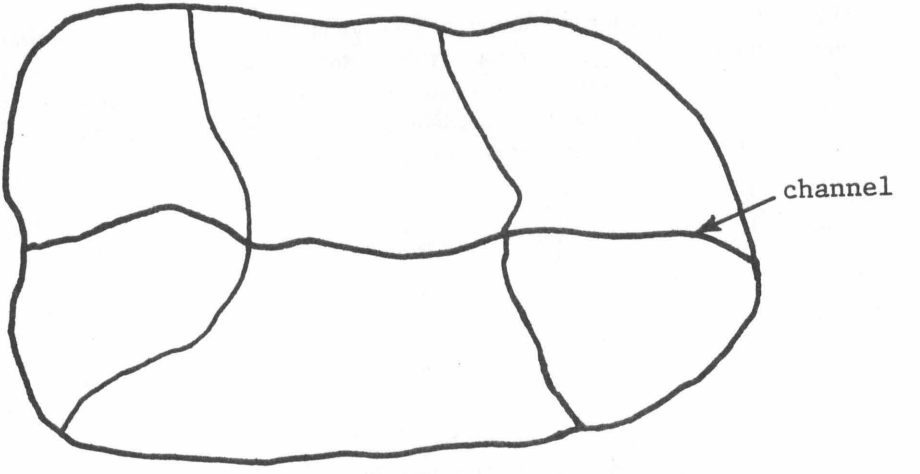

(a) Actual domain

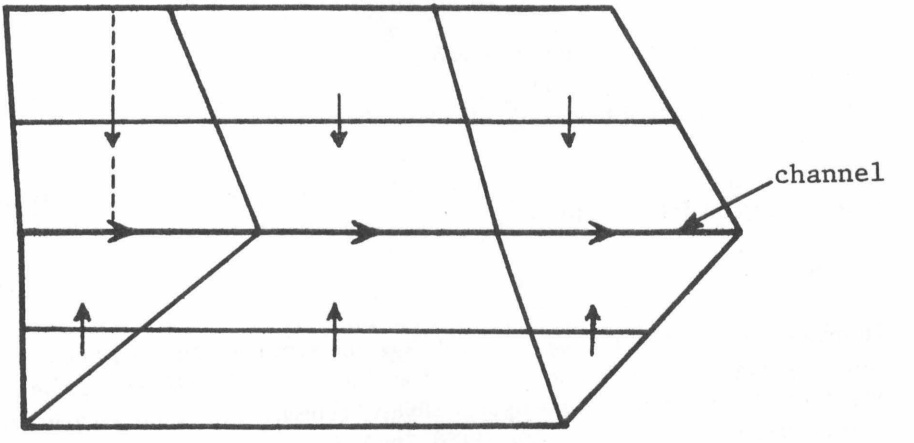

(b) Discretized domain

where:

V = the velocity of flow;
Q = the discharge;
R = hydraulic radius (area/wetted perimeter);
A = cross sectional area; and,
η = the Manning retardance coefficient.

II. Derivation of the Element Equations

A one-dimensional analysis was assumed to be satisfactory for this study. The example watershed shown in Figure 18a, in which there is one main stream, is considered the actual domain. The watershed is shown with the stream divided into three equidistant sections. These sections form the channel elements in the discretized domain of Figure 18b. The lines projecting out from these divisions in the actual domain are the boundaries of the drainage areas of each channel section, and the corresponding lines in Figure 18b define the six "strips." Each strip is solved independently of any other strip in conformance with the one-dimensional method of solution. The arrows in the strips represent the direction of flow which is always perpendicular to the direction of flow in the channel elements. The dashed line in the upper left strip represents the one-dimensional line elements equivalent to the elements shown in the strip. A strip may be divided into any number of elements as desired, with the dividing lines being drawn parallel to the channel elements as shown in Figure 18b. In this case each strip in the watershed contains two elements and three nodes. The channel contains three elements and four nodes. The overland flow plane and the channel are solved independently of each other where lateral inflow to the overland flow plane is rainfall excess and lateral inflow to the channel is output from the overland flow plane.

A simple natural coordinate system for a one-dimensional element (Figure 19) is represented as [Desai, 1974]:

$$X = 1/2\,(1 - L)\,X_1 + 1/2\,(1 + L)\,X_2 \qquad [30]$$

where:

$$L = \frac{x - x_3}{\ell/2},\quad x_3 = (x_1 + x_2)/2,\quad l = x_2 - x_1$$

Following Galerkins's procedure (Equation 14), the following equations for the discharge and areas can be written:

$$Q(x, t) = \sum_{i=1}^{n} N_i(x)\,Q_i(t) \qquad [31]$$

$$A(x, t) = \sum_{i=1}^{n} N_i(x)\,A_i(t) \qquad [32]$$

FIGURE 19
A One-Dimensional Finite Element Representation
(Adapted from Desai and Abel, 1972)

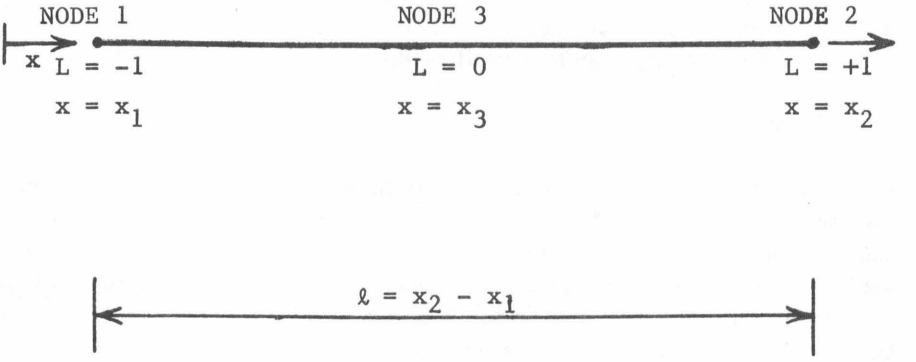

where:

$N_i(x)$ = the shape function;
$Q_i(t)$ = Q as a function of time only; and,
$A_i(t)$ = A as a function of time only.

In matrix form, these can be expressed for one element as:

$$Q(x,t) = 1/2 \left[(1-L) \quad (1+L)\right] \begin{Bmatrix} Q_1(t) \\ Q_2(t) \end{Bmatrix} \qquad [33]$$

$$A(x,t) = 1/2 \left[(1-L) \quad (1+L)\right] \begin{Bmatrix} A_1(t) \\ A_2(t) \end{Bmatrix} \qquad [34]$$

Taking the derivatives of Q with respect to x and A with respect to t for corresponding expressions in Equation 25 yields:

$$\frac{\partial Q}{\partial x} = \frac{1}{\ell} \left[-1 \quad 1\right] \left\{Q(t)\right\} \qquad [35]$$

$$\frac{\partial A}{\partial t} = 1/2 \left[(1-L) \quad (1+L)\right] \left\{\dot{A}(t)\right\} \qquad [36]$$

where:

ℓ = the length of the element;
$Q(t)$ = a column matrix (2 x 1) of flow; and,
$\dot{A}(t)$ = a column matrix (2 x 1) of the time differential of the area.

Substituting the above terms into the continuity equation (Equation 25) yields:

$$[N] \left\{\dot{A}(t)\right\} + 1/\ell \, [-1 \quad 1] \left\{Q(t)\right\} - q = \epsilon \qquad [37]$$

where:

$[N]$ = $1/2 \, [(1 - L) \quad (1 + L)]$, and,
ϵ = the error or residual.

Applying Galerkin's method further, with the shape function used as the weighting function, gives the following equation:

$$\sum_{i=1}^{NE} \int [N]^T \left([N] \left\{\dot{A}(t)\right\} + \frac{Q_2(t) - Q_1(t)}{\ell} - q \right) dL = 0 \qquad [38]$$

where:

NE = the number of elements.

Performing the integration term by term:

$$\int [N]^T [N] \left\{\dot{A}(t)\right\} dL = 1/4 \int_{-1}^{1} \begin{Bmatrix} (1-L) \\ (1+L) \end{Bmatrix} \begin{bmatrix} (1-L) & (1+L) \end{bmatrix} dL \left\{\dot{A}(t)\right\}$$

$$= 1/4 \int_{-1}^{1} \begin{bmatrix} (1-L)^2 & (1-L)(1+L) \\ (1-L)(1+L) & (1+L)^2 \end{bmatrix} dL \left\{\dot{A}(t)\right\}$$

$$= 1/4 \begin{bmatrix} \frac{-(1-L)^3}{3} & L - \frac{L^3}{3} \\ L - \frac{L^3}{3} & \frac{(1+L)^3}{3} \end{bmatrix}_{-1}^{1} \left\{\dot{A}(t)\right\} = \begin{bmatrix} \frac{2}{3} & \frac{1}{3} \\ \frac{1}{3} & \frac{2}{3} \end{bmatrix} \left\{\dot{A}(t)\right\}$$

and

$$\int [N]^T \frac{Q_2(t) - Q_1(t)}{\ell} dL = \tfrac{1}{2} \int_{-1}^{1} \begin{Bmatrix} (1-L) \\ (1+L) \end{Bmatrix} dL \, \frac{Q_2(t) - Q_1(t)}{\ell}$$

$$= \tfrac{1}{2} \begin{Bmatrix} (1-L) \\ (1+L) \end{Bmatrix} \Bigg|_{-1}^{1} \frac{Q_2(t) - Q_1(t)}{\ell} = \tfrac{1}{2} \begin{Bmatrix} 2 \\ 2 \end{Bmatrix} \frac{Q_2(t) - Q_1(t)}{\ell}$$

$$= \begin{Bmatrix} 1 \\ 1 \end{Bmatrix} \frac{Q_2(t) - Q_1(t)}{\ell}$$

Similarly,

$$\int [N]^T q \, dL = \begin{Bmatrix} 1 \\ 1 \end{Bmatrix} q$$

Combining the terms gives the following element equation:

$$\begin{bmatrix} \frac{2}{3} & \frac{1}{3} \\ \frac{1}{3} & \frac{2}{3} \end{bmatrix} \{\dot{A}(t)\} + \frac{Q_2(t) - Q_1(t)}{\ell} \begin{Bmatrix} 1 \\ 1 \end{Bmatrix} - q \begin{Bmatrix} 1 \\ 1 \end{Bmatrix} = 0 \qquad [39]$$

The above equation represents the single element equation for this one-dimensional finite element analysis.

If the time differential of the area is represented by:

$$\dot{A}(t) = \frac{A(t + \Delta t) - A(t)}{\Delta t}$$

where:

Δt = the time increment,

the equation for one element becomes:

$$\frac{1}{\Delta t} \begin{bmatrix} \frac{2}{3} & \frac{1}{3} \\ \frac{1}{3} & \frac{2}{3} \end{bmatrix} \begin{Bmatrix} A_1 \\ A_2 \end{Bmatrix}_{t + \Delta t}$$

$$- \frac{1}{\Delta t} \begin{bmatrix} \frac{2}{3} & \frac{1}{3} \\ \frac{1}{3} & \frac{2}{3} \end{bmatrix} \begin{Bmatrix} A_1 \\ A_2 \end{Bmatrix}_t + \frac{Q_2(t) - Q_1(t)}{\ell} \begin{Bmatrix} 1 \\ 1 \end{Bmatrix} = q \begin{Bmatrix} 1 \\ 1 \end{Bmatrix} \qquad [40]$$

III. Assemblage of the Element Equations

For the element equation to be adapted to a finite element grid consisting of more than one element, it must be arranged in a form which embodies the total number of elements. Application of the direct stiffness method to the element equation gives the equation for the assemblage in the following form:

$$\frac{1}{\Delta t} [K] \{A(t + \Delta t)\} - \frac{1}{\Delta t} [K] \{A(t)\} + \frac{Q_2(t) - Q_1(t)}{\ell} \{k\} = q\{k\} \qquad [41]$$

where:

$[K]$ = square matrix (nxn);
n = the number of nodes, and
$\{k\}$ = column matrix (nx1).

As an example for two elements and three nodes, the assembled element equation would be written as:

$$\frac{1}{\Delta t}\begin{bmatrix} \frac{2}{3} & \frac{1}{3} & 0 \\ \frac{1}{3} & \frac{4}{3} & \frac{1}{3} \\ 0 & \frac{1}{3} & \frac{2}{3} \end{bmatrix}\begin{Bmatrix} A_1 \\ A_2 \\ A_3 \end{Bmatrix}_{t+\Delta t} - \frac{1}{\Delta t}\begin{bmatrix} \frac{2}{3} & \frac{1}{3} & 0 \\ \frac{1}{3} & \frac{4}{3} & \frac{1}{3} \\ 0 & \frac{1}{3} & \frac{2}{3} \end{bmatrix}\begin{Bmatrix} A_1 \\ A_2 \\ A_3 \end{Bmatrix}_{t}$$

$$+ \frac{Q_2(t) - Q_1(t)}{\ell}\begin{Bmatrix} 1 \\ 2 \\ 1 \end{Bmatrix} = q\begin{Bmatrix} 1 \\ 2 \\ 1 \end{Bmatrix} \qquad [42]$$

In the above equation the third term may be written as:

$$\frac{1}{\ell}\begin{Bmatrix} Q_2(t) - Q_1(t) \\ [Q_2(t) - Q_1(t)] + [Q_3(t) - Q_2(t)] \\ Q_3(t) - Q_2(t) \end{Bmatrix} = 1/\ell\begin{Bmatrix} Q_2(t) - Q_1(t) \\ Q_3(t) - Q_1(t) \\ Q_3(t) - Q_2(t) \end{Bmatrix} \qquad [43]$$

where the subscripts of Q are the numbering of the nodes of the elements.

The fourth term may be represented by:

$$\begin{Bmatrix} q^{I} \\ q^{I} + q^{II} \\ q^{II} \end{Bmatrix} \qquad [44]$$

where:

q^{I} = lateral inflow into first element, and
q^{II} = lateral inflow into second element.

IV. Initial and Boundary Conditions

Continuing with the above example, it can be shown how several initial conditions may be made which contribute to the ease of solution and allow a "marching" procedure to be used. For the overland flow plane or the channel at time, t = 0, several terms have the value of zero, hence the equation becomes:

$$\frac{1}{\Delta t}\begin{bmatrix} \frac{2}{3} & \frac{1}{3} & 0 \\ \frac{1}{3} & \frac{4}{3} & \frac{1}{3} \\ 0 & \frac{1}{3} & \frac{2}{3} \end{bmatrix} \begin{Bmatrix} A_1 \\ A_2 \\ A_3 \end{Bmatrix}_{t+\Delta t} = \begin{Bmatrix} q^{I} \\ q^{I} + q^{II} \\ q^{II} \end{Bmatrix} \qquad [45]$$

After solving the equations simultaneously for the values, A_1 $(t + \Delta t)$, A_2 $(t + \Delta t)$, and A_3 $(t + \Delta t)$, the Manning equation is then used to solve for the values of Q_2 $(t + \Delta t)$ and Q_3 $(t + \Delta t)$.

At the upper boundaries of the strips and channel the flow is zero at all times, t, which is an existing boundary condition that further simplifies the solution of the problem.

In compliance with the "marching" procedure, the equations must then be solvable, because at the next time step, $t = \Delta t$. The above values of A_1 $(t + \Delta t)$, A_2 $(t + \Delta t)$, A_3 $(t + \Delta t)$, Q_2 $(t + \Delta t)$, and Q_3 $(t + \Delta t)$, solved for the above would become A_1 (t), A_2 (t), A_3 (t), Q_2 (t), and Q_3 (t), respectively. This procedure is continued for the time period desired.

DEVELOPMENT OF THE COMPUTER PROGRAM FOR FLOOD ROUTING

A computer program for the model was written at Virginia Polytechnic Institute and State University in the Fortran IV language. The solution procedure in the program is based on the finite element computer program of Judah [1972], which also routes overland and channel flow. However, the routine presented herein goes into much greater detail in that it allows for variation in the input parameters across the watershed. In addition, flood-detention structures and reservoirs can be included in the watershed system.

The program is written in subroutines to allow even more refinements to be made at a later date, without a major alteration of the entire program. A copy of the computer program can be obtained upon request. Several aspects of the organization, writing, and operation of the program are described below. Further details are planned in a later water center bulletin.

I. Sequence of the Computer Program

The general sequence of the finite element program written for this model is as follows:

1. With rainfall excess as input, calculate the Froude number and the kinematic wave number, K, at the downstream node of the strip. When the Froude number is greater than .5 (providing greater confidence in the results than the value of 2) and/or K is less than 10, print the actual values and the corresponding time step.

2. Solve for the area of flow at each node of the strip from the assembled element equation, and calculate the discharge at each node from the Manning equation.

3. Repeat steps 1 and 2 for each time step using the values of Q and A solved for in the previous time step.

4. Repeat steps 1, 2, and 3 for each strip.

5. With the flow across the downstream node of each strip as input, solve for the areas of flow at each node of the channel, and calculate the discharge at each node from the Manning equation.

6. Repeat step 5 for each time step using the values of Q and A solved for in the previous time step.

II. Band Width

The general procedure of a finite element program is to solve for the assembled matrices in the assembled element equation, the size of each depending on the number of nodes in a strip. If n is the number of nodes, the square matrix defined in Equation 40 would be of the size, n X n, and the column matrix, also defined in Equation 40, would be of the size, n X 1. As a result, the number of simultaneous equations would be equal to the number of nodes, n.

A feature which greatly simplifies the arrangement of the assembled square matrix is that of band width. Band width is directly related to the way in which the elements are numbered. Because of the one-dimensional scheme, the arrangement of the flow planes into independently solved strips, and the consecutive numbering of the nodes within a strip, the band width becomes the minimum possible band width of two. This simplifies the procedure of setting up the matrices and the solution of the simultaneous equations as the matrix is one with a tri-diagonal band width with all the other coefficients being equal to zero. Formulas for calculating band width can be found in most texts dealing with finite element and matrix techniques [e.g. Desai and Abel, 1972].

III. Input Requirements for the Model

A watershed varies greatly with respect to its hydrologic properties. The primary advantage of the use of the finite element method is that spatial variations can be considered by simply including the appropriate values for each element. Factors such as slope, Manning roughness coeffiecient and lateral inflow (rainfall, and subsequently, rainfall excess), most often vary from element to element. All of these, and many other factors, combine and interact to make the hydrologic response of each element different. All factors need to be defined when possible and given proper consideration in constructing the element and strip configurations to retain hydrologic homogeneity. Other data which must be included are the number of strips, number of elements and nodes in each strip, and the geometric length and width of the elements, in addition to initial and boundary conditions.

Because of the similarity between the finite element analysis for the overland flow and channel flow routines, the data input requirements for both are the same, with the exception that lateral inflow to the channel becomes the output from the overland flow routine.

APPLICATION OF MODELS TO SOUTH RIVER WATERSHED

As was previously noted, this project was conducted in two phases. During Phase I, a precipitation excess generator was developed. Phase II consisted of the development of a flood routing model. When combined, these two models form the basis for a storm hydrograph model. The models were structured to handle spatial variations in rainfall, soils, cover, management practice, topographic features, etc.

Initial testing of the complete model was begun on the South River Watershed located in Augusta County, Virginia. Additional testing and refinement of the model will be accomplished as monies can be secured for this purpose.

I. Description of the Study Area

Approximately 236 square miles along the southeast and east boundaries of Augusta County are drained by the South River and its tributaries (Figure 20). The study area was defined by USDA-SCS [1974] to include the following stream reaches:

> "South River, from Interstate 81 through Waynesboro to its confluence with North River—about 38 miles; two miles along Pratts Run tributary from Route 250 down to Waynesboro city limits; five miles along Back Creek tributary from about one mile above the community of Sherando down to its confluence with South River; and about one mile along Jones Hollow tributary within the city of Waynesboro."

The general relief is that of broad rolling valley flanked on the east and west by mountains. Drainage is in the Potomac River Watershed. The area is rapidly becoming urbanized and industrialized, particularly in the area around Waynesboro.

A recent soil survey completed by the Soil Conservation Service (SCS) in cooperation with Virginia Polytechnic Insitutute and State University and the Augusta County Extension Staff [SCS, 1972] gives detail on soils existing in the drainage area. This report contains the latest knowledge on the soils of the area and should be consulted for detailed soil descriptions.

The many different kinds of soils are defined generally as follows:

> "Some have formed from limestone, shale, sandstone, or a mixture of these, on rolling to steep valley uplands. Other have formed from sandstone, quartzite, or shale on steep mountain slopes and ridges. Still others have formed in alluvial materials of the terraces and flood plains on nearly level to sloping topography. Some have heavy clay subsoils, others are sandy throughout, and some have dense compacted layers called fragipans."

FIGURE 20
The South River Watershed

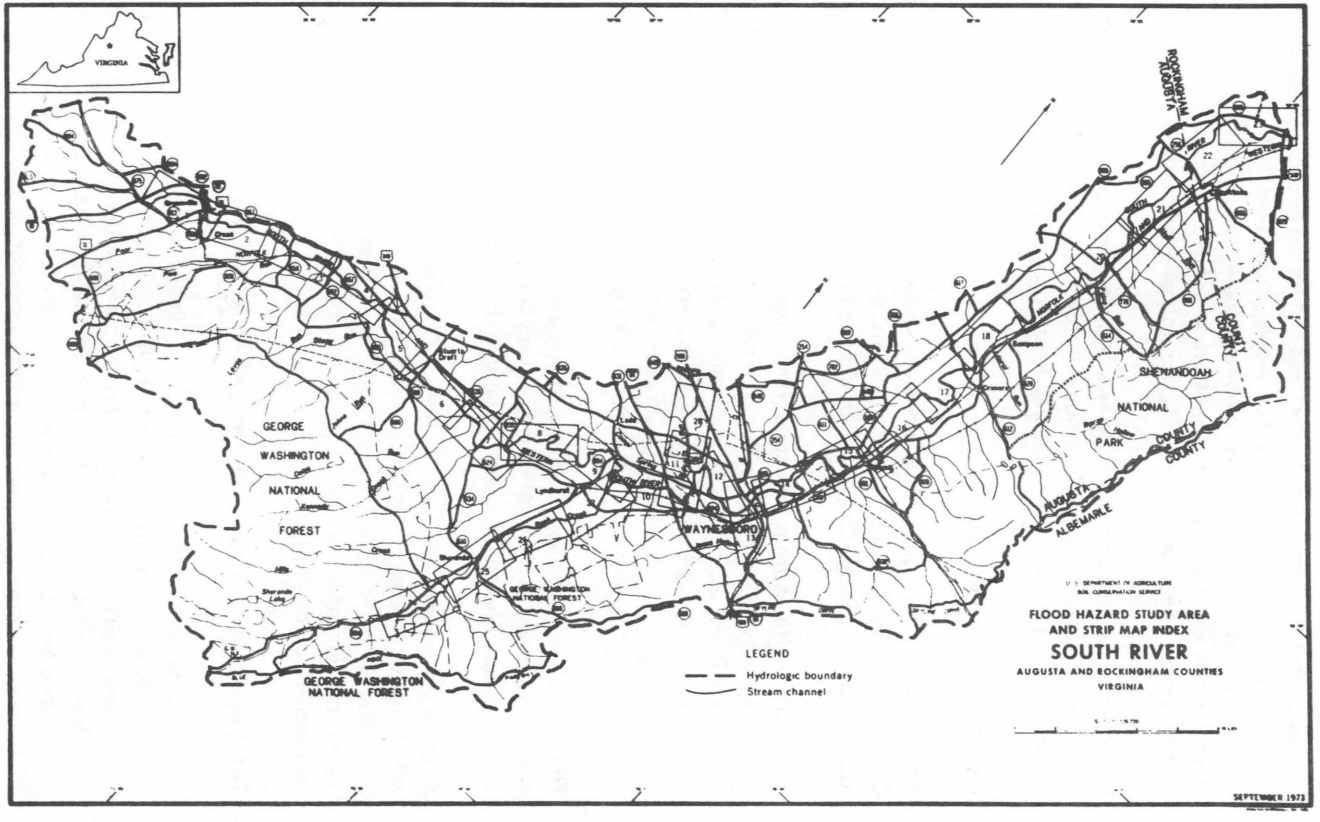

These soils support a very wide and diverse arrangement of agricultural activity.

For this model application, only the upper portion of the watershed was analyzed, or the drainage area to the point where the gaging station at Waynesboro is located. This area, hereafter referred to as the upper South River watershed, comprises 136 square miles, and is shown in Figure 21. This action was taken since there are no other gaging stations further downstream along the South River and. therefore, consideration of the watershed below Waynesboro would be useless for the purposes of calibrating the model.

The South River, being the main channel in the watershed, would ordinarily be the channel in the channel routine while the rest of the watershed would be included in the overland flow routine. However, in the case of this watershed, there is a relatively large tributary of the South River. It was decided that this stream, Back Creek, should also be incorporated into the channel routine. For this to be accomplished, three channels were defined: (1) the South River to the confluence of the South River and Back Creek, (2) Back Creek to the same confluence, and (3) the South River downstream of this confluence.

Considering this, three sub-drainage areas or overland flow planes must be defined and each solved independently of the others. This discretization phase of the study area is shown in Figure 21. For the case of three overland flow planes, a major change must be made because the boundary condition of $Q_1 = 0$ at the upper nodes of the channels does not apply to the third channel. The value of Q_1 must be equal to the sum of the discharges at the last nodes of the other two channels at any given time, t.

Although this computer program is written specifically for the case of three overland flow planes and three channels, it is a simple procedure to make adjustments in the program to handle more than three. The appropriate changes must be made in the boundary conditions of the pertinent channels, however, and cross-sectional data for the additional channels must be available.

II. Flood-Detention Structures

The existence of flood-detention structures necessitated additional refinements in the flood routing solution. The location and drainage areas of these structures are shown in Figure 22. The structures drain approximately 32 square miles and were designed to contain runoff from a 100-year flood event. Because flow from the reservoirs is released depending upon the level and volume of the water in the reservoirs, their influence had to be incorporated into the program in order to obtain realistic simulations.

When a strip in a given finite element grid contains a flood-detention structure, the first step taken by the computer program is to combine all the elements in that strip

<u>**FIGURE 21**</u>

Drainage Area Above Waynesboro Showing the Three Overland Flow Planes Used in This Study

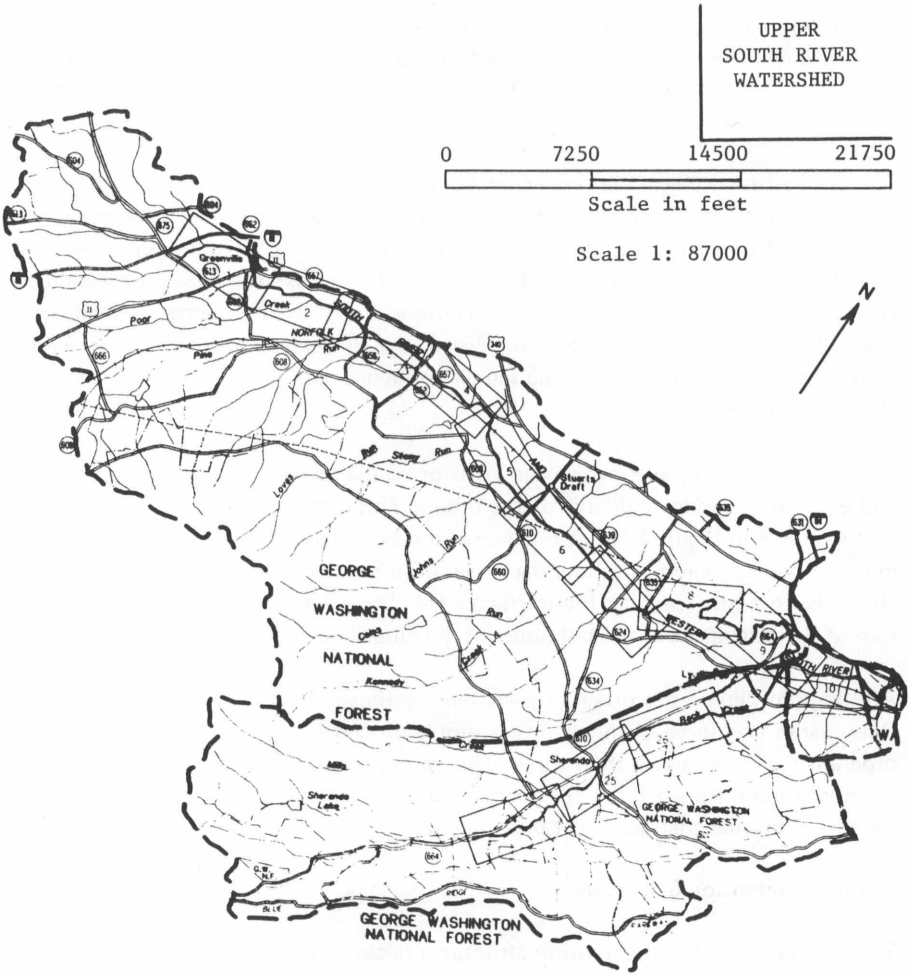

FIGURE 22

Locations and Drainage Areas of the 12 Flood-Detention Structures on the South River Watershed

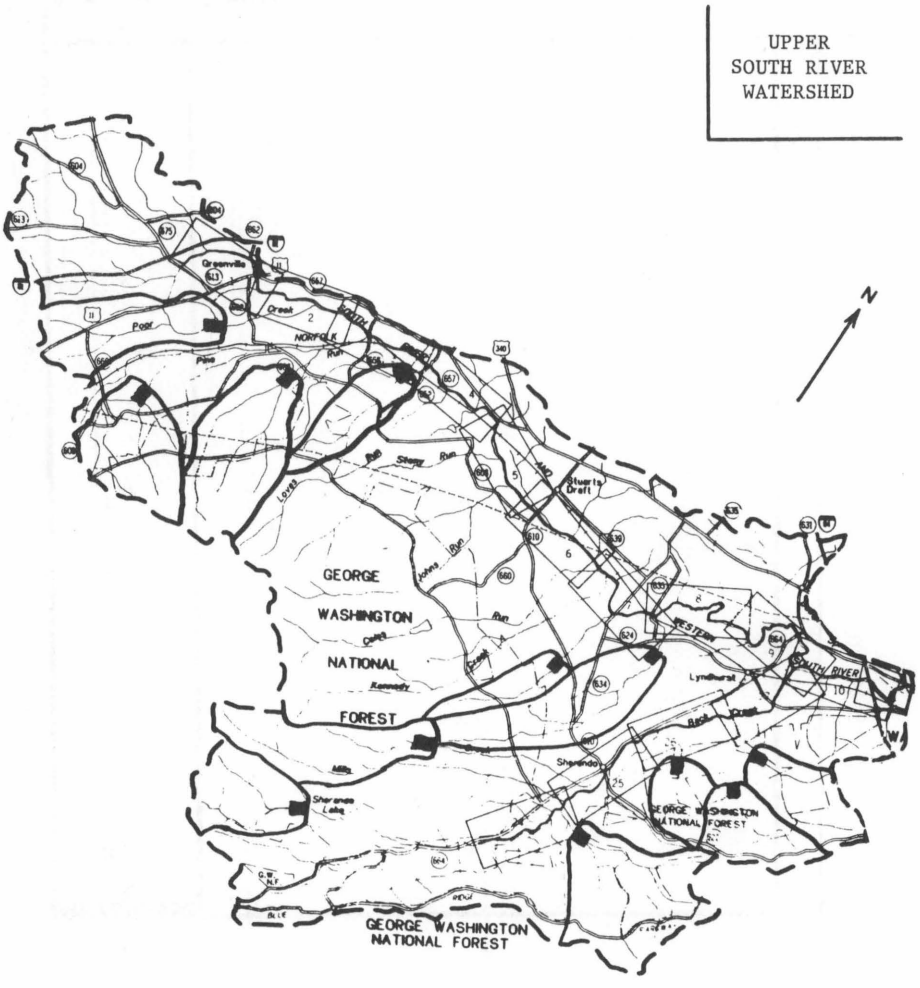

FIGURE 23

Schematic Representation of an Element Containing a Flood-Detention Structure

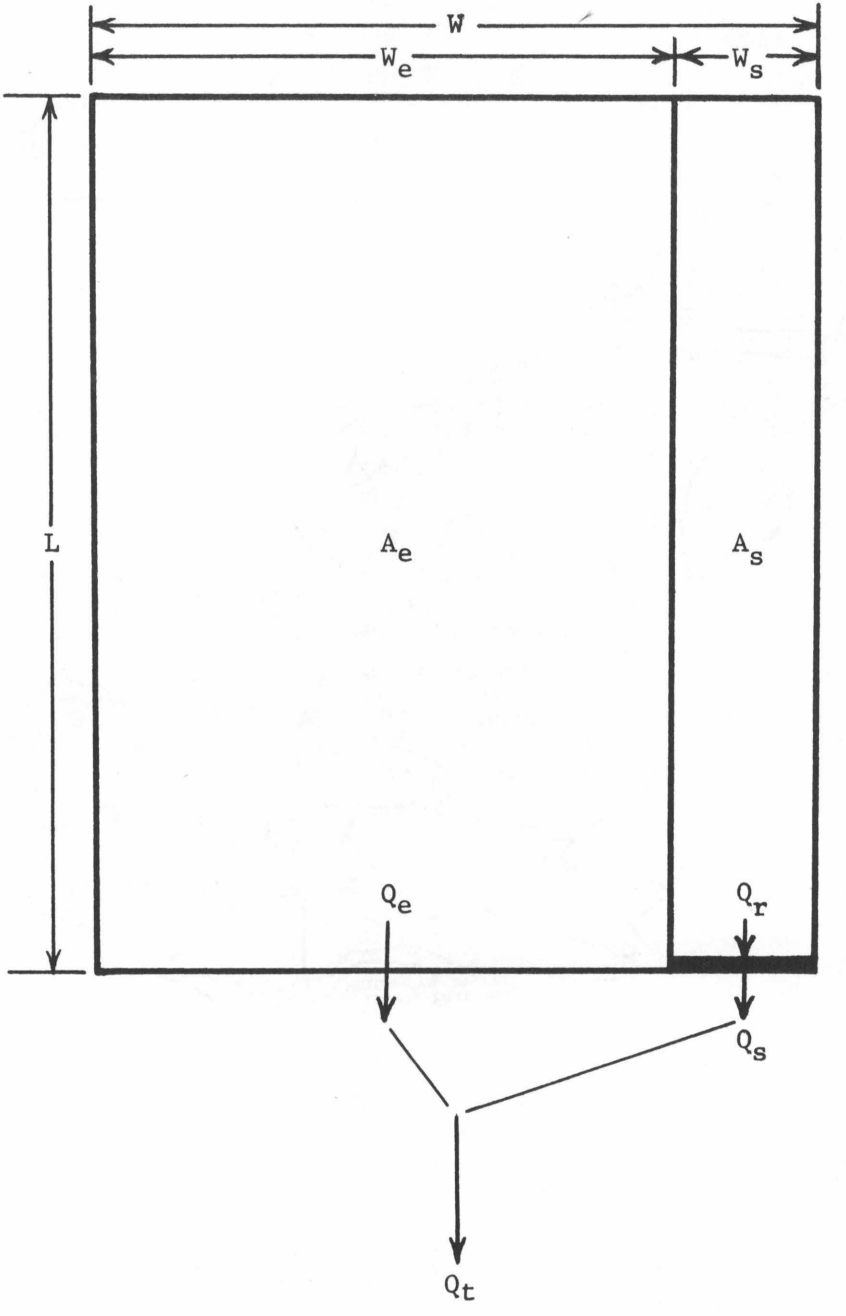

into one element. Weighted averages of the elements' hydrologic properties are taken to determine the hydrologic properties of the single element in the strip.

The next step is to divide the single element strip into two elements, as shown in Figure 23. One element represents the drainage area, A_s, above the flood-detention structure and the other element represents the remaining area, A_e, in the strip which drains directly into the channel.

The drainage area, A_s, is entered as an input parameter for each structure. Since the length of this element is equal to the strip length, L, its width can be calculated by $W_s = A_s/L$. Proper adjustment is made in the computer program to define the dimensions of the remaining element.

The two elements which replaced the original strip are routed independently of each other, but both have the same hydrologic properties as determined above.

For each time step, the volume of the reservoir is calculated as a function of the flow across the downstream node of the element representing the drainage area of the reservoir, which is the flow into the reservoir, Q_r. Discharge from the structure, Q_s, is determined by interpolation from known discharge rates which correspond with reservoir volumes. Several discharge rates and their corresponding volumes must be entered for each flood-detention structure as an imput parameter. Once Q_s is determined, it is combined with Q_e to equal the flow into the channel, Q_t.

Where several flood-detention structures are located in a given strip, additional elements are formed, the size of each dependent upon the drainage area above each flood-dentention structure. Therefore, three elements would be devised for a strip containing two flood-detention structures.

III. Input Parameters

The major input parameters and information regarding their acquisition and assumptions associated with them are described in the following sections.

IV. Rainfall Excess

Rainfall excess is the major input parameter for the overland flow routing in this model. Rainfall data may be easily obtainable, however, accurate values of rainfall excess are very difficult to obtain. The technique previously described was used to generate precipitation excess. A brief description of the procedure as applied to the South River Watershed follows.

An extensive summary of the watershed topography was conducted in order to divide the watershed into hydrologic response units depending upon soil characteristics and

land use. Following previous guidelines, over one hundred hydrologic response units were identified. These units were coded and digitized. Grid maps were created. The finite element grids based on geometric consideration were overlaid and percentages of each hydrologic response unit within an element were determined.

Rainfall excess was determined for each hydrologic response unit using the previously described model. A weighted average for each element was taken to obtain a single representative rainfall excess value for a given element. This was accomplished by thresholding all elements to remove from the computations all response units which seemingly made very little contribution to the overall rainfall excess value for a given element. Elements contributing 5 to 6.5 percent or less were generally deleted. This move resulted in the total number of hydrologic response units being reduced to 69.

The method made it a relatively simple matter to arrive at a new rainfall excess value after land-use changes had been incorporated into the watershed. Since the hydrologic response units were based on land-use conditions, the new percentages of land-use types within an element could be determined and then weighted to find the new rainfall excess value for that element since the rainfall excess value for each hydrologic response unit had been previously obtained.

V. Slope

This parameter is used in Manning's equation and was obtained from U.S. Geological Survey topographic maps of the area. By placing the finite element grid configuration on the maps, an average elevation was obtained for the upper and lower nodes of each element. The slopes were calculated as a function of the difference in the elevations and the distance between the nodes.

For the channel, the elevations at various stations along the channel were used, where cross-section data was available. This data was provided by the Soil Conservation Service. When these stations did not coincide with the channel element nodes, interpolation was used, based on the distance between nodes.

VI. Manning Roughness Coefficient (η)

This parameter greatly influences the magnitude of flow and care must be taken in its selection. Estimates for Manning's η were provided by SCS. When the nodal points of an element did not coincide with known cross sections, an average Manning η was found by a method of interpolation similar to that given above for defining average slopes. This value was used for the initial value of Manning η, but was adjusted somewhat during the calibaration of the model. The resultant Manning η values are somewhat higher than those for a natural channel because, in working with high flows, the major part of the flow occurs in the floodplain, where friction is greatly increased.

The effects of obstructions and low-lying bridges in the floodplain would also have the obvious effect of increasing the Manning η.

The values of Manning η for the overland flow elements represented a greater challenge as attempts were made to select representative values for the actual roughness conditions. Since flow in the overland flow element varies greatly, it can be seen how this value is little more than a tool by which to calibrate the model. For this reason, Manning η values for the overland flow elements were adjusted until the results of the model approached that of the actual recorded hydrograph. For the first runs, however, values were roughly estimated from data provided by Petryk and Bosmajian [1975] and Satterlund [1972].

Since Manning η is a direct result of the type of land use, a system of calculating Manning η had to be devised which would be consistent with any changes that had to be made later. Therefore, the information on land use which was used in the computation of rainfall excess was used for the solution of the Manning η coefficient. If the percentage of each land-use type—woods, agriculture 1, agriculture 2, residential, and impervious—are known and a Manning η value assigned to each type, a weighted average can be made to determine a Manning η for the entire element. In this manner, when changes are made in land use, or when the percentages of land-use types in a given element are changed, a consistent means of changing the Manning η of the element is provided.

Upon calibrating the model, the following Manning η coefficients were assigned: woods—0.30, agriculture 1—0.35, agriculture 2—0.40, residential—0.25, and impervious—0.02.

VII. Top Width

This parameter is used to calculate the hydraulic radius in the Manning equation and is defined as the width of the elements at the nodes where the flows were calculated. Since the overland flow concept represents a rectangular cross-section of flow with shallow depth, the hydraulic radius was set equal to the area divided by the top width. From this assumption, the hydraulic radius was set equal to the depth of flow for wide channels.

The channel geometry at the nodes had to be defined for channels. This information was obtained from channel cross-section data. The area of flow and top width of the channel were entered as data wherever the channel geometry changed abruptly. The program interpolates to obtain the proper top width after the area of flow is computed at the channel node points. The hydraulic radius was assumed to be equal to the area of flow divided by the top width. This assumption is valid for high flow conditions where flow occurs in the floodplain, although it may not be valid during low flows where flow is confined to the natural river channel.

FIGURE 24

Discretization of the Watershed into Six Elements

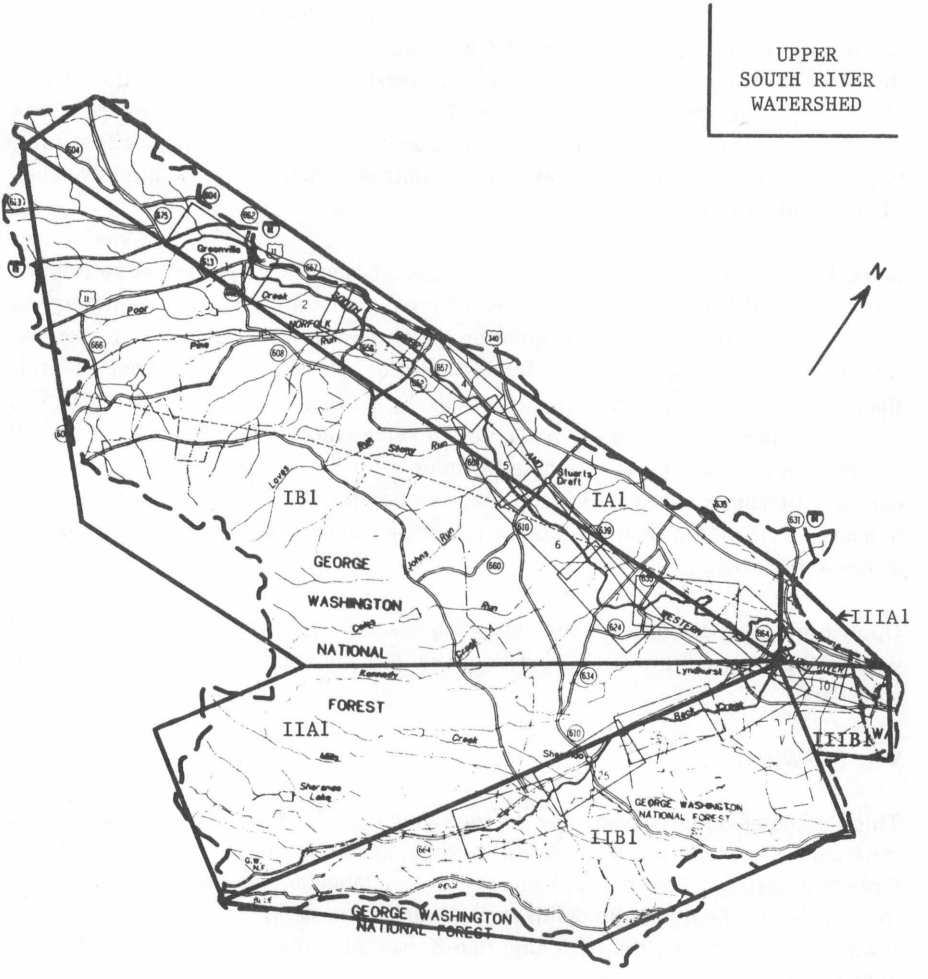

FIGURE 25

Discretization of the Watershed into 24 Elements

TABLE 9

Overland Geometry for the 24-Element Grid

Overland Flow Plane No.	Strip No.	Element No.	Length (ft.)	Average Width (ft.)	Slope (ft./ft.)	Manning η
I	A	1	7656	29568	.028	.297
	B	1	13200	7788	.016	.343
		2	13200	23364	.010	.336
	C	1	7656	16984	.020	.323
	D	1	13200	23672	.065	.316
		2	13200	20328	.025	.309
	E	1	7656	19624	.024	.244
	F	1	13200	9782	.103	.292
		2	13200	19110	.027	.310
	G	1	7656	17512	.017	.340
	H	1	13200	9328	.006	.338
II	A	1	8976	15928	.041	.286
		2	8976	18216	.024	.266
	B	1	8976	4340	.108	.300
		2	8712	14520	.043	.300
	C	1	8976	9900	.111	.280
		2	8976	19580	.071	.291
	D	1	8712	14740	.111	.300
		2	8712	17820	.047	.286
	E	1	8976	9680	.011	.231
	F	1	8712	15532	.066	.308
		2	8712	18084	.019	.294
III	A	1	8712	6336	.003	.264
	B	1	7920	10032	.057	.121

TABLE 10

Channel geometry for the 24-Element Grid

Channel No.	Element No.	Length (ft.)	Slope (ft./ft.)	Manning η
I	1	31152	.013	.100
	2	18656	.004	.085
	3	18656	.001	.085
	4	18656	.001	.105
II	1	19360	.039	.120
	2	19360	.010	.115
	3	19360	.005	.115
III	1	12672	.002	.130

VIII. Element Dimensions

The discretization of the watershed into strips and elements is a matter of both convenience and judgment. After the watershed was divided into the three overland flow planes described earlier, the next step was to define the channel elements. Points were defined along the length of the channel to give the lengths of the channel elements. From these points, lines were drawn outward over the watershed, based on the boundaries of the drainage areas of the flow to the already defined channel elements. The lines then formed the strips in which the overland flow is routed independently of any other strips. To further discretize the watershed, lines parallel to the channel elements were drawn at equidistant points along the length of the strips to create more than one element per strip.

Two finite element grids were devised for the application of this model. Figure 24 shows a grid comprised of six elements. This grid represents the coarsest grid possible for the case of three overland flow planes. A 24-element grid is shown in Figure 25.

The elements in the grids are numbered for use with Tables 9, 10, 12, and 13. In this type of numbering system the Roman numeral signifies the overland flow plane in which an element appears, the capital letter identifies the strip, and the Arabic numeral identifies the element within that strip. For example, the element numbered IID1 in Figure 25 would be the first element in the fourth strip of the second overland flow plane.

Table 9 shows the overland geometry and Table 10 shows the channel geometry. The values of Manning η shown in Table 9 are those obtained from using the Manning η values for specific land use types discussed earlier. The values of Manning η for the channel also represent those obtained after the calibration of the model.

FIGURE 26

Hurricane Camille in Virginia with Rainfall Given in Inches

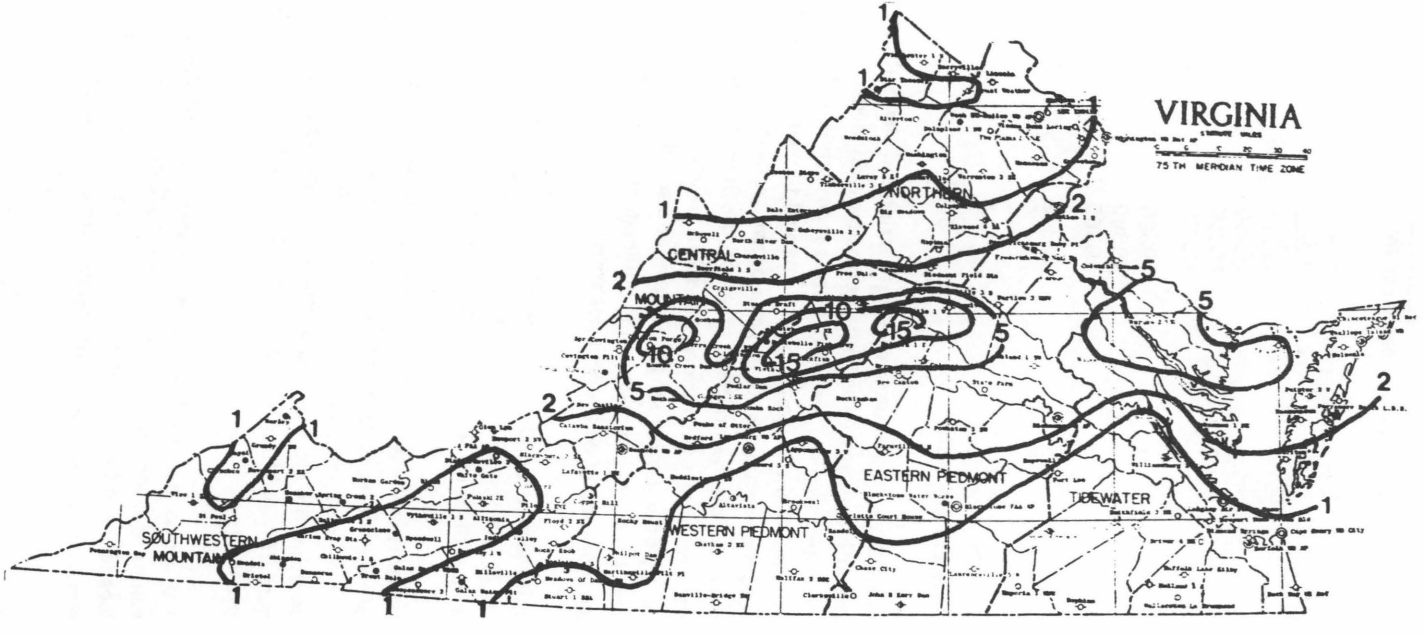

SIMULATING HURRICANE CAMILLE

In seeking a near 100-year event to calibrate the model and observe the effects of land-use changes, Hurricane Camille was chosen. The storm was a tropical depression which hit the state of Virginia on the night of August 19, 1969 and continued until the morning of August 20. Some isolated areas of Virginia near the South River watershed were soaked with over 20 inches of rainfall in a 15-hour period, while total rainfall over the upper South River watershed ranged from about 3 to 11 inches.

Hourly precipitation data was not available for any stations within this watershed; however, a station just southwest of the watershed—Montebello Fish Nursery—provided this data. No other nearby stations with hourly data were found suitable for this particular storm and watershed. Because of the uneven distribution of the rainfall over the watershed and much of Virginia, as shown in Figure 26, an adjustment was made in distributing the hourly data.

In Figure 27, the positions of the 5-inch and 10-inch isohyetal lines on the upper South River watershed are shown. The approximate location of the 10-inch isohyetal line was used to divide the watershed into two parts as far as the rainfall distribution is concerned. Data from the Montebello Fish Nursery station was then applied to that part of the watershed below this line (elements IIA1, IIA2, IIB1, IIB2, IID1, and IID2 of the 24-element grid). For the area of the watershed above this line, half of the rainfall values for the Montebello Fish Nursery station for each hour were used.

After making this assumption, the total of the hourly rainfall data under this method approached the total of the daily rainfall data for stations in and near the watershed, where these daily totals were available. This fact gave some assurance that the above assumption was a valid one.

The rainfall values were then used as input data in the rainfall excess model for each hydrologic response unit. By the weighted average process, a rainfall excess value was obtained for each element, depending on the hydrologic response units within each element. These values, for each element and for each hour of the storm, are given in Table 11 along with the two sets of rainfall which are entered in the rainfall excess model.

The rainfall excess values were then entered in the finite element model. The results for the 24-element grid and the results after the Manning roughness coefficient had been adjusted to provide a closer fit, are shown in Figure 28. A time increment of 900 seconds was used. For comparison, the recorded hydrograph is also shown. An even closer fit could be achieved by further adjustment of Manning η and possibly other parameters—such as the slope of the individual elements. A variable Manning η, depending on the length of time the rain has been falling, and/or whether or not

TABLE 11

Weighted Rainfall Excess Values for Elements in the 24-Element Grid for Hurricane Camille with Present Land-Use Conditions

Element	Hour 1	2	3	4	5	6	7	8	9	10	11	12
rainfall	0.4750	0.4900	0.5050	0.5150	0.5300	0.5100	0.5100	0.5300	0.4750	0.2800	0.2950	0.3500
IA1	0.0520	0.0537	0.0570	0.1437	0.3806	0.4813	0.4813	0.5034	0.4461	0.2565	0.2299	0.2906
IB1	0.0146	0.0152	0.0155	0.0158	0.0351	0.0639	0.0732	0.2263	0.2994	0.1638	0.2063	0.3370
IB2	0.0334	0.0358	0.0586	0.1801	0.3298	0.3648	0.3796	0.4436	0.4221	0.2474	0.2491	0.3276
IC1	0.0330	0.0360	0.0598	0.1446	0.2126	0.2113	0.2793	0.3650	0.3952	0.2408	0.2143	0.2959
ID1	0.0414	0.0431	0.0638	0.1434	0.1716	0.3891	0.4160	0.4340	0.4700	0.2800	0.1108	0.1706
ID2	0.0485	0.0544	0.2097	0.0728	0.2692	0.3677	0.4125	0.4583	0.4305	0.2524	0.1524	0.2233
IE1	0.1169	0.1225	0.1284	0.1751	0.2837	0.3261	0.3549	0.4057	0.3822	0.2097	0.2356	0.3128
IF1	0.0146	0.0152	0.0224	0.0564	0.0816	0.3046	0.3088	0.3329	0.4700	0.2800	0.0792	0.1396
IF2	0.0538	0.0692	0.0851	0.1434	0.1986	0.2479	0.2907	0.3825	0.3872	0.2268	0.1923	0.2699
IG1	0.0033	0.0150	0.0278	0.1594	0.3677	0.4597	0.4834	0.5107	0.4578	0.2712	0.2840	0.3480
IH1	0.0123	0.0187	0.0314	0.0743	0.1537	0.1900	0.2222	0.3329	0.3576	0.2075	0.2461	0.3486

IIC1	0.0329	0.0459	0.1161	0.1353	0.1925	0.3175	0.3306	0.3478	0.4312	0.2393	0.0936	0.1782
IIC2	0.0282	0.0294	0.0407	0.1019	0.1862	0.3411	0.3411	0.3559	0.4406	0.2672	0.1697	0.2372
IIE1	0.2803	0.2895	0.2980	0.3039	0.3127	0.3009	0.3009	0.3828	0.3879	0.2230	0.2585	0.3500
IIF1	0.0001	0.1543	0.5000	0.5100	0.5300	0.5100	0.5100	0.5300	0.4700	0.2800	0.1231	0.1831
IIF2	0.0570	0.0936	0.2256	0.2301	0.3217	0.3599	0.3604	0.3804	0.3204	0.1304	0.0968	0.1562
IIIA1	0.1093	0.1444	0.1718	0.1982	0.2561	0.3202	0.3635	0.4135	0.3860	0.2246	0.2222	0.2854
IIIB1	0.3055	0.3152	0.3248	0.3313	0.3932	0.4264	0.4264	0.4458	0.3992	0.2095	0.2249	0.2816
rainfall	0.9500	0.9800	1.0100	1.0300	1.0600	1.0200	1.0200	1.0600	0.9500	0.5600	0.5900	0.7000
IIA1	0.0897	0.2514	0.5270	1.0241	1.0600	1.0200	1.0200	1.0600	0.9500	0.5600	0.5900	0.7000
IIA2	0.0582	0.1837	0.5314	0.8451	1.0105	0.9978	1.0173	1.0600	0.9500	0.5600	0.5900	0.7000
IIB1	0.1410	0.4183	0.5681	0.9778	1.0433	1.0177	1.0200	1.0600	0.9500	0.5600	0.5900	0.7000
IIB2	0.1799	0.3552	0.6256	1.0294	1.0600	1.0200	1.0200	1.0600	0.9500	0.5600	0.5900	0.7000
IID1	0.0321	0.1448	0.6886	1.0257	1.0574	1.0183	1.0200	1.0600	0.9500	0.5600	0.5900	0.7000
IID2	0.1226	0.3408	0.7689	1.0300	1.0660	1.0200	1.0200	1.0600	0.9500	0.5600	0.5900	0.7000

FIGURE 27

Positions of the 5- and 10-inch Isohyetal Lines on the South River Watershed for Hurricane Camille

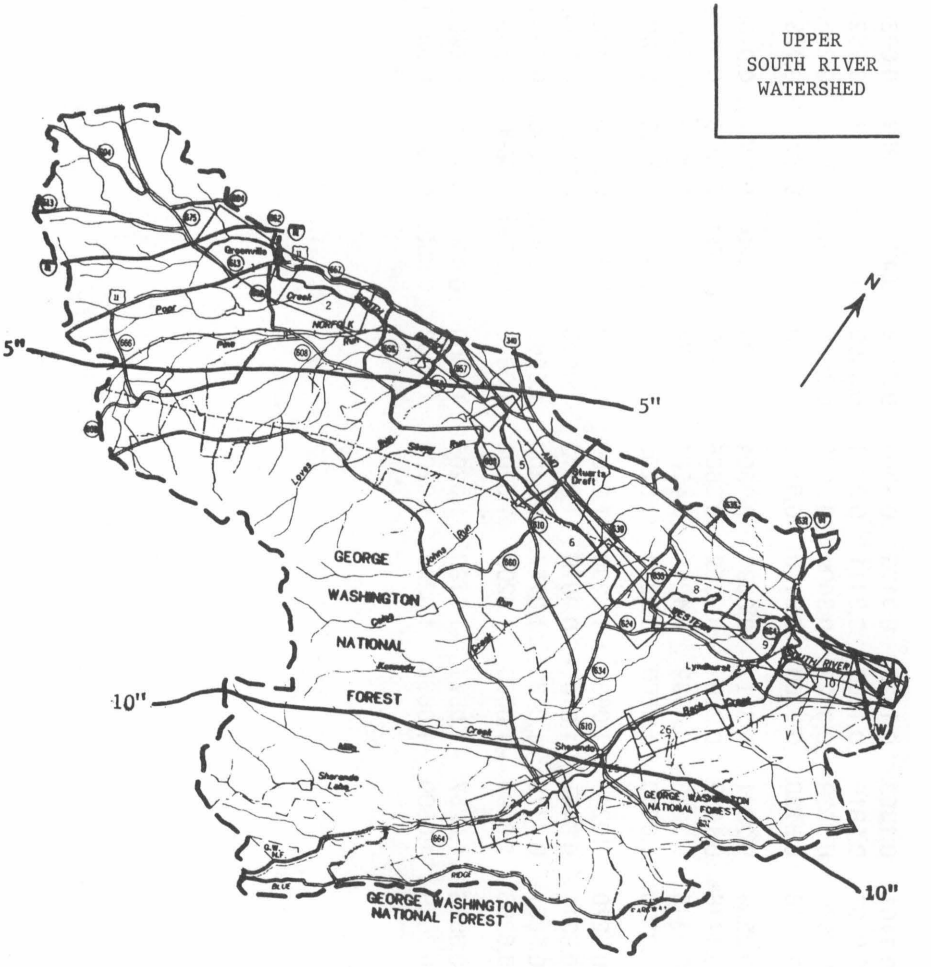

FIGURE 28

Comparison of Observed and Calculated Discharge for Hurricane Camille, Using the 24-Element Grid And a Time Increment of 900 Seconds

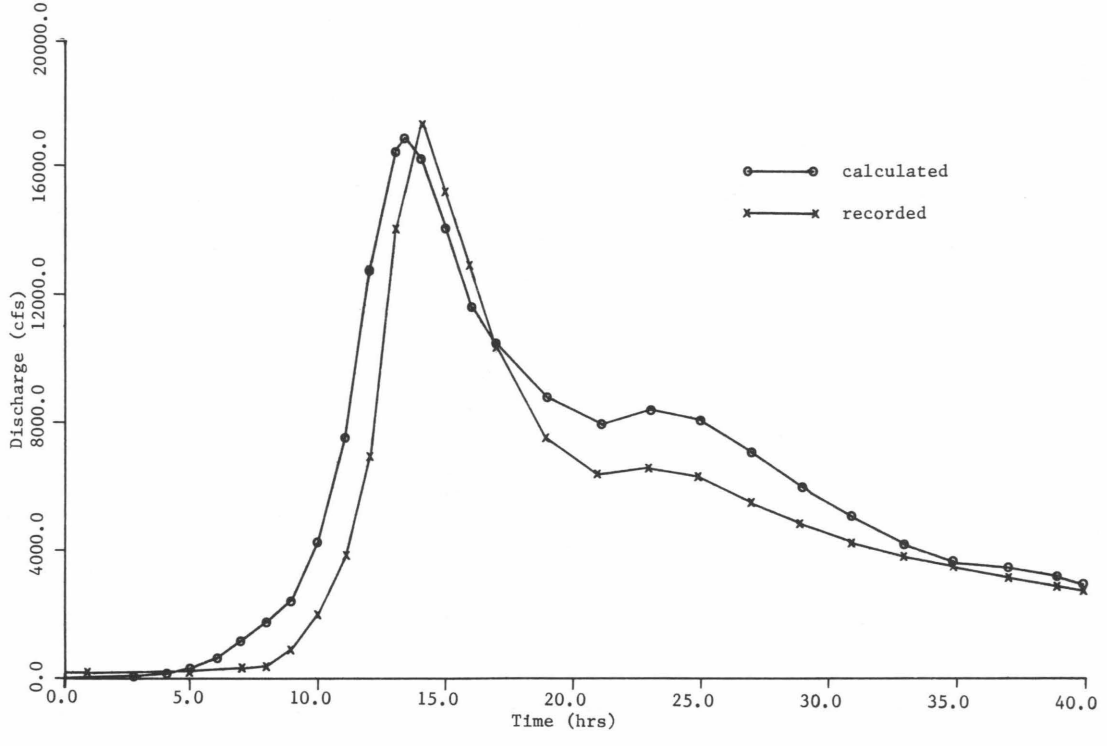

FIGURE 29

Comparison of the Calculated Discharge for Hurricane Camille, Using the 24-Element Grid with Three Different Time Increments

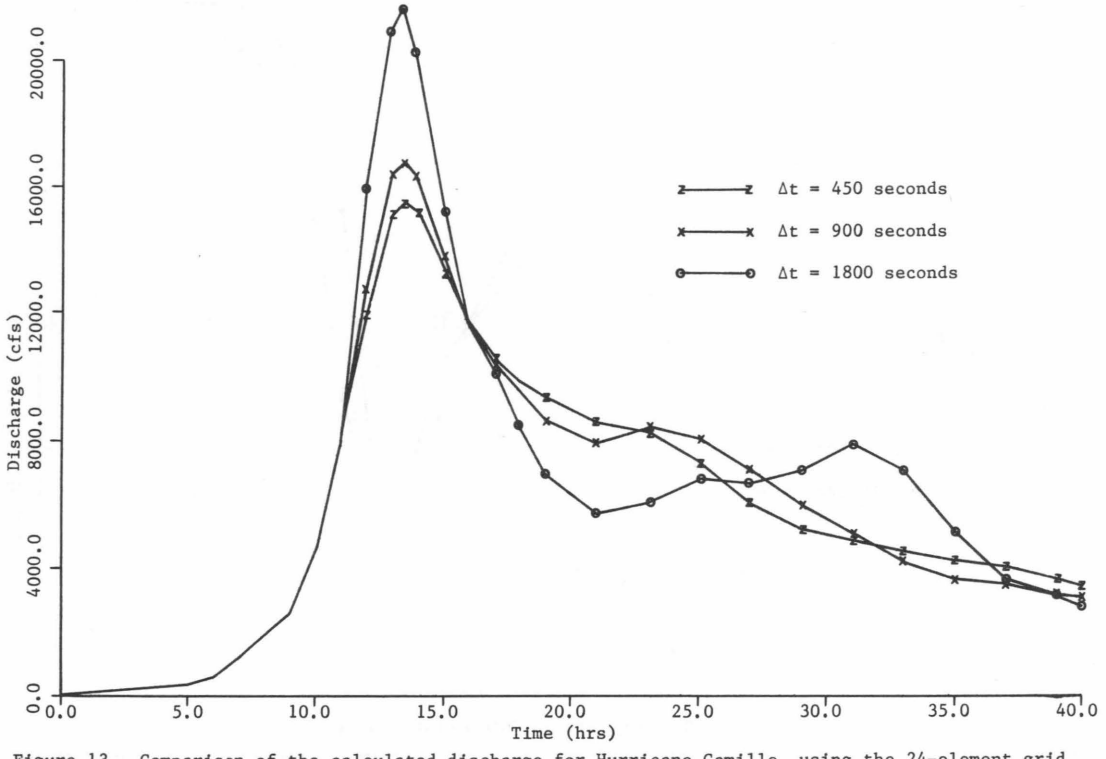

Figure 13. Comparison of the calculated discharge for Hurricane Camille, using the 24-element grid with 3 different time increments.

the rain has stopped, would no doubt cause the rise of the hydrograph to lag somewhat, thus approaching the rise of the recorded hydrograph. A variable Manning η for the channel would also be a definite improvement.

The calculated hydrograph in Figure 28, however, is adequate for the purposes of this model in showing the effects of land-use changes. While the recorded peak discharge of 17,400 cfs represents the 100-year high flow for the South River gaging station at Waynesboro, the calculated hydrograph gave a peak discharge of 16,798 cfs, which was considered to be sufficiently close to the recorded peak.

I. Effect of Changes in the Time Increment

Several other similar runs were made on the 24-element grid with different time increments to determine the effect of this change upon the discharge hydrograph. Time increments of 450 seconds and 1,800 seconds were used. The results of these runs are shown in Figure 29 in comparison with the originally calculated discharge hydrograph obtained from using a time increment of 900 seconds.

The differences in the hydrographs can be expected for time increment changes such as these in a finite element analysis, but this difference may be attributed in part to the nature of the STRUC routine in calculating flow into and out of the reservoirs for the time steps. In the case of the hydrograph obtained by using a time of 1,800 seconds, part of the large increase in the peak flow may be due to the fact that the model is exhibiting some instability. There are several elements in the 24-element grid which have a length of less than 8,000 feet. A time increment of 1,800 seconds may be close to the maximum time increment which can be used and still prevent instability.

II. The Effect of Changes in the Finite Element Grid

In order to evaluate the model with a coarser finite element grid, the 6-element grid shown in Figure 24 was used. Tables 12 and 13 give the watershed and channel geometry for the elements in this grid and Table 14 gives the rainfall excess values for Hurricane Camille for each of the 6 elements. These values are essentially the weighed averages of the excess values of the 24-element grid. In the same way the values for slope and Manning η for the elements in the 6-element grid are essentially the weighted averages of the values of slope and Manning η for the elements of the 24-element grid.

The results of this run are shown in Figure 30 along with the results obtained for the elements obtained for the 24-element grid under present land-use conditions. A time increment of 1,800 seconds was used for this run. The peak is noticeably less than that for the 24-element grid. Observing these curves, it appears that the volume of rainfall excess, or the area under the curves, is less for the 6-element grid than for the 24-element grid. Although the nature of the hydrograph is unknown beyond 40

TABLE 12
Overland Geometry for the 6-Element Grid

Overland Flow Plane No.	Strip No.	Element No.	Length (ft.)	Average Width (ft.)	Slope (ft./ft.)	Manning η
I	A	1	7656	83688	.023	.300
	B	1	26400	56232	.031	.317
II	A	1	17952	36432	.043	.273
	B	1	17424	42768	.065	.297
III	A	1	8712	6336	.003	.262
	B	1	7920	10032	.057	.121

TABLE 13
Channel Geometry for the 6-Element Grid

Channel No.	Element No.	Length (ft.)	Slope	Manning η
I	1	87120	.006	.095
II	1	58080	.018	.117
III	1	12672	.002	.130

TABLE 14

Weighted Rainfall Excess Values for Elements in the 6-Element Grid for Hurricane Camille with Present Land-Use Conditions

Element	Hour 1	2	3	4	5	6	7	8	9	10	11	12
rainfall	0.4750	0.4900	0.5050	0.5150	0.5300	0.5100	0.5100	0.5300	0.4750	0.2800	0.2950	0.3500
IA1	0.0556	0.0600	0.0666	0.1485	0.3172	0.3851	0.4036	0.4506	0.4184	0.2404	0.2402	0.3119
IB1	0.0369	0.0420	0.0836	0.1173	0.2094	0.3130	0.3409	0.4036	0.4216	0.2474	0.1772	0.2573
IIA1	0.0830	0.1532	0.3148	0.5530	0.6037	0.6495	0.6562	0.7279	0.6762	0.3978	0.3698	0.4635
IIB1	0.0565	0.1489	0.3300	0.4297	0.5138	0.5937	0.5941	0.6190	0.5490	0.3130	0.2500	0.3213
IIIA1	0.1093	0.1444	0.1718	0.1982	0.2561	0.3202	0.3635	0.4135	0.3860	0.2246	0.2222	0.2854
IIIB1	0.3055	0.3152	0.3248	0.3313	0.3932	0.4264	0.4264	0.4458	0.3992	0.2095	0.2249	0.2816

FIGURE 30

Comparison of the Calculated Discharge for Hurricane Camille, with Present Land-Use Conditions, Using the 6-Element Grid (Δt = 1,800 sec) and the 24-Element Grid (Δt = 900 sec)

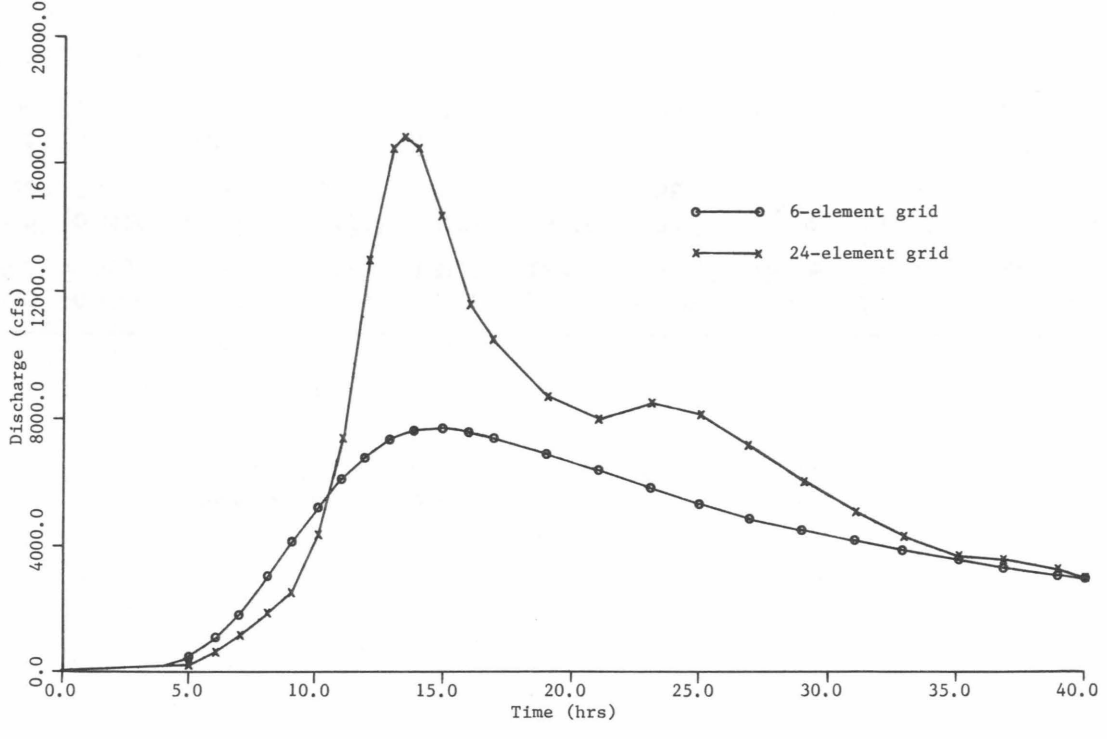

hours, this can be partially explained by the fact that rainfall excess for those elements without flood-detention structures in the 24-element grid, was greater than the values of rainfall excess for the larger elements of the 6-element grid; therefore, more of the quantity of the rainfall excess is routed to the reservoirs, which reduces the quantity of flow directly to the channels. If a time increment of 900 seconds had been used for the 6-element grid, the peak of the hydrograph would have been even less, following the pattern established in Figure 29. Since many of the elements in the 24-element grid are half the length of those in the 6-element grid, the time increment was doubled to arrive at 1,800 seconds.

It is readily noted from Figure 30 that the 6-element grid is unsuitable for flood routing on this watershed. The large size and nonhomogeneity of the watershed make it undesirable to define its hydrologic properties in terms of the large elements of the 6-element grid.

Observing Figure 28, good agreement can be obtained from a finite element grid composed of 24 elements, although even better agreement can be expected with the use of a finer grid consisting of several more elements. This may be necessary to achieve a close fit between the recorded and calculated hydrographs for a different storm. Further usage and testing of the model will confirm whether this is necessary or not.

An obvious result of the utilization of a finer grid is an increase in the computation time and storage requirements resulting in increased computer costs. Some observations regarding these points were made and are discussed below.

III. Computation Time and Storage Requirements

For the 6-element grid hydrograph shown in Figure 30 and for a time increment of 1,800 seconds for 40 hours of real-time simulation, the computation time was 18 seconds. For the 24-element grid hydrograph with a time increment of 900 seconds for 40 hours of real-time simulation, the computation time was 25 seconds. From these observations, a much finer grid did not result in a major computation time increase. It is possible that an even finer grid than the 24-element grid may be devised that will not greatly increase the computation time. One aspect which must be considered is that as the element sizes decrease further, the time interval must also decrease to meet the stability criterion. This factor may contribute greatly to an increase in the total computation time.

A check of the storage requirements revealed that over four times the storage space required for the 6-element qrid was necessary for the 24-element grid. The fact that the time increment was reduced for the smaller elements of the 24-element grid accounted for approximately 60 percent of this increase. A further increase in the number of elements could be expected to cause a similar increase in the storage requirements and may not be justified in view of the agreement obtained by a finite element grid of fewer elements.

FIGURE 31

Comparison of the Calculated Discharge for Hurricane Camille, with Flood-Detention Structures Included and Flood-Detention Structures Excluded

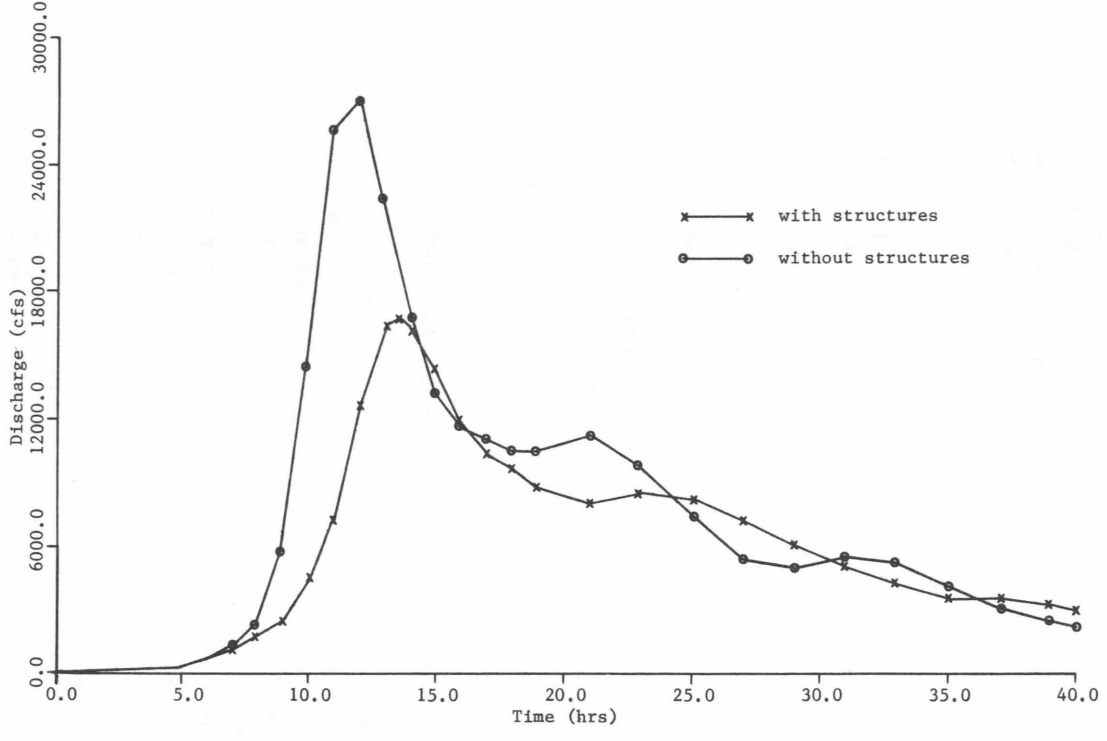

IV. Effect of Flood-Detention Structures

The flood-detention structures mentioned earlier contribute much to the shape of the hydrograph. Figure 31 shows a comparison of Hurricane Camille's effect on the upper South River watershed with the 12 structures present and again with all 12 structures removed from the watershed. The 24-element grid and a time increment of 900 seconds were used.

A primary usage of this model in planning would be to determine the effect of additional flood-detention structures upon the downstream hydrograph. To illustrate this feature, an additional flood-detention structure was incorporated into the model in element IG1 of the 24-element grid. This flood-detention structure is a proposed structure and its location and drainage area are shown in Figure 32. Data, such as the reservoir volume and discharge rates were available for this proposed structure.

With this data entered, the model was run again for Hurricane Camille and the results are shown in Figure 33. The results are essentially what would be expected, with little change in the hydrograph until the peak is passed and the major effect appears on the second, smaller peak. This is due to the fact that most of the rainfall in this particular element, for the first few hours of the storm, was infiltrated into the soil. Also, it was observed in the calculation of these discharges that the major part of the flow at Waynesboro from Hurricane Camille was contributed by the flow from Back Creek, and the proposed flood-detention structure is small compared to some of the other flood-detention structures already on the watershed.

V. Effect of Land-Use Changes

In an effort to determine the effect of land-use changes on the watershed in a realistic sense, data from the Tayloe Murphy Institute, in its publication entitled, *Population Projections, 1980-2000 for Virginia Counties, Cities, and Planning Districts,* was used. Table 15 shows its population increase projections for Augusta County and Waynesboro in terms of the average annual percentage.

In light of these figures, it was decided to use an average annual increase percentage of two and one-half percent, distributed over the entire watershed, to show the extreme effect of land-use changes due to population increases. The year 2000 was selected which represents an overall increase in population from 1970 to 2000 of about 110 percent.

To incorporate this population increase into the model, each element was reevaluated in terms of its land-use characteristics. The residential and impervious areas of an element—direct results of populated areas—were increased by 110 percent, with the agricultural areas being decreased by the same factor. As previously mentioned, this type of action would result in a transformation of the rainfall excess and Manning η

FIGURE 32

Location and Drainage Area of the Proposed Flood-Detention Structure

FIGURE 33

Comparison of the Calculated Discharge for Hurricane Camille, With and Without the Proposed Flood-Detention Structure

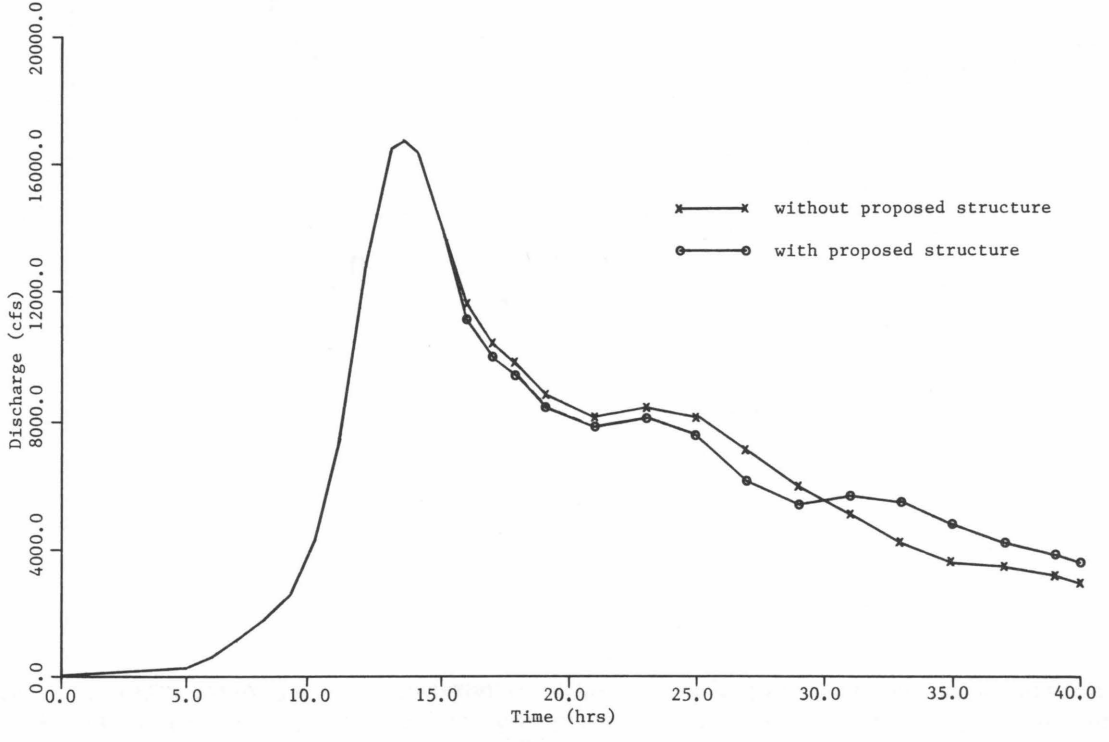

FIGURE 34

Comparison of the Calculated Discharge for Hurricane Camille, with Present and Future Land-Use Conditions (Two and One-Half Percent Annual Population Increase), Using the 24-Element Grid and a Time Increment of 900 Seconds

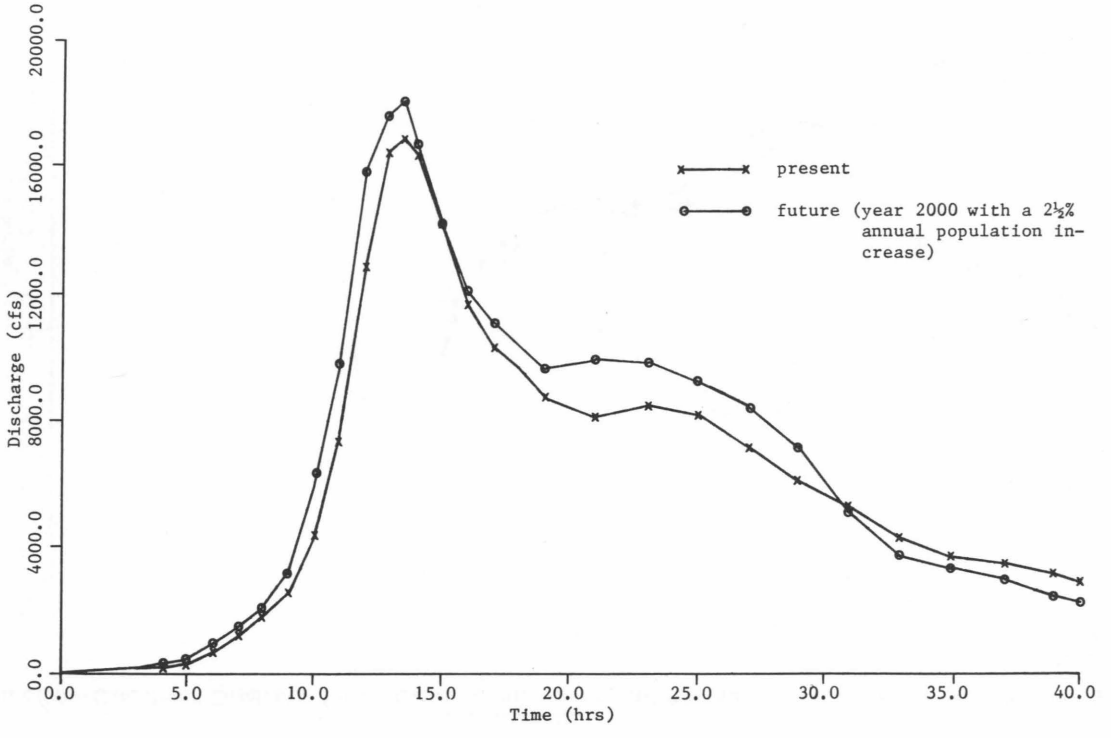

FIGURE 35

Depth Versus Time for Hurricane Camille and the 24-Element Grid, Under Present Land-Use Conditions and the Two Cases of Future Land-Use Conditions

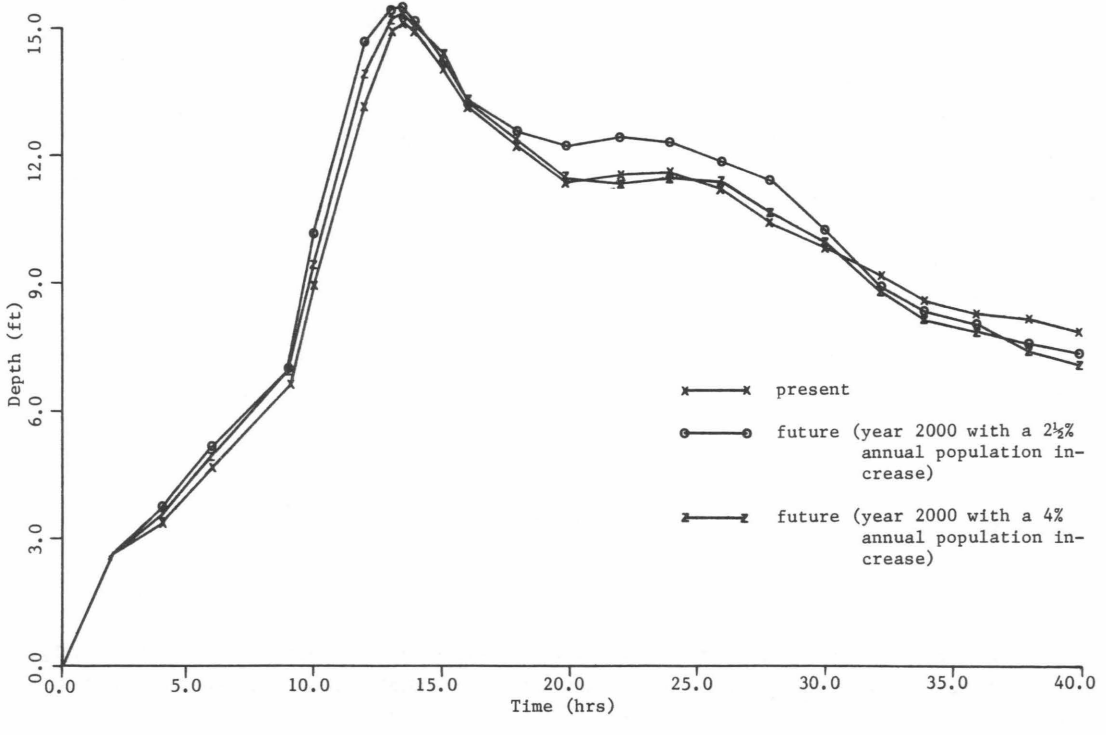

FIGURE 36

Comparison of the Calculated Discharge for Hurricane Camille, with Present and Future Land-Use Conditions (Four Percent Annual Population Increase), Using the 24-Element Grid and a Time Increment of 900 Seconds

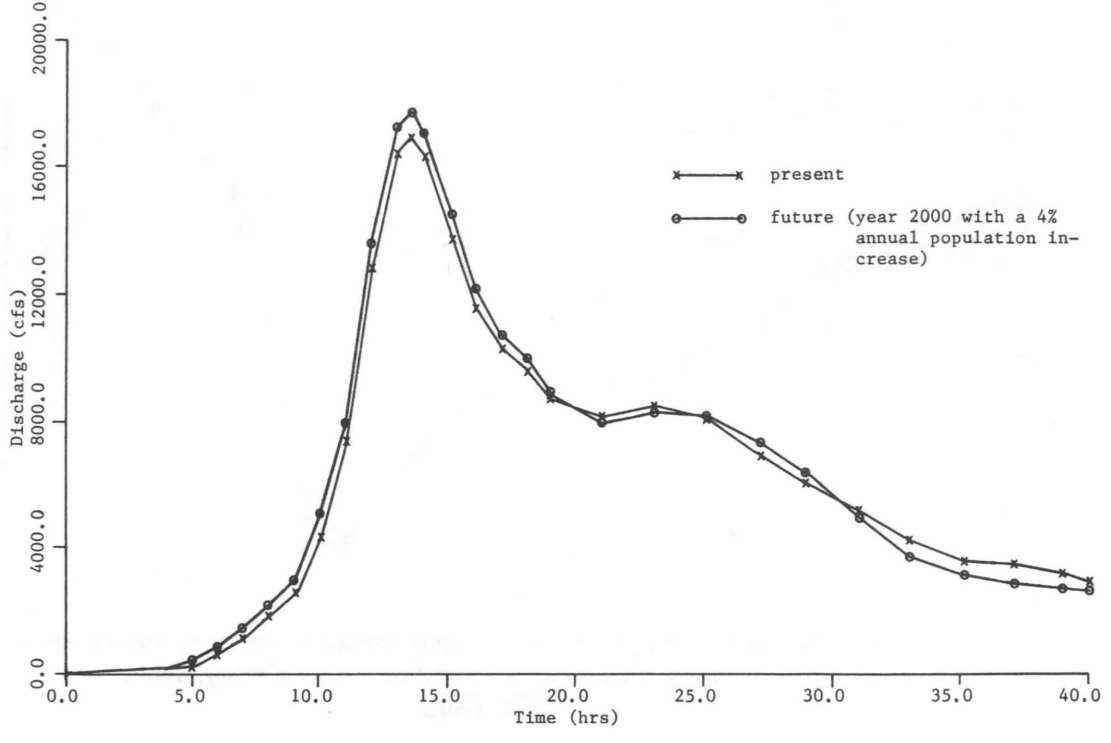

TABLE 15

Projected Average Annual Rate of Change of Population for Augusta County and City of Waynesboro

	1960-1970	1970-1972	1972-1980	1980-1985	1985-1990	1990-1995	1995-2000
Augusta County	1.7%	3.0%	2.2%	1.8%	1.7%	1.6%	1.6
Waynesboro City	0.6	1.2	0.3	0.5	0.4	0.2	0.2

TABLE 16

Comparison of Manning η Under Present Land-Use Conditions and Future Land-Use Conditions in the Year 2000, for the 24-Element Grid

Element	Manning η Present	Future (2½% increase)	Future (4% increase)
IA1	0.297	0.258	0.240
IB1	0.343	0.333	0.343
IB2	0.336	0.302	0.299
IC1	0.323	0.297	0.323
ID1	0.316	0.275	0.316
ID2	0.309	0.297	0.309
IE1	0.244	0.140	0.140
IF1	0.292	0.283	0.292
IF2	0.310	0.273	0.252
IG1	0.340	0.329	0.309
IH1	0.338	0.327	0.314
IIA1	0.286	0.260	0.286
IIA2	0.266	0.230	0.266
IIB1	0.300	0.300	0.300
IIB2	0.300	0.300	0.300
IIC1	0.286	0.258	0.286
IIC2	0.291	0.277	0.291
IID1	0.300	0.300	0.300
IID2	0.286	0.272	0.286
IIE1	0.231	0.184	0.158
IIF1	0.308	0.308	0.308
IIF2	0.294	0.267	0.266
IIIA1	0.264	0.227	0.227
IIB1	0.121	0.090	0.090

TABLE 17

Weighted Rainfall Excess Values for Elements in the 24-Element Grid for Hurricane Camille with Future Land-Use Conditions Based on a Two and One-Half Percent Annual Population Increase to the Year 2000

Element	Hour 1	2	3	4	5	6	7	8	9	10	11	12
rainfall	0.4750	0.4900	0.5050	0.5150	0.5300	0.5100	0.5100	0.5300	0.4750	0.2800	0.2950	0.3500
IA1	0.1081	0.1127	0.1162	0.1950	0.4342	0.5100	0.5100	0.5300	0.4700	0.2800	0.2601	0.3201
IB1	0.0285	0.0294	0.0303	0.0309	0.0324	0.0554	0.0612	0.2147	0.2863	0.1575	0.2022	0.3359
IB2	0.0719	0.0761	0.0826	0.2058	0.3414	0.3680	0.3747	0.4399	0.4395	0.2384	0.2565	0.3479
IC1	0.0713	0.0735	0.0919	0.1863	0.2544	0.2448	0.3037	0.3880	0.4035	0.2438	0.1906	0.2886
ID1	0.0903	0.0931	0.1106	0.1438	0.1672	0.3891	0.4160	0.4360	0.4700	0.2800	0.1318	0.1902
ID2	0.0903	0.0931	0.1257	0.3458	0.4452	0.4284	0.4402	0.4808	0.4370	0.2558	0.1480	0.2116
IE1	0.2280	0.2352	0.2424	0.2597	0.3230	0.3382	0.3632	0.4069	0.3663	0.1874	0.2108	0.2771
IF1	0.0285	0.0294	0.0362	0.0698	0.0954	0.3173	0.3173	0.3373	0.4700	0.2800	0.0753	0.1350
IF2	0.1024	0.1133	0.1383	0.1706	0.2067	0.2428	0.2874	0.3854	0.3834	0.2345	0.2082	0.2866
IG1	0.0001	0.0210	0.0336	0.2121	0.3761	0.4748	0.5100	0.5300	0.4700	0.2800	0.2900	0.3500
IH1	0.0259	0.0350	0.0416	0.0893	0.1321	0.1534	0.1590	0.2950	0.3325	0.1951	0.2389	0.3500

IIC1	0.0713	0.1735	0.0758	0.0773	0.0795	0.3103	0.3103	0.3303	0.4700	0.2800	0.0910	0.1468
IIC2	0.0475	0.0490	0.0505	0.0538	0.1013	0.3006	0.3066	0.3224	0.4302	0.2650	0.1866	0.2466
IIE1	0.2173	0.2592	0.2901	0.3141	0.3405	0.3356	0.3576	0.4084	0.3937	0.2528	0.2662	0.2979
IIF1	0.0001	0.1543	0.5000	0.5100	0.5300	0.5100	0.5100	0.5300	0.4700	0.2800	0.1232	0.1831
IIF2	0.0713	0.1031	0.2150	0.2193	0.3141	0.3794	0.3794	0.3994	0.3394	0.1494	0.0982	0.1574
IIIA1	0.1646	0.1994	0.2240	0.2329	0.3100	0.3237	0.3481	0.3875	0.3424	0.1858	0.2387	0.3037
IIIB1	0.3325	0.3430	0.3535	0.3605	0.4164	0.4284	0.4284	0.4484	0.3884	0.1984	0.2119	0.2684
rainfall	0.9500	0.9800	1.0100	1.0300	1.0600	1.0200	1.0200	1.0600	0.9500	0.5600	0.5900	0.7000
IIA1	0.2147	0.4418	0.5742	1.0100	1.0189	1.0200	1.0200	1.0600	0.9500	0.5600	0.5900	0.7000
IIA2	0.2878	0.4421	0.6686	1.0300	1.0600	1.0200	1.0200	1.0600	0.9500	0.5600	0.5900	0.7000
IIB1	0.1410	0.4183	0.5681	0.9778	1.0433	1.0177	1.0200	1.0600	0.9500	0.5600	0.5900	0.7000
IIB2	0.1799	0.3552	0.6256	1.0294	1.0600	1.0200	1.0200	1.0660	0.9500	0.5600	0.5900	0.7000
IID1	0.0321	0.1448	0.6886	1.0257	1.0574	1.0183	1.0200	1.0600	0.9500	0.5600	0.5900	0.7000
IID2	0.1693	0.3894	0.7965	1.0300	1.0600	1.0200	1.0200	1.0600	0.9500	0.5600	0.5900	0.7000

TABLE 18

Weighted Rainfall Excess Values for Elements in the 24-Element Grid for Hurricane Camille with Future Land-Use Conditions Based on a Four Percent Annual Population Increase for Selected Elements to the Year 2000

Element	Hour 1	2	3	4	5	6	7	8	9	10	11	12
rainfall	0.4750	0.4900	0.5050	0.5150	0.5300	0.5100	0.5100	0.5300	0.4750	0.2800	0.2950	0.3500
IA1	0.1211	0.1367	0.1302	0.2302	0.4543	0.4892	0.4917	0.5137	0.4554	0.2667	0.2777	0.3385
IB1	0.0146	0.0152	0.0155	0.0158	0.0351	0.0639	0.0732	0.2263	0.2994	0.1638	0.2063	0.3370
IB2	0.0572	0.0733	0.1009	0.1816	0.3846	0.3433	0.3530	0.4207	0.4021	0.2299	0.2540	0.3343
IC1	0.0330	0.0360	0.0598	0.1446	0.2126	0.2113	0.2793	0.3650	0.3952	0.2408	0.2143	0.2959
ID1	0.0414	0.0431	0.0638	0.1434	0.1716	0.3891	0.4160	0.4340	0.4700	0.2800	0.1108	0.1706
ID2	0.0485	0.0544	0.2097	0.0728	0.2692	0.3677	0.4125	0.4583	0.4305	0.2524	0.1524	0.2233
IE1	0.2280	0.2352	0.2424	0.2597	0.3230	0.3382	0.3632	0.4069	0.3663	0.1874	0.2108	0.2771
IF1	0.0146	0.0152	0.0224	0.0564	0.0816	0.3046	0.3088	0.3329	0.4700	0.2800	0.0792	0.1396
IF2	0.1032	0.1304	0.1570	0.2088	0.2538	0.2860	0.3178	0.4024	0.3357	0.1883	0.2032	0.2809
IG1	0.0195	0.0475	0.0650	0.1860	0.3706	0.4631	0.5100	0.5300	0.4700	0.2800	0.2900	0.3500
IH1	0.0395	0.0540	0.0645	0.1086	0.1488	0.1665	0.1725	0.2997	0.3347	0.2007	0.2421	0.3500

IIC1	0.0329	0.0459	0.1161	0.1353	0.1925	0.3175	0.3306	0.3478	0.4312	0.2393	0.0936	0.1782
IIC2	0.0282	0.0294	0.0407	0.1019	0.1862	0.3411	0.3411	0.3559	0.4406	0.2672	0.1697	0.2372
IIE1	0.2313	0.2882	0.3302	0.3636	0.4000	0.3944	0.4055	0.4337	0.4091	0.2800	0.2900	0.3500
IIF	0.0001	0.1543	0.5000	0.5100	0.5300	0.5100	0.5100	0.5300	0.4700	0.2800	0.1231	0.1831
IIF2	0.0774	0.1169	0.2350	0.2437	0.2833	0.2621	0.3638	0.3850	0.3303	0.1542	0.1227	0.1819
IIIA1	0.1093	0.1444	0.1718	0.1982	0.2561	0.3202	0.3635	0.4135	0.3860	0.2246	0.2222	0.2854
IIIB1	0.3055	0.3152	0.3248	0.3313	0.3932	0.4264	0.4264	0.4458	0.3992	0.2095	0.2249	0.2816
rainfall	0.9500	0.9800	1.0100	1.0300	1.0600	1.0200	1.0200	1.0600	0.9500	0.5600	0.5900	0.7000
IIA1	0.0897	0.2514	0.5270	1.0241	1.0600	1.0200	1.0200	1.0600	0.9500	0.5600	0.5900	0.7000
IIA2	0.0582	0.1837	0.5314	0.8451	1.0105	0.9978	1.0173	1.0600	0.9500	0.5600	0.5900	0.7000
IIB1	0.1410	0.4183	0.5681	0.9778	1.0433	1.0177	1.0200	1.0600	0.9500	0.5600	0.5900	0.7000
IIB2	0.1799	0.3552	0.6256	1.0294	1.0600	1.0200	1.0200	1.0600	0.9500	0.5600	0.5900	0.7000
IID1	0.0321	0.1448	0.6886	1.0257	1.0574	1.0183	1.0200	1.0600	0.9500	0.5600	0.5900	0.7000
IID2	0.1226	0.3408	0.7689	1.0300	1.0600	1.0200	1.0200	1.0600	0.9500	0.5600	0.5900	0.7000

values for the affected elements. The changes in Manning η are shown in Table 16. Table 17 shows the new rainfall excess values for each element, after the increase in population was considered. The future discharge hydrograph is shown in Figure 34, along with the original calculated hydrograph under present land-use conditions. Both of these were run with a time increment of 900 seconds, with the only differences being the changes in the Manning η and rainfall excess values due to land-use.

There is relatively little increase in the peak of the hydrograph, considering the large increase in the population. This 110 percent increase in population resulted in a peak discharge of 17,916 cfs, whereas the peak with present land-use conditions was 16,798 cfs. This represents an increase of only 6.7 percent over the previous peak. An even more significant fact is that the depth of flow at the gaging station at Waynesboro increased by only 0.4 feet, or 2.7 percent over the previous depth of flow, for the peak conditions. Figure 35 shows depth versus time for this station for the present hydrograph, the two and one-half percent annual increase hydrograph, and another future hydrograph due to a change which will be discussed below. It is obvious from these hydrographs and the depth versus time plots that no great amount of additional flood damage would result from these projected land-use conditions for a similar storm.

To more correctly represent the pattern of population increases in the watershed, it was decided to limit the population increases to those elements which are primarily residential at the present time, since those elements which are wooded mountainous areas would be unlikely to experience any significant increase in population. To accomplish this, an average annual rate of change of four percent was used for elements which at present overlay towns and residential areas or are near potential residential areas. This criterion was applied to the following elements of the 24-element grid: IA1, IB2, IE1, IF2, IG1, IH1, IIE1, IIF2, IIIA1, and IIIB1.

Table 16, which gave the new Manning η values for the two and one-half percent increase also gives the new Manning η values for the four percent increase, along with Manning η under present land-use conditions. Table 18 gives all of the new rainfall excess values used for this run.

The results of these changes in the watershed are shown in Figure 36 in comparison with the discharge hydrograph resulting from the storm under present land-use conditions. Under the four percent annual increase conditions for those elements which are most likely to experience a major population increase, the peak discharge is 17,500 cfs, which is somewhat less than that obtained from the case of a two and one-half percent annual increase distributed over the entire watershed. This reaffirms the assumption that no major increase in flood damage due to a similar storm would result from these projected land-use conditions at Waynesboro. As mentioned previously, Figure 35 shows depth versus time for this condition in comparison with the depth versus time curve under present land-use conditions at Waynesboro, for Hurricane Camille.

CONCLUSIONS AND RECOMMENDATIONS

Listed below are several conclusions arrived at during this study.

1. The finite element technique, in conjunction with Galerkin's residual method as revealed by this particular model and the work of other investigators, has proven to be easily programmable and applicable to the problem of numerical flood routing.

2. The model can easily accommodate natural watersheds which have complex geometry, highly variable hydrologic properties resulting in part from diverse land-use, and variable rainfall distribution resulting in highly diverse rainfall excess values across the watershed.

3. This finite element model, used along with the rainfall excess model discussed previously, can easily accommodate land-use changes by changing several of the major input parameters.

4. Since the rainfall excess parameter is the most significant factor in calculating the the discharge of a river, major effort should be made toward obtaining good rainfall values and a proper distribution of this rainfall over the watershed.

5. For the South River drainage basin, land-use changes, resulting from population increases, have little effect upon the response of the river, in terms of increasing the magnitude of flow for the particular storm discussed herein. A 50-year flood event would likely experience a greater proportional increase after land-use changes have taken place. Additional flood-detention structures can be modeled to determine their effect upon the response of the river and, therefore, the model provides a valuable tool in planning structures such as these. The model could also be used effectively in determining the effect of channel improvements, such as dredging, upon the depth flow for given discharges at points along the channel.

Several aspects which should be considered in future research and further development of the model are listed below.

1. The rainfall excess model and the finite element flood routing model used in this report were run as two separate computer programs. To eliminate the work which is now necessary between the two models, it is suggested that they both be incorporated into one general program. This will reduce much of the time which is now required to run the model. When this is done and the finite element model has been calibrated for a specific watershed, it will be necessary to enter only rainfall values for a given storm to obtain a discharge hydrograph. Changes in land-use resulting in a change in some of the input parameters still can be easily made.

2. When devising a finite element grid for a given watershed, a separate element

should be drawn for the drainage area of any existing flood-detention structure. In this manner, flow into and around a reservoir can be modeled more nearly in terms of the hydrologic properties of the land over which it flows.

3. A change which may be necessary for particular watersheds is that of modifying the model to handle a flood-detention structure which exists in the channel of the CHANL routine. One may wish to observe also the effect of such a channel structure which may be placed there in the future.

4. A variable Manning η, as discussed previously, is an improvement which would more accurately represent the actual flow conditions. A Manning η value depending on depth or velocity of flow for the channel flow, and a Manning η dependent upon whether the rain is falling or has stopped falling for the overland flow would be an obvious improvement in the model.

5. When attempting to determine the effects of such channel improvements as dredging and bridge modification, the channel elements should be devised in the grid construction to allow these improvements to be modeled. It may be necessary to place the channel element nodes at these locations or accommodate more elements in the channel.

6. The following changes are obvious improvements and their consideration is totally dependent upon the limit of the computer costs of running this model:

(a) A finite element grid consisting of more (and smaller) elements, and
(b) More of the streams in a given watershed being incorporated into the CHANL routine, when cross-sectional data for these streams are available.

7. Consideration should be given to development of techniques for computerizing the selection of hydrologic response units.

8. Consideration also should be given to development of mathematical relationships to describe the interaction between hydrologic response units.

LITERATURE CITED

Al-Mashidani, G. and Taylor, C., 1974. "Finite Element Solutions of the Shallow Water Equations–Surface Runoff." *Finite Element Methods in Flow Problems,* UAH Press, Huntsville, Alabama.

Amein, M., 1968. "An Implicit Method for Numerical Flood Routing." *Water Resources Research* 4(4).

Amein, M. and Fang, C. S., 1970. "Implicit Flood Routing in Natural Channels." *Journal of the Hydraulics Division, ASCE* 95(HY4).

Balloffet, A., 1969. "One-Dimentional Analysis of Floods and Tides in Open Channels." *Journal of the Hydraulics Division, ASCE* 95(HY4).

Baltzer, R. A. and Lai, C., 1968. "Computer Simulations of Unsteady Flows in Waterways." *Journal of the Hydraulics Division, ASCE* 94(HY14).

Barnes, B. S., 1940. "Discussion of Analysis of Runoff Characteristics," *Trans ASCE* 105:106.

Bouma, J., Hillel, D. I., Hole, F. D., and Amerman, C. R., 1971. "Field Measurement of Unsaturated Hydraulic Conductivity by Infiltration Through Artificial Crusts." In *Soil Science Society of America Proceedings* 35:362-364.

Brakensiek, D. L., 1967. "Kinematic Flood Routing." *Trans. of ASAE* 10(3).

Claborn, B. J. and Moore, W. L., 1970. *Numerical Simulation of Watershed Hydrology*. Tech. Rep. HYD14-7001, Dept. of Civil Engineering, The University of Texas.

Contractor, D. N. and Wiggert, J. M., 1972. *Numerical Studies of Unsteady Flow in the James River.* Bulletin 51, Virginia Water Resources Research Center. Virginia Polytechnic Institute and State University.

Crawford, N. H. and Linsley, R. K., 1962. *The Synthesis of Continuous Streamflow Hydrographs on a Digital Computer*. Department of Civil Engineering, Stanford University.

Crawford, N. H. and Linsley, R. K., 1966. *Digital Simulation in Hydrology: Stanford Watershed Model IV.* Tech. Rep. No. 39, Dept. of Civil Engineering, Stanford University.

Dawdy, David R., 1969. "Mathematical Modeling in Hydrology, the Progress of Hydrology." In *Proceedings of the First International Seminar for Hydrology Professors.* Vol. I. Department of Civil Engineering, University of Illinois. pp. 346-361.

Dawdy, David R., Lichty, Robert W., and Bergmann, James M., 1970. *A Rainfall-Runoff Simulation Model for Estimation of Flood Peaks for Small Drainage Basins—A Progress Report.* USGS Professional Paper 506B. 28 p.

Desai, C. S. and Abel, J. L., 1972. *Introduction to the Finite Element Method.* Van Nostrand Reinheld Co., New York.

Desai, C. S., 1974. "Finite Element Methods for Flow in Porous Media." *Finite Element Methods in Flow Problems.* UAH Press, Huntsville, Alabama.

Eagleson, P. S., 1970. *Dynamic Hydrology.* McGraw-Hill Book Co.

England, C. B., 1970. *Land Capability: A Hydrologic Response Unit in Agricultural Watersheds.* ARS 41-172, Agricultural Research Service, U. S. Department of Agriculture.

Freeze, R. Allen and Harlan, R. L., 1969. "Blueprint for a Physically-Based, Digitally-Simulated Hydrologic Response Model." *Journal of Hydrology* 9:237-258.

Garrison, J. M., Granju, J. P., and Price, J. T., 1969. "Unsteady Flow Simulation in Rivers and Reservoirs." *Journal of the Hydraulics Division, ASCE* 95(HY5).

Greco, F. and Panattoni, L., 1975. "An Implicit Method to Solve Saint-Venant Equations." *Journal of Hydrology* 24.

Green, W. H. and Ampt, G. A., 1911. "Studies on Soil Physics I. The Flow of Air and Water Through Soils." *J. Agric. Sci.* 4:1-24.

Holtan, H. N., 1961. *A Concept for Infiltration Estimates in Watershed Engineering.* ARS 41-51. Agricultural Research Service, U. S. Dept. of Agriculture.

Holtan, H. N., England, C. B., and Shanholtz, V. O., 1967. "Concepts in Hydrologic Soil Grouping." *Trans. of ASAE* 10:(3)407-410.

Holtan, H. N., England, C. B., Lawless, G. P., and Schumaker, G. A., 1968. *Moisture Tension Data for Selected Soils in Experimental Watersheds.* ARS 41-144. Agricultural Research Service, U. S. Dept. of Agriculture.

Holtan, H. N. and Lopez, N. C., 1971. *USDAHL-70, Model of Watershed Hydrology.* USDA Tech. Bulletin No. 1435. 84 p.

Horton, R. E., 1939. "Analysis of Runoff Plot Experiments with Varying Infiltration Capacity." *Trans. Am. Geoph. Union.* Part IV. p. 693.

Ishihara, Y., 1963. "Hydraulic Mechanism of Runoff." In *Proceedings of a Conference on Hydraulics and Fluid Mechanics.* Pergamon Press.

James, L. Douglas, 1965. "Using a Digital Computer to Estimate the Effects of Urban Development on Flood Peaks." *Water Resources Research* 1:223-233.

Judah, O. M. 1972. "Simulation of Runoff Hydrographs from Natural Watersheds by Finite Element Method." Ph. D. Thesis, Virginia Polytechnic Institute and State University.

Kostyakov, A. N., 1932. "On the Dynamics of the Coefficient of Water-Percolation in Soils and on the Necessity for Studying it from a Dynamic Point of View for Purposes of Amelioration." *Trans. 6th Com. Intern. Soc. Soil Sci.* Russian Part, A:17-21.

Langford, K. J. Turner, 1972. "An Experimental Study of the Application of Kinematic-Wave Theory to Overland Flow." *Journal of Hydrology* 18(2).

Larson, C. L., 1973. "Hydrologic Effects of Modifying Small Watersheds—Is Prediction by Hydrologic Modeling Possible?" *Trans. of ASAE* 16(3):560-564, 568.

Liggett, J. A. and Woolhiser, D. A., 1967a. "Difference Solutions of the Shallow Water Equation." *Journal of the Engineering Mechanics Division, ASCE* 93(EM2).

Liggett, J. A. and Woolhiser, D. A., 1967b. "Unsteady One-Dimensional Flow Over a Plane—the Rising Hydrograph." *Water Resources Research* 3(3).

Lighthill, M. J. and Whitham, G. B., 1955. "On Kinematic Waves—I. Flood Movement in Long Rivers." In *Proceedings of the Royal Society of London* 229.

Ligon, James R., Law, Albert G., and Higgins, D. H., 1969. *Evaluation and Application of a Digital Simulation Model*. Report No. 12, Water Resources Research Institute, Clemson University.

Mein, R. G. and Larson, C. L., 1971. *Modeling the Infilitration Component of the Rainfall-Runoff Process*. Bulletin 43, Minnesota Water Resources Research Center, University of Minnesota.

Morgali, J. R. and Linsley, R. K., 1965. "Computer Analysis of Overland Flow." *Journal of the Hydraulics Division, ASCE* 91(HY3).

Morgali, R., Jr., 1970. "Laminar and Turbulant Overland Flow Hydrographs."*Journal of the Hydraulics Division, ASCE* 96(HY2).

National Weather Service, 1972. *National Weather Service River Forecast Procedures.* NOAA Technical Memorandum NWS HYDRO-14.

Oden, J. T., 1969. "A General Theory of Finite Elements." *International Journal for Numerical Methods in Engineering* 1(2).

Oden, J. T. and Somogyi, D., 1969. "Finite Element Application in Fluid Dynamics." *Journal of the Engineering Mechanics Division, ASCE* 95(EM4).

Petryk, S. and Bosmajian, G., III, 1975. "Analysis of Flow Through Vegetation." *Journal of the Hydraulics Division, ASCE* 101(HY7).

Philip, J. R., 1957. "The Theory of Infiltration, 4. Sorptivity and Algebraic Infiltration Equations." *Soil Sci.* 83:257-264.

Price, R. K., 1974. "Comparison of Four Numerical Methods for Flood Routing." *Journal of the Hydraulics Division, ASCE* 100(HY7).

Rastogi, R. A., 1971. "Nonlinear Response to a Small Drainage Basin Model." *Journal of Hydrology* 14.

Ricca, V. T., 1974. *The Ohio State University Version of the Stanford Streamflow Simulation Model.* 2nd printing. Ohio Water Resources Center, Ohio State University.

Richards, L. A., 1931. "Capillary Conduction of Liquids Through Porous Mediums." *Physics* 1:318-333.

Satterlund, D. R., 1972. *Wildland Watershed Management.* Ronald Press Co., New York.

Schulze, F. E., 1966. *Recent Trends in Hydrograph Synthesis.* Committee for Hydrologic Research, Technical Meeting 21, The Hague, Netherlands.

Shanholtz, V. P., Burford, J. B., and Lillard, J. H., 1972. *Evaluation of a Deterministic Model for Predicting Water Yields from Small Agricultural Watersheds in Virginia.* Research Division Bulletin 78, Virginia Polytechnic Institute and State University. 213 pp.

Skaggs, R. W., Huggins, L. F., Monke, E. J., and Foster, G. R., 1968. "Experimental-Evaluation of Infiltration Equations." Presentation at ASAE meeting at Utah State University.

Soil Conservation Society, 1972. "Hydrology." *National Engineering Handbook* Section 4. U.S. Department of Agriculture.

Soil Conservation Service, 1972. *Soils of Augusta County*. Report No. 14 Augusta County Extension Agency, Virginia.

Southern Regional Research Reports, 1975. (In press).

Factors Affecting Water Yields from Small Watersheds and Shallow Ground Aquifers. C. T. Hann, Editor. SRR Report 198. North Carolina Agricultural Experiment Station.

Data Summaries for Small Watersheds in the Southern Region. T. V. Wilson, Editor. SRR Report 199. South Carolina Agricultural Experiment Station.

Shanholtz, V. O. and Carr, J. C. *Evaluation of a Model for Simulating Streamflow from Small Watersheds*. SRR Report 200. Virginia Agricultural Experiment Station

Haan, C. T. *Evaluation of a Model for Simulating Monthly Water Yields from Small Watersheds*. SRR Report 201. Kentucky Agricultural Experiment Station.

Shelton, C. H., et al. *Field Procedures for Predicting Water Yields and Peak Runoff Rates from Small Watersheds.* SRR Report 202. Tennessee Agricultural Experiment Station.

Wilson, T. V., et al. *Water Yields from Shallow Ground Aquifers.* SRR Report 203. South Carolina Agricultural Experiment Station.

Stoker, J. J., 1953. *Numerical Solution of Flood Prediction and River Regulation Problems—Report I—Derivation of Basic Theory and Formulation of Numerical Methods of Attack.* Report No. IMM-200, Institute of Mathematical Sciences, New York University.

Strelkoff, T., 1970. "Numerical Solution of Saint-Venant Equations." *Journal of the Hydraulics Division, ASCE* 96(HY1).

Tennessee Valley Authority, 1972. *Upper Bear Creek Experimental Project—A Continuous Daily Streamflow Model.* TVA Research Paper No. 8.

Tong, P., 1971. "The Finite Element Method in Fluid Flow Analysis." *Recent Advances in Matrix Methods of Structural Analysis and Design*.

United States Army Corps of Engineers, 1973. "Hydrograph Analysis." *Hydrologic Engineering Methods for Water Resources Development.* Vol. 4. The Hydrologic Engineering Center.

Vreugdenhill, C. B., 1968. "Discussion of Difference Solutions of the Shallow Water Equation by J. A. Liggett and D. A. Woolhiser." *Journal of the Engineering Mechanics Division, ASCE*. 94(EM1).

Wooding, R. A., 1965a. "A Hydraulic Model for the Catchment Stream Problems I—Kinematic Wave Theory." *Journal of Hydrology* 3.

Wooding, R. A., 1965b. "A Hydraulic Model for the Catchment Stream Problems II—Numerical Solutions. *Journal of Hydrology* 3.

Wooding, R. A., 1966. "A Hydraulic Model for the Catchment Stream Problems III—Comparison with Runoff Observation." *Journal of Hydrology* 4.

Woolhiser, D. A., 1973. "Hydrologic and Watershed Modeling—State of Art." *Trans. of ASAE* 16(3):553-559.

Wylie, E. B., 1970. "Unsteady Free-Surface Flow Computations." *Journal of the Hydraulics Division, ASCE*. 96(HY11).

Yevjevich, V. M., 1964. *Bibliography and Discussion of Flood Routing Methods and Unsteady Flow in Channels.* U.S. Government Printing Office.

Zienkiewicz, O. C. and Cheung, Y. K., 1965. "Finite Elements in the Solution of Field Problems." *The Engineer* 220(5722):507-510.

Zienkiewicz, O. C. and Parekh, C. J., 1970. "Transient Field Problems: Two-Dimensional and Three-Dimensional Analysis by Isoparametric Finite Elements." *International Journal for Numerical Methods in Engineering* 2(4).

SUPPORTING REFERENCES

Bell, R. C., 1966. *Improved Techniques for Estimating Runoff with Brief Records.* Report No. 91, Water Research Laboratory. The University of New South Wales, Australia.

Bergstrom, S. and Forsman, A., 1973. "Development of a Conceptual Deterministic Rainfall-Runoff Model." *Nordic Hydrology* 4(3):147-170.

Boughton, W. C., 1965. *A New Simulation Technique for Estimating Catchment Yield.* Report No. 78, Water Research Laboratory, The University of New South Wales. Australia.

Boughton, W. C., 1968. "Evaluating the Variables in a Mathematical Catchment Model." *Civil Engineering Trans.* (Australia) CE10(1):31-39.

Boughton, W. C., 1969. "A Mathematical Catchment Model for Estimating Runoff." *Journal of Hydrology* (New Zealand). p. 75-100.

Clarke, R. T., 1973. "A Review of Some Mathematical Models Used in Hydrology with Observation on Their Calibration and Use." *Journal of Hydrology* 19:1-20.

Dawdy, David R. and O'Donnel, Terrence, 1965. "Mathematical Models of Catchment Behavior." *Proc. ASCE* 91(HY4):123-137m.

Dunn, D. E., 1970. *An Experiment in Finite-Difference Watershed Modeling.* Report No. 13, Water Resources Research Center. Montana State University.

Grip, H., 1973. "A Deterministic Parametric Water-Balance Model." *Nordic Hydrology* 4(3):191-205.

Haan, C. T., 1972. "A Water Yield Model for Small Watersheds." *Water Resources Research* 8(1).

Holtan, H. N., Stiltner, G. J., Henson, W. H. and Lopez, N. C., 1974. *USDAHL-74 Revised Model of Watershed Hydrology.* Plant Physiology Institute Report No. 4, ARS, U. S. Department of Agriculture.

Huggins, L. F. and Monke, E. J., 1970. *Mathematical Simulation of Hydrologic Events of Ungaged Watersheds*. Technical Report 14, Water Resources Research Center, Purdue University.

Johnson, H. P., 1973. "Hydrologic and Watershed Modeling in Summary." *Trans. of ASAE* 16(3):585-586.

Jones, J. R., *The Estimation of Runoff from Small Rural Catchments.* Hydrology Symposium. The Institute of Engineers, Austrialia. pp. 17-24.

Laurenson, E. M. and Jones. J. R., 1968. "Yield Estimates for Small Rural Catchments in Austrialia." *Civil Eng. Trans.* (Austr.) CE10(1):160-166.

Lee, M. T. and Delleur, J. W., 1972. *A Program for Estimating Runoff from Indiana Watersheds, Part III. Analysis of Biomorphologic Data and a Dynamic Contributing Area Model for Runoff Estimation.* Tech. Rep. 24, Water Resources Research Center, Purdue University.

Machmeier, R. E. and Larson, C. L., 1968. "Runoff Hydrographs for Mathematical Watershed Model." *Proc. ASCE* 94(HY6):1453-74.

Nielson, S. A. and Hansen, E., 1973. "Numerical Simulation of the Rainfall-Runoff Process on a Daily Basis." *Nordic Hydrology* 4(3):171-190.

McMahon, J. W. and McMahon, T. A., 1971. "A Model for the Simulation of Streamflow Data from Climatic Records." *Journal of Hydrology* 13:297-324.

Rockwood, D. M., 1964. *Streamflow Simulation and Reservoir Regulation.* Tech. Bulletin 22, U. S. Corps of Engineers, North Pacific Division.

Sittner, W. T., Schauss, C. E., and Munro, J. C., 1969. "Continuous Hydrograph Synthesis with an API-Type Hydrologic Model." *Water Resources Research* 5:1007-1022.

Smith, R. E. and Woolhiser, D. A., 1971. *Mathematical Simulation of Infiltrating Watersheds*. Hydrology Paper No. 47, Colorado State University.

Snyder, W. M., Mills, W. C. and Stephens, J. C., 1971. "A Three-Component, Non-Linear Water-Yield Model." *Proceedings of the First Bilateral U.S./Japan Seminar in Hydrology*. Water Resources Publications, Fort Collins, Colorado.

VIRGINIA WATER RESOURCES RESEARCH CENTER
BLACKSBURG, VIRGINIA 24061